

7-11-2015

Investigation of methods and validation techniques for plastic injection mold weight reduction

Bitá Mohjernia
University of Windsor

Follow this and additional works at: <http://scholar.uwindsor.ca/etd>

Recommended Citation

Mohjernia, Bitá, "Investigation of methods and validation techniques for plastic injection mold weight reduction" (2015). *Electronic Theses and Dissertations*. Paper 5308.

This online database contains the full-text of PhD dissertations and Masters' theses of University of Windsor students from 1954 forward. These documents are made available for personal study and research purposes only, in accordance with the Canadian Copyright Act and the Creative Commons license—CC BY-NC-ND (Attribution, Non-Commercial, No Derivative Works). Under this license, works must always be attributed to the copyright holder (original author), cannot be used for any commercial purposes, and may not be altered. Any other use would require the permission of the copyright holder. Students may inquire about withdrawing their dissertation and/or thesis from this database. For additional inquiries, please contact the repository administrator via email (scholarship@uwindsor.ca) or by telephone at 519-253-3000ext. 3208.

**Investigation of methods and validation techniques for plastic injection mold weight
reduction**

By

Bitá Mohajernia

A Thesis

Submitted to the Faculty of Graduate Studies

Through the Department of **Mechanical, Automotive & Materials Engineering**

in Partial Fulfillment of the Requirements for

the Degree of **Master of Science**

at the University of Windsor

Windsor, Ontario, Canada

2015

© 2015 Bitá Mohajernia

**Investigation of methods and validation techniques for plastic injection mold weight
reduction**

by

Bitra Mohajernia

APPROVED BY:

Dr. Ahmed Azab, Reader

Industrial & Manufacturing Systems Engineering

Dr. Nader Zamani, Reader

Mechanical, Automotive & Materials Engineering

Dr. Jill Urbanic, Advisor

Mechanical, Automotive & Materials Engineering

Dr. Peter Frise, Co-advisor

Mechanical, Automotive & Materials Engineering

17 April 2015

DECLARATION OF ORIGINALITY

I hereby certify that I am the sole author of this thesis and that no part of this thesis has been published or submitted for publication.

I certify that, to the best of my knowledge, my thesis does not infringe upon anyone's copyright nor violate any proprietary rights and that any ideas, techniques, quotations, or any other material from the work of other people included in my thesis, published or otherwise, are fully acknowledged in accordance with the standard referencing practices. Furthermore, to the extent that I have included copyrighted material that surpasses the bounds of fair dealing within the meaning of the Canada Copyright Act, I certify that I have obtained a written permission from the copyright owner(s) to include such material(s) in my thesis and have included copies of such copyright clearances to my appendix.

I declare that this is a true copy of my thesis, including any final revisions, as approved by my proposal committee and the Graduate Studies office, and that this proposal has not been submitted for a higher degree to any other University or Institution.

ABSTRACT

Mold making techniques have focused on meeting the customers' functional and process requirements; however, today, molds are increasing in size and sophistication. Presently, mold weight saving techniques focus on pockets to reduce the mass of the mold and supporting components (platen plate), but the overall size is still large. Reducing the overall size of the mold is desirable. It is proposed to use Finite Element Analysis simulation tools to model the forces, and pressures to determine where material can be removed. The potential results of this project will reduce manufacturing costs. In this study, a light weight structure is defined by optimal distribution of material to carry external loads. Topology optimization methods are utilized to improve structural stiffness while decreasing the weight and overall envelope of the mold (OptiStruct software).

Results show 8% of weight reduction and the maximum displacement difference of less than 0.005 mm , between original and optimized structure and Von Mises stress in the safe domain.

ACKNOWLEDGEMENTS

I would like to express my deepest appreciation to all those who provided me the possibility to complete this thesis. I am thankful to my supervisor, Dr. Jill Urbanic, whose advice and knowledge added to my graduate experience. Her insight has inspired me, and I would appreciate her support. I would also want to express my gratitude to my co-advisor Dr. Frise for his support. I would like to appreciate my committee members, Dr. Ahmad Azab and Dr. Nader Zamani for their valuable suggestions. Furthermore, a special thanks goes to Omega Tools personnel for their patience, kindness and their valuable experience which guided me in this thesis. I am especially grateful to my beloved parents and husband who always encourage and support me.

TABLE OF CONTENTS

DECLARATION OF ORIGINALITY	iii
ABSTRACT.....	iv
LIST OF TABLES	ix
LIST OF FIGURES	x
LIST OF APPENDICES.....	xiii
LIST OF ABBREVIATIONS.....	xiv
CHAPTER 1- Introduction	1
1.1 Plastic injection mold	1
1.2 Plastic injection machine.....	4
1.3 Cycle sequence in injection molding.....	4
1.4 Process of designing an injection mold	6
1.5 Manufacturing guidelines standard for extremely high volume mold	7
1.5.1 Mold base.....	7
1.5.2 Cavity and core.....	7
1.5.3 Cooling.....	7
1.5.4 Ejection	8
1.6 Mold failures.....	8
1.7 Mold maintenance.....	8
Problem Description.....	10
Objective	11
CHAPTER 2- Literature review	13
2.1 Plastic injection mold design	13
2.2 Plastic injection process optimization	13
2.3 Plastic injection mold weight reduction.....	13
2.4 Structural optimization	13
2.5 Thermal analysis and design of plastic injection molds	14
2.6 Table of literature review.....	15
CHAPTER 3- Methodology	18

3.1	<i>FEA analysis</i>	18
3.2	<i>Structural optimization</i>	18
3.3	<i>Topology optimization:</i>	20
3.4	<i>Software Selection</i>	23
3.5	<i>SIMP method in Optistruct</i>	23
3.6	<i>A trial case for 2D Topology optimization problem</i>	24
CHAPTER 4- Model description, analysis setup, structural optimization and validation ..		37
4.1	<i>Mold geometry</i>	37
4.2	<i>Geometry cleanup:</i>	40
4.2.1	<i>Removing unnecessary details:</i>	40
4.2.2	<i>Refining topology to achieve a quality mesh</i>	41
4.3	<i>Meshing</i>	42
4.3.1	<i>2D meshing</i>	42
4.3.2	<i>3D meshing:</i>	43
4.4	<i>Element quality check</i>	43
4.5	<i>Assigning material and properties</i>	44
4.6	<i>Defining design space and non-design space</i>	44
4.7	<i>Analysis setup</i>	45
4.7.1	<i>Constraints</i>	45
4.7.2	<i>Loads</i>	46
4.7.3	<i>Defining optimization criteria</i>	50
4.8	<i>Results of static analysis of primary model</i>	52
4.9	<i>Results of topology optimization</i>	54
4.10	<i>Results interpretation and redesign of the die</i>	58
4.11	<i>Mold with smaller overall size</i>	60
4.12	<i>Validating results by installing mold deflection sensors</i>	61
CHAPTER 5- A coupled heat transfer/structural analysis		68
5.1	<i>Cavity Temperature</i>	68
5.2	<i>Coupled thermal/ structure analysis result</i>	71
CHAPTER 6- Summary, conclusion and future works		74
6.1	<i>Summary and conclusion</i>	74
6.2	<i>Future works</i>	75

REFERENCES	77
APPENDICES	80
VITA AUCTORIS	89

LIST OF TABLES

Table 1.1 Standard material used for mold manufacturing and their costs.....	3
Table 1.2 Steps of project.....	12
Table 2.1 Summary of literature review.....	17
Table 3.1 Original and optimized c-clip weight comparison.....	28
Table 3.2 Displacement changes based on load and time for original C-clip.....	32
Table 3.3 Displacement changes based on load and time for optimized C-clip.....	33
Table 3.4 Numerical values of theoretical and experimental displacement for original and optimized c-clip and the calculated error.....	34
Table 3.5 Original and optimized c-clip weight comparison based on theory.....	36
Table 3.6 Original and optimized c-clip weight comparison based on theory.....	36
Table 4.1 Material properties of P20 steel tool.....	40
Table 4.2 Demonstration of element quality.....	44
Table 4.3 Inputs of FE model in Optistruct.....	52
Table 4.4 Results of static analysis of primary model.....	52
Table 4.5 Results of static analysis of optimized interpreted model.....	59
Table 4.6 Results of static analysis of proposed model.....	61
Table 5.1 Sensor's application and depth of tip to mold surface table.....	69
Table 5.2 Inputs of FE model in Optistruct.....	71

LIST OF FIGURES

Fig 1.1 Injection molding machine, mold block, platen plates, injection and ejection systems[1].....	3
Fig 1.2 Sequence of injection molding, First stage, Injection [2].....	5
Fig 1.3 Sequence of injection molding, second stage Solidification [2].....	5
Fig 1.4 Sequence of injection molding Ejection [2].....	6
Fig 1.5 Front view of a cavity block illustrating the size and complexity of a standard application (all dimensions are in inches).....	10
Fig 1.6 Top view of the cavity block (all dimensions are in inches).....	11
Fig 3.1 Three categories of structural optimization a) Sizing optimization of a truss structure, b) Shape optimization and c) Topology optimization. The initial problems are shown at the left and the optimized solutions are shown at the right [3].....	20
Fig 3.2 Topology optimization problem set up (yellow triangles are constraints and applied loads are demonstrated with blue arrows).....	25
Fig 3.3 Displacement contour for the original c-clip along Z axis each color corresponds to a range of displacement (m), varying between 1.0 E-5 m and 2.6 E-4 m.....	26
Fig 3.4 Element density contour plot.....	26
Fig 3.5 Optimized model of c-clip after performing topology optimization.....	27
Fig 3.6 Displacement contour for the optimized geometry, each color corresponds to a range of displacement (m) varying between -1.6 E-5 m and 3.8 E-4 m.....	27
Fig 3.7 Von Mises stresses (Pa) contour for the optimized geometry.....	28
Fig 3.8 C-clip in tensile test machine (Instron).....	29
Fig 3.9 Optimized model with iso value of 0.15.....	31
Fig 3.10 Load-displacement diagram, original c-clip.....	32
Fig 3.11 Load-displacement diagram, optimized c-clip.....	33
Fig 3.12 Displacement- Iso value diagram for theory and experiment tests.....	35
Fig 3.13 Optimized geometry based on theoretical result.....	35
Fig 4.1 Mold block consisting core, yellow part, and cavity, blue part, from industrial partner.....	37
Fig 4.2 Mold block mounted in injection molding machine.....	38
Fig 4.3 Front view of cavity block.....	38
Fig 4.4 Side view of cavity block.....	38

Fig 4.5 Front view of core block.....	39
Fig 4.6 Side view of core block.....	39
Fig 4.7 Original CAD model.....	41
Fig 4.8 Cleaned-up model	41
Fig 4.9 Topology refinement examples [4].....	42
Fig 4.10 Triangular and quadrilateral elements.....	42
Fig 4.11 3D elements, tetra, penta and hexa.....	43
Fig 4.12 Meshed cavity and tetrahedral elements in meshed cavity.....	43
Fig 4.13 Model configuration consisting design space (purple mesh) and non-design space (blue mesh).....	45
Fig 4.14 Constrained cavity block.....	46
Fig 4.15 Button style cavity pressure sensor [5].....	47
Fig 4.16 Button style cavity pressure sensor dimensions [5].....	47
Fig 4.17 Pressure sensors located behind the ejector pin [5].....	48
Fig 4.18 Cavity pressure sensors are installed in the core block.....	48
Fig 4.19 Pressure-time diagram, Cavity pressure is plotted for both sensors in each cavity.....	49
Fig 4.20 Loaded model, red arrows show the applied pressure to the mold.....	50
Fig 4.21 Displacement contour plot for primary model.....	53
Fig 4.22 Topology optimized mold, top block is the cavity block and bottom block is the core block.....	54
Fig 4.23 Results of topology optimized mold, only the design space has been demonstrated, top view.....	54
Fig 4.24 Element density plot for topology optimization results, top view and bottom view.....	56
Fig 4.25 IGES file extracted from topology results using Ossmooth.....	57
Fig 4.26 Optimized interpreted geometry.....	58
Fig 4.27 Displacement contour plot for optimized interpreted model.....	59
Fig 4.28 Stress contour plot for optimized interpreted model.....	60
Fig 4.29 Displacement contour plot for proposed model.....	61
Fig 4.30 Deflection sensors placement on cavity half.....	62
Fig 4.31 Mold deflection sensor installed in cavity block on parting line [6].....	63
Fig 4.32 Deflection-time diagram, original model.....	64
Fig 4.33 Deflection-time diagram, optimized model.....	64

Fig 4.34 The mold is clamped and peak pressure of cavities are demonstrated with green and blue lines) has happened $t=3.112$ S.....	65
Fig 4.35 The mold is clamped and peak pressure of cavities are demonstrated with green and blue lines) has happened $t=3.3$ S.....	65
Fig 4.36 Deflection (mils)-time(s) diagram for $t = 2$ S to $t = 4$ S, original structure.....	66
Fig 4.37 Deflection (mils)-time(s) diagram for $t = 2$ S to $t = 4$ S, Optimized structure.....	67
Fig 5.1 Cavity temperature sensors [7].....	68
Fig 5.2 Cavity temperature sensor and depth of tip to the cavity surface [7].....	69
Fig 5.3 Cavity temperature sensors and module, installed in cavity block.....	69
Fig 5.4 Temperature-time diagram, Cavity temperature is plotted for both sensors in each cavity.....	70
Fig 5.5 deflection contour due to coupled thermal structure analysis of original model.....	71
Fig 5.6 deflection contour due to coupled thermal structure analysis of optimized interpreted model.....	72
Fig 5.7 deflection contour due to coupled thermal structure analysis of smaller model.....	72
Fig 6.1 Compliance curve vs iteration numbers for optimization with VOF of 0.5.....	74
Fig 6.2 Demonstration of real optimal and optimized interpreted model.....	75

LIST OF APPENDICES

Appendix A: Deflection contour for original model, optimized interpreted model and smaller model.....	80
Appendix B: Deflection contour for coupled structure/thermal analysis results.....	83
Appendix C: Mesh quality check.....	86
Appendix D: Workflow of structural optimization.....	87

LIST OF ABBREVIATIONS

FEA	Finite Element Analysis
IGES	Initial Graphics Exchange Specification
SIMP	Solid Isotropic Material with Penalization
CM	Corrective Maintenance
PM	Preventive Maintenance
MMS	Minimum Member Size
VOF	Volume Fraction

CHAPTER 1

INTRODUCTION

Preface:

The Windsor area is known for its mold making capabilities. The companies design and build prototype and production tooling, and are involved with design for manufacturing activities related to improving the process costs without impacting process design. They may be involved in production activities as well. The industrial sponsor for this research is a mold manufacturing company that, offers a wide range of solutions for complex tooling challenges in the plastic injection molding industry. They have 30 year's experience and capabilities in all aspects of the tooling industry, from new builds to engineering modifications and trouble shooting of the tooling issues.

Background, plastic injection molding

The plastic injection molding process is one of the key processes in producing plastic parts of almost any complexity. Injection molding is the most common method of producing plastic parts. The process involves injecting molten plastic at a high pressure into a mold, shaped into the form of a part. The increasing size and complexity of these plastic parts requires larger, heavier and costlier molds which are designed traditionally and based on trial and error methods. However, this enlarging of the mold size cannot be performed indefinitely, since it introduces cost, time, and performance related issues. The plastic injection mold design starts with refining the design of the component for the injection molding process. Once the component is designed, the mold elements are designed, and the plastic injection molding criteria is established.

In the design process of an injection mold, it is desirable to optimize the design for the mold structure (as well as the part being molded) in predetermined circumstances for given sets of loads and boundary conditions.

1.1 Plastic injection mold

The mold tool, which is usually made from hardened steel (high volume production) , provides the shape of the plastic parts. Using a well-designed and well-made (surface finish / polish) mold tool is vital in ensuring the quality of the plastic part produced. An injection mold is a heat exchanger that solidifies the molten plastic into the

desired shape. The mold assembly consists of platens, cavity block and core block, usually made of tool steel (P20), which are described in detail in this chapter. The main function of mold is to shape the liquefied plastic inside the mold cavity and eject the solidified molded part. The stationary component of the mold is named the cavity block and the moving part of the mold is named the core block. The core block is connected to the cavity block with the use of tie bars. In addition to the cavity and core blocks, there are other components in the mold, each of which serves a function during the molding cycle.

A mold should have distribution channels through which the molten plastic flows from the nozzle of the injection barrel into the cavity. The distribution channel consists of the following:

- Sprue: Sprue is a passage through which the plastic is introduced into a mold.
- Runner: Runner is a system that feeds material into the cavity.
- Gate: Gate in mold constricts the flow of plastic into the cavity.

The mold needs an ejection system to eject the molded part out the cavity at the end of the molding cycle. Ejector pins are built into the moving half of the mold. They are used to push the solidified component out of the cavity. The cavity is divided between the two mold halves in such a way that the natural shrinkage of the molding causes the part to stick to the moving half. When the mold opens, the ejector pins push the part out of the cavity. A cooling system is also required for the mold. Water is circulated to remove heat from the hot plastic. Air should be removed from the mold cavity using a vacuum when the plastic enters the cavity. Much of the air passes through the small ejector pin. In addition, narrow air vents are often machined into the parting line of the mold. These channels allow air to escape to the outside. These components are illustrated in Figure 1.1.

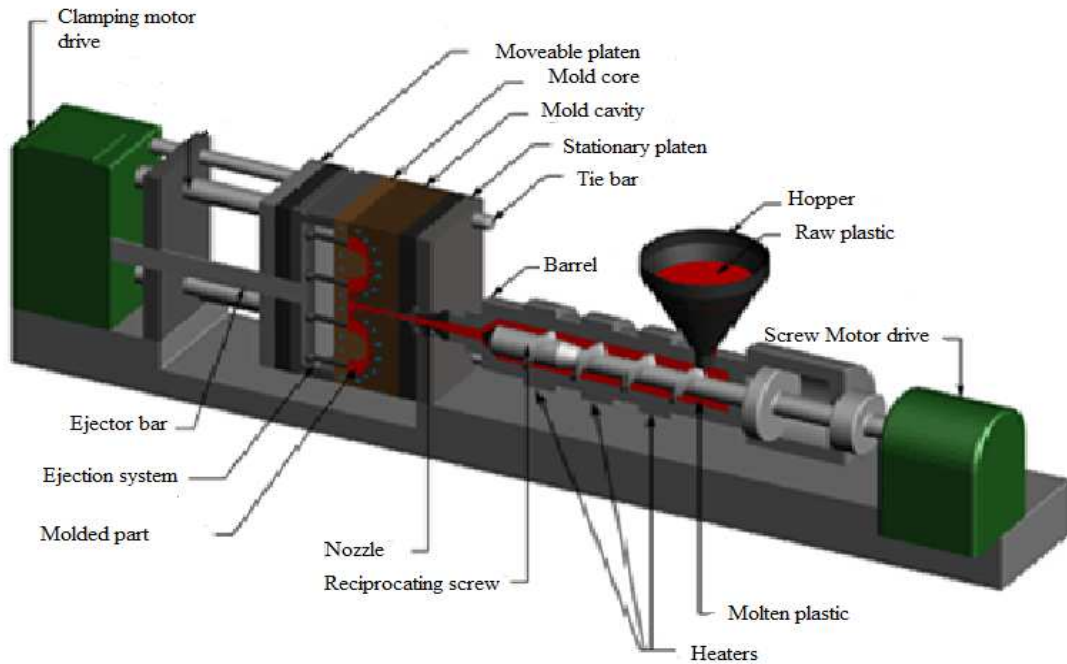


Fig 1.1 Injection molding machine, mold block, platen plates, injection and ejection systems[1]

Plastic injection molds are usually made of steel tool. The following table demonstrates the type of material for manufacturing different parts of the mold.

Steel type	Usage	Price per pound
P20	Core and cavity blocks, the components used to de-mold any undercuts such as lifters and slides	1.5 \$
1020, 4140	back plates, ejector plates	1\$
TM180	For area that is difficult to cool with P20 steel, TM180 is used, TM180 is a beryllium free copper/ nickel alloy with excellent thermal conductivity properties	18\$

Table 1.1 Standard material used for mold manufacturing and their costs

1.2 Plastic injection machine

An injection molding machine consists of two principal components: the plastic injection unit and the clamping unit.

- The plastic injection unit:

The injection unit consists of a barrel that is fed from one end by a hopper containing a plastic pellets. There is a reciprocating screw inside the barrel. The screw turns inside the barrel. It mixes and heats the plastic simultaneously. The screw moves forward to inject molten plastic into the mold. A nonreturnable valve mounted near the tip of the screw prevents the melt from flowing backward. Generally, the functions of the injection unit are to melt and homogenize the plastic, and then inject it into the mold cavity.

- The mold clamping unit:

The clamping unit of injection machine holds the two halves of the mold in proper alignment with each other, keeps the mold closed during injection, and opens and closes the mold at the appropriate times. The clamping unit consists of two platens (a fixed platen and movable platen), and a mechanism for moving the moveable platen. The mechanism is basically a power press that acts by means of a hydraulic piston [8].

1.3 Cycle sequence in injection molding

Injection: Before the injection process starts, the core and cavity blocks should be closed securely. The clamping unit of the machine produces the required clamping force for the two halves. Plastic, usually in form of pellets, is fed into the hopper. The hopper is a funnel shape device, which is located on the top of barrel, and it is the entrance of resin into the barrel. As the resin enters the injection barrel, it is driven forward by rotation of screw, which is powered by the hydraulic motor. The resin melt as the turning screw drags it to the nozzle end. This is referred to as drag flow, which causes the polymer molecules to slide over each other creating the frictional heat, which melts the material. The injection system (heaters and barrel with single screw extruder) heats the thermal plastic material to appropriate viscosity and then injected that into the mold.

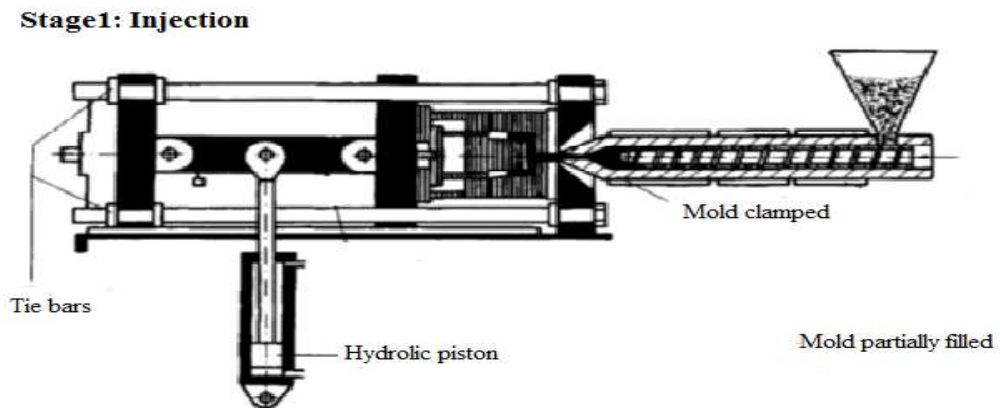


Fig 1.2 Sequence of injection molding, First stage, Injection [2]

Solidification: The molten plastic inside the cavity starts to cool. Shrinkage happens during cooling; therefore, the packing of the material in the injection stage allows additional material to flow into the mold and reduce the amount of visible shrinkage.

Stage 2: Holding pressure and solidification

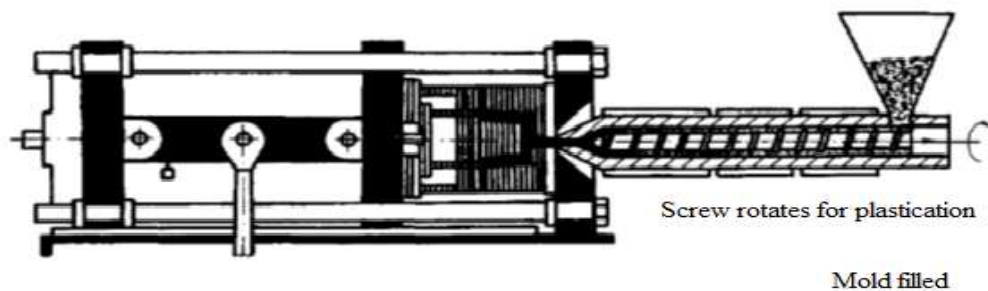


Fig 1.3 Sequence of injection molding, second stage Solidification [2]

Ejection: When the molded part solidified to an extent that it could retain its shape without external support, the clamping unit of the machine opens the core and the plastic part is pushed out of the cavity by ejector pins.

Stage 3: Ejection

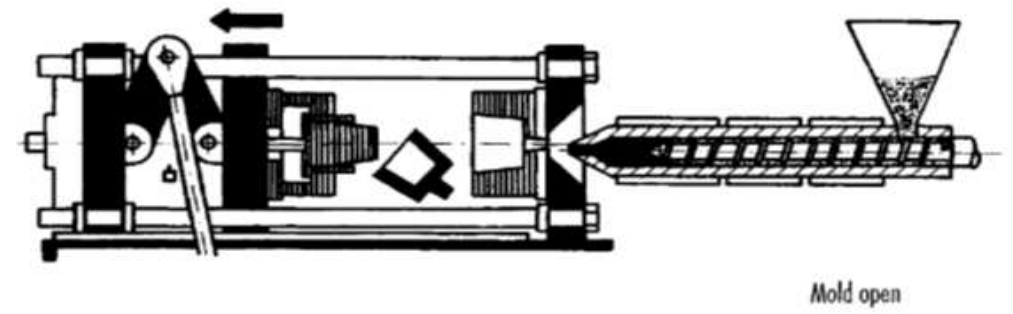


Fig 1.4 Sequence of injection molding, Ejection [2]

1.4 Process of designing an injection mold

The design of an injection mold is a complicated task. A mold designer first gathers all the required information related to the part design. The designer decides on the type of injection machine and mold according to the customer's requirement and arranges all the steps of the design from the primary design to the detailed design. The mold designer has to design the cavity of the mold, which accurately shapes the part, and the runner system and position and orientation of different parts of the injection mold and make sure that the entire mold assembly works appropriately. Designers apply engineering techniques and trial and error methods to come up with their desired mold layout. There are three steps for the general design flow:

Step 1

Collect comprehensive information around part's geometry and its layout. Perform design modifications to ensure about the manufacturability of the final design.

Step2

Develop of core and cavity: Determine the parting lines of the core and cavity according to their manufacturability considerations. Check the core and cavity designs carefully for interferences.

Step3

Design the gating, ejection system, venting system, cooling lines and finally determine the mold final layout. This is discussed further in section 1.5.

1.5 Manufacturing guidelines standard for extremely high volume mold

(Extremely high volume production injection molds built for lifetime cycles exceeding one million)

- Mold should run in a full automatic cycle.
- Primary mold layout should be approved by the tooling engineer before constructing the mold.
- Final mold design must be updated with all modifications prior to mold approval.
- All screws, bolts, leader pins/bushings, ejector pins, ejector blades, etc. should be standard stock items wherever possible.

1.5.1 Mold base

- All mold base plates should be fabricated from stainless steel material.
- Straight parting line interlocks should be on both sides of the vertical and horizontal axes.

1.5.2 Cavity and core

- All molding surfaces should be made of hardened tool steel and heat treated to a minimum of 48 Rockwell “C” hardness.
- Venting is required because of entrapment of air in the mold cavity. When venting is improperly designed, “gas burn” happens. Gas burn is small spot on plastic part. [9]. Example design guidelines are:
 - a. Last to fill areas must always have appropriate venting.
 - b. Deep pockets must be vented wherever possible.

1.5.3 Cooling

- Water lines should be distributed in both the core and cavity blocks.
- The water inlet and outlet locations should be located so they do not interfere with the molding machine tie bars and mold clamp slots.
- All water inlets and outlets should be stamped and identified on the mold base. Identify inlets as “IN 1”, “IN 2”, etc. Identify outlets as “OUT 1”, “OUT 2”, etc.

1.5.4 Ejection

- The ejector plates should run on guided bushings.
- Bushings shall be self-lubricated.
- The ejector plate travel must be sufficient for full part ejection and consistent automatic molding cycle operation.
- The ejector pins and sleeves shall be industry standard sizes wherever possible. All exceptions must be noted and approved by the design engineer.
- All ejector plates should have return springs where the mold design and mold operation allows.

1.6 Mold failures

Mold failure can occur due to deformation, cracking, wear, erosion, etching and pitting. In order to reduce the likelihood of above mentioned failures, the following criteria should be met:

- Mold design should be compatible with the mold material selected for that and with the required planned procedure.
- Perform the appropriate heat treatment procedure for the steel used in the mold structure.
- Use high hard P20 steel where the plastic material is very abrasive.
- Control of all finishing operations. Surface finishing is a broad range of industrial processes that alter the surface of a manufactured item to achieve a certain property. Finishing processes may be employed to: improve appearance, adhesion or wettability, corrosion resistance, wear resistance, hardness, and other surface flaws, and control the surface friction.
- Controlling mold operation specifically over loading.

1.7 Mold maintenance

Maintenance can be defined as the necessary activities that are performed to keep the equipment in specific working conditions. Mold maintenance is performed with the objective of maximizing the equipment availability in its working condition to achieve the desired output quality. Maintenance should be realized in a cost effective way and

conform to safety and environmental regulations [10]. Mold maintenance can be classified in to two categories:

1. Scheduled or preventive maintenance (PM).
2. Corrective maintenance (CM).

PM is conducted to decrease the failure probability of a certain system, which involves adjusting operation parameters and repairing or replacing a component of the system before the system breaks down. Preventive replacement describes the action done during a PM.

CM is the action to be taken on the system immediately up on its failure to restore it back to its desire functioning condition. The frequency of conducting CM is not deterministic. The system is subjected to many factors during its operation. Fatigue cycle properties of components and operating parameters are just some examples of factors that makes CM forecasting complex. Failure replacement describes the action done during a CM.

While performing preventive maintenance, it is important to identify the components, which should be considered for replacement even if they still appear to be in perfect condition or components which can be allowed to run until the next PM.

There are four basic maintenance policies

1. Failure base maintenance (FBM).

FBM is a corrective maintenance which is prescribed only on occurrence of failure.

2. Use based maintenance (UBM).

UBM assumes that failure behavior is known following a trend of increasing failure rate since the previous maintenance.

3. Condition based maintenance (CBM).

CBM assumes that there exists a system parameter that can be used to predict the failure behavior. It is activated when the value of a given system parameter reaches or surpasses a preset value.

4. Opportunity based maintenance (OBM) Failure of one component gives the chance to carry out preventive maintenance on other components which have not failed yet.

Problem Description

In today's mold industry, in spite of the many simulation options available, initial stock block sizes are dimensioned based on a trial and error method. Only a small percentage of mold manufacturers employ simulation software to validate their mold designs, and typically this focuses on material flow and cooling challenges. Most of this market is not benefiting from the advantages offered by simulation options targeting the basic mold design. Although trends have increased within companies to familiarize themselves with these types of software, the high cost of simulation software tools, and inaccessibility to experienced and qualified work force to utilize them has been always an issue. In the following pictures, the current trial and error method for dimensioning the block sizes has been displayed.

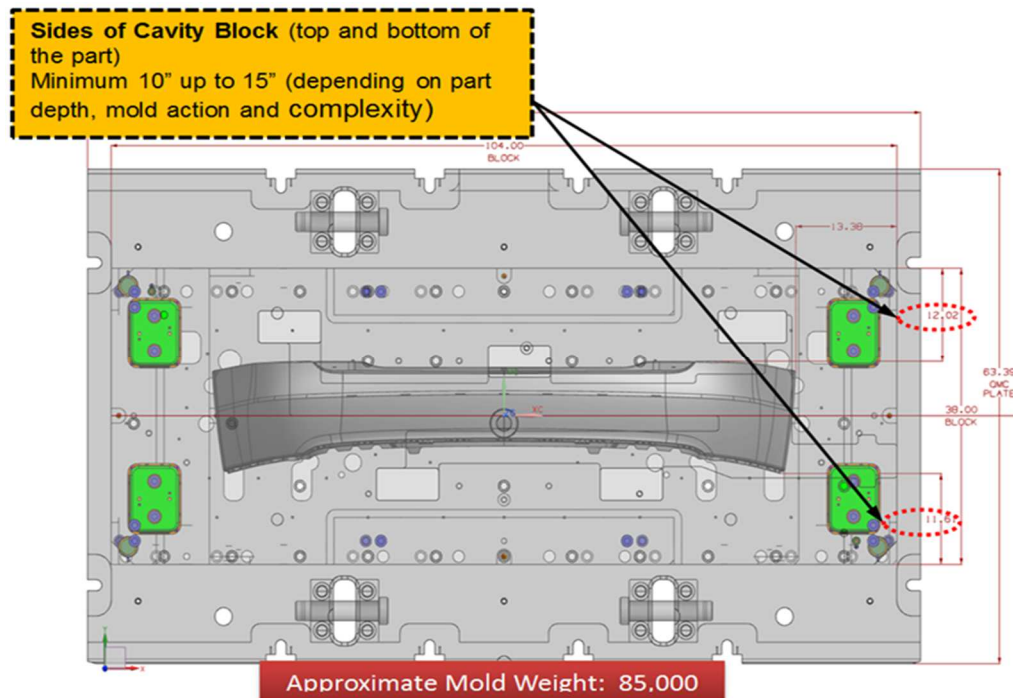


Fig 1.5 Front view of a cavity block illustrating the size and complexity of a standard application (all dimensions are in inches)

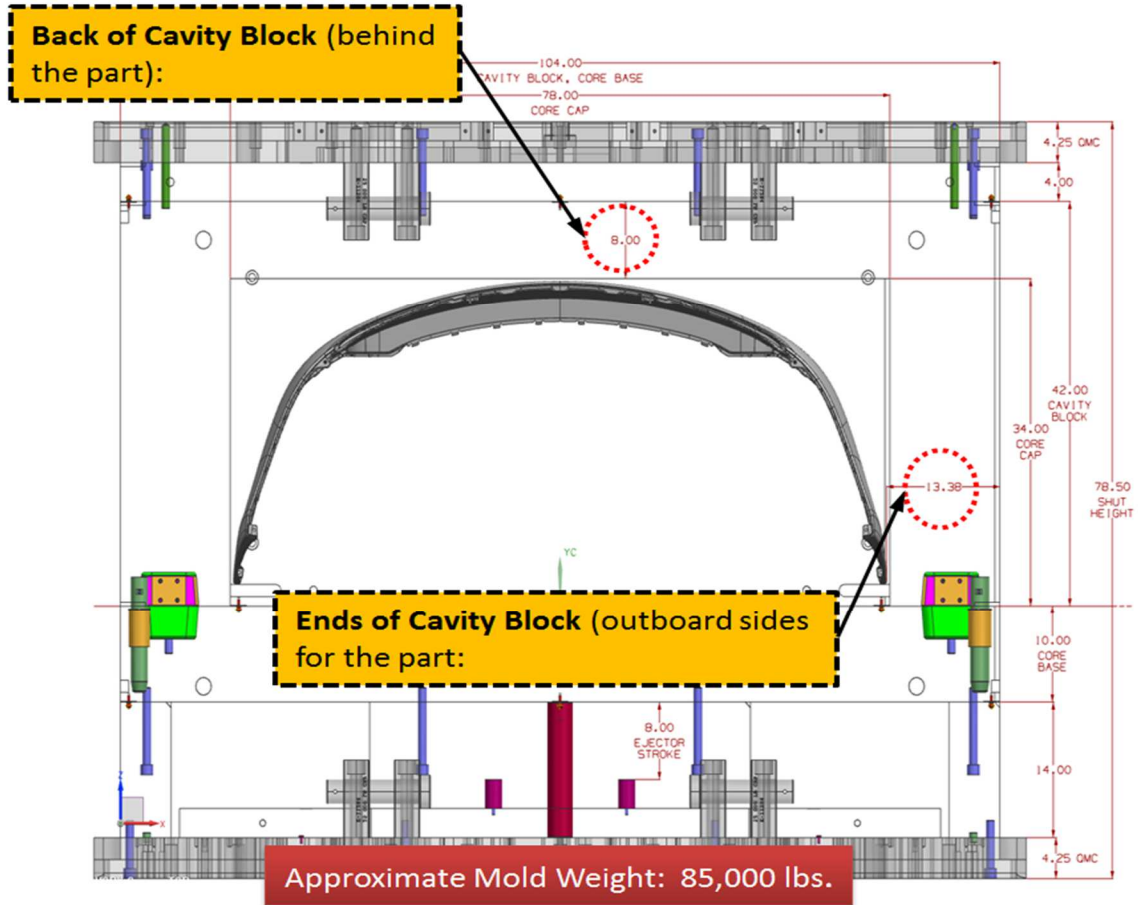


Fig 1.6 Top view of the cavity block (all dimensions are in inches)

Objective

The main purpose of this research is to redesign and manufacture a mold that has been structurally optimized for specific load cases while reducing its weight, based on topology optimization results. The Optistruct software is employed in this research. Maximizing the stiffness of the structure, with constraints on the volume fraction while reducing the weight and overall size of the structure is the primary objective of this research. Key to this goal is validating this optimization process with experimental data to correlate the simulation and experimental results. The methodology of topology optimization is used to reach to the optimized structure. Following the steps below (Table 1.2) will lead us to our objective.

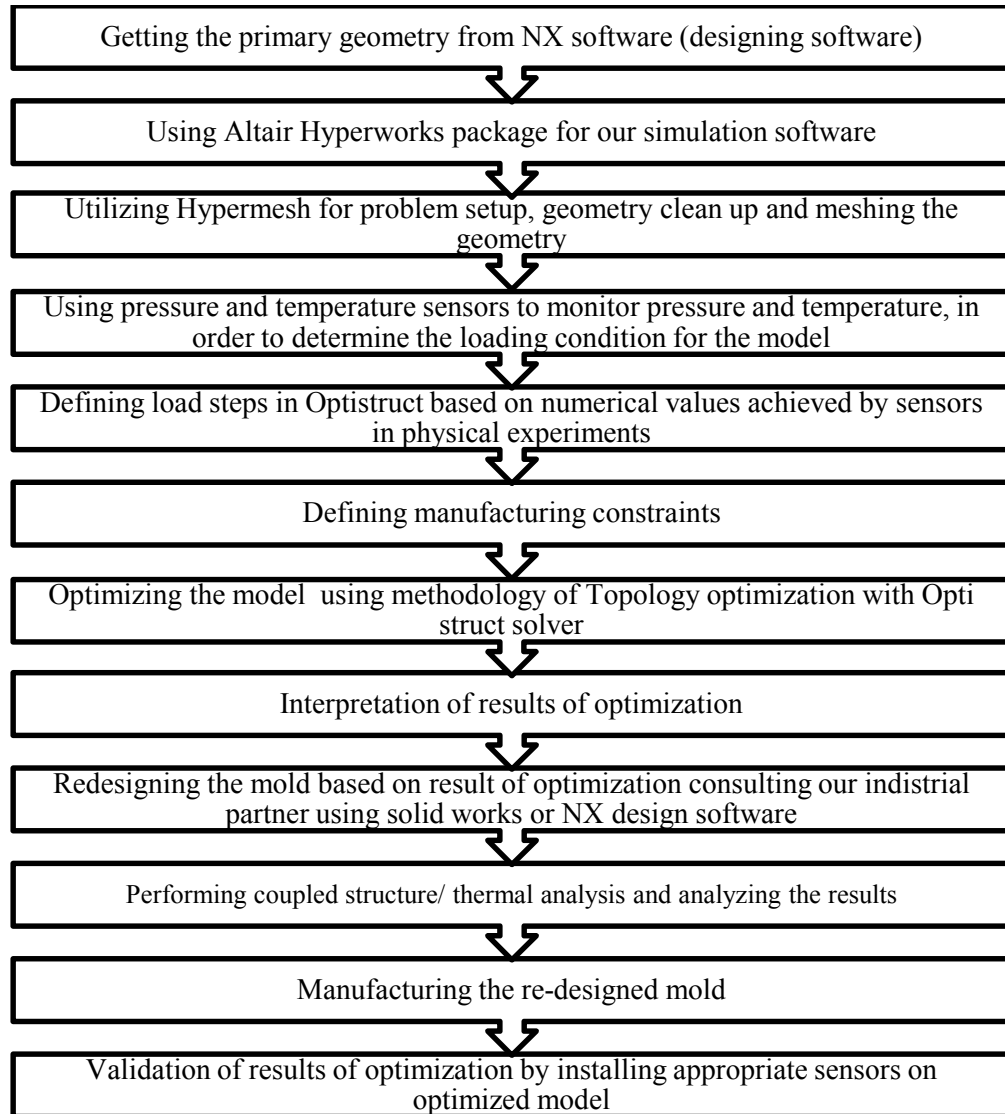


Table 1.2 Steps of project

Each step is elaborated in the following chapters. In chapter 2, a literature review, which summarizes the research focus for mold design and methodology of topology optimization are presented. The simulation strategies and a 2D topology optimization problem are presented in chapter 3. The model description, analysis set up and topology optimization are discussed in chapter 4. A coupled heat thermal/structure analysis is carried out, and presented in chapter 5. How the theory comes to practice (validation), summary, conclusions, and future work are represented in the last chapter 6.

CHAPTER 2

LITERATURE REVIEW

This chapter focuses on literature review of related work to plastic injection molding, mold design and optimization, mold weight reduction, structural optimization and coupled heat structure analysis of structures.

2.1 Plastic injection mold design

Michaeli et al, W in 2004, presented an approach in details to mechanical design of injection mold with the aid of FEA. They performed calculation of mold filling and mold deformation by linking injection molding simulation to FEA package [11]. Alaneme in 2009 investigated the failure analysis of the mold, which showed that the short service life of the die component is due to incorrect heat treatment which did not remove the cold worked structures [12]. Dong-Gyu Ahn in 2010, investigate into manufacturing a high energy efficiency mold using a rapid manufacturing process hybrid RM process combining direct metal rapid tooling [13].

2.2 Plastic injection process optimization

In 2004, Chen, W et al, combined numerical simulation software, genetic algorithms and multilayer neural networks to optimize process parameters considering parameters such as mold temperature melt temperature, injection time and injection pressure[14]. Zongbao Chen and Lih-Sheng Turng in 2005 searched in regards to quality control of injection molding. They organized prior studies into four categories process setup, machine control, process control and quality control [15].

2.3 Plastic injection mold weight reduction

There is no published research directly related to mold weight reduction strategies.

2.4 Structural optimization

The foundation of structural optimization dates back to 1904, when Michell found a formula for structures with minimum weight given stress constraints on design domain of trusses[16] . In 1985 Ringertz worked on topology optimization of trusses for

minimization of weight subject to stress and displacement constraints [17]. In 2007, Achtziger and Stolpe used a branch-and-bound method to find the globally optimal solution to truss topology optimization problems [18]. Karakaya and Soykasap 2011, used a genetic algorithm to optimize composite plates which is an example of 1D topology optimization problem[19]. The disadvantage of genetic algorithms for topology optimization is that they become prohibitively expensive for large systems [20]. Kemin Zhou in 2011, presented a method to minimize structural volume under stress constraints subject to multiple load cases for trusses.

Denghong Xiao in 2012, used Topology optimization methodology to generate robust electric bicycle main frame which was an example of 3D topology optimization problem with volume fraction constraint but the industrial application and validation of the achieved results has not been assessed.

2.5 Thermal analysis and design of plastic injection molds

S.H. Tang et al in 2006 present the design of a plastic injection mold and performing thermal analysis for the mold. Their main objective in thermal analysis of the mold was analyzing the effect of residual stress on product dimension. The thermal analysis of plastic injection mold has provided an understanding of the effect of thermal residual stress on deformed shape of the specimen [21].

The literature related to this research is summarized in Table 2.1.

2.6 Table of literature review

Authors	Topology optimization	Mold mass/weight reduction	FEA analysis	Minimum compliance	plastic injection molding	Mold design	Volume fraction	Threshold value	Coupled heat/structure analysis	Comments
Michaeli, W (2004)			✓		✓	✓				Presents an approach in details to mechanical design of injection mold with the aid of FEA and performing calculation of mold filling and mold deformation by linking injection molding simulation to FEA package
Dong-Gyu (2010)					✓	✓				Investigation into manufacturing high energy efficiency mold using rapid manufacturing process
Ling, Z (2010)					✓	✓				A method is proposed for multi objective optimization design of mold platen with help of FEA and neighborhood cross section genetic algorithm (NCGA) to improve structure performance of mold platen
Villarreal (2011)					✓	✓				This paper presents a research aimed at creating a virtual plastic injection molding (VPIM) environment, which is designed and implemented based on techniques such as virtual Reality(VR), multidiscipline simulation, and scientific visualization.
Abul B (2010)					✓	✓				Cooling channel of mold with copper tube inside has been examined and FEA thermal analysis has been performed with ANSYS simulation software. Mold Flow has been used to get process parameters for analysis
Yongqing Fu (2013)	✓			✓			✓	✓		In this paper, an optimization approach for black-and-white and hinge-removal topology designs is studied.
Asger Nyman (2014)	✓			✓			✓			Present a method for automatic generation of 3D models based on shape and topology optimization.

Authors	Topology optimization	Mold mass/weight reduction	FEA analysis	Minimum compliance	plastic injection molding	Mold design	Volume fraction	Threshold value	Coupled heat/structure analysis	Comments
Hyun-Jun Kim (2010)	✓			✓			✓	✓		A topology optimization program, which is based on the C language is developed in this study
Gilles Marck (2013)	✓		✓						✓	The design of efficient structure for heat and mass transfer problems involves the implementation of topology optimization
SUN RuJie (2013)	✓			✓						The procedure of airfoil optimization is carried out. On the basis of the combination of design of experiment (DOE), response surface method (RSM) and genetic algorithm (GA)
Erik Holmberg (2014)	✓		✓	✓						Present topology optimization problem with fatigue constraints.
Thomas A. Reist (2010)	✓		✓	✓			✓			Application of topology optimization to prosthetic design, and details the structural optimization of a new prosthetic knee joint
Denghong Xiao (2012)	✓		✓	✓			✓	✓		Topology optimization technology is applied to generate robust electric bicycle main frame
Krishnan Suresh (2012)	✓		✓	✓			✓			Introduce an efficient algorithm and implementation for large-scale 3-D topology optimization.
Chien-Jong Shih (2010)	✓		✓	✓			✓	✓		A practical integrated topology design optimization of minimizing compliance with the empirical Von Mises stress constraint is presented in this paper.
X. Huang (2010)	✓		✓	✓			✓	✓		This paper shows the possibility of solving any topology optimization problems with multiple constraints using the BESO method
Kemin Zhou (2011)	✓			✓						Present a method to minimize structural volume under stress constraints subject to multiple load cases.
Dongmei Li (2010)	✓								✓	In this paper, the sequential coupling method is used to solve the equivalent nodal temperature load, which is regarded as the physical force load imposed in the elastic field.

Authors	Topology optimization	Mold mass/weight reduction	FEA analysis	Minimum compliance	plastic injection molding	Mold design	Volume fraction	Threshold value	Coupled heat/structure analysis	Comments
Alaneme (2009)						✓				Failure analysis of mold, showed that the short service life of die component is due to incorrect heat treatment which did not remove the cold worked structure
Dong-Gyu Ahn and Hyun-Woo (2010)						✓				Investigate into manufacturing high energy efficiency mold using rapid manufacturing process
Ling, Z (2010)						✓				They proposed a method for multi objective optimization design of mold platen with help of FEA
S.H. Tang (2006)									✓	Present the design of a plastic injection mold and performing thermal analysis for the mold.

Table 2.1 Summary of literature review

CHAPTER 3 METHODOLOGY

3.1 FEA analysis

Finite element analysis (FEA) is a technique that is used to obtain numerical solution for engineering problems with complex nature that are difficult or sometimes impossible to be solved analytically. It is important to note that FEA is a simulation tool and is not reality. In general, the reality of problem dynamics is described by geometric model whereas the simulation is conducted on the mathematical model. A mathematical model is an idealized model in which the geometry, material properties, loads and boundary conditions are simplified. For instance, distribution of load over a small area may be considered as concentrated force applied on a point which in reality is not possible or a support might be considered fixed although there is not any totally rigid support. FEA is basically applied to a mathematical model. FEA analysis has four basic steps. The first step is discretizing the CAD model into discrete elements (a mesh). The model is discretized by dividing into a mesh of finite elements and numbering the nodes that would define these elements. The second step involves determining matrices that describe the behavior of each element. The third step is combining these matrices in to a large matrix equation and solving this equation to determine the values of field quantities at the nodes. When the equations are solved in some cases, for instance mechanical problems, stresses are of interest in addition to the displacement. These are calculated after solution of the global equation system. The last step engages the checking of the results. The results should be examined to insure they are consistent with the physics of the problem. This step is performed by post-processing functions of FEA software which show the results graphically [22].

3.2 Structural optimization

A structure in mechanics science is an assemblage of material that is supposed to sustain a load. Structural optimization refers to designing and fabricating that structure to carry loads in the best way possible. In this methodology, the model is modified iteratively to accomplish the objective and satisfy the constraints. Different objectives

such as mass, stiffness, etc can be considered for optimization of the structure. In order to achieve the pre-determined objective some constraints and limitations are needed to be defined. In a structural optimization problem, the following functions and variables are defined:

1. Objective function (f), is a function that should be maximized or minimized
2. Design variables (x), is a controllable parameter defined by the designer. They can be anything that affect the performance of structure such as thickness, etc. Moreover, they are usually bounded by maximum and minimum values.
3. Response, for any given values of the design variables there is a response from the structure. Responses are used to evaluate the performance of the structure. Examples of responses are displacement, volume fraction and compliance.
4. Constraint is a condition which must be satisfied. Design variables and responses should be constrained with minimum and maximum values to make sure that the performance of the structures is in the allowed interval. Typical constraints are maximum allowable mass and displacement or minimum allowable stiffness.

In general, structural optimization problem determines the optimal value of design variables x in a way that maximizes or minimizes the objective function, f , and satisfies the defined constraints. There are three types of structural optimization problem based on Christensen and Klarbring [23]. The kind of optimization that is performed depends on properties of design variable.

Size optimization:

Size optimization is the simplest type of optimization. In this type of optimization the shape of the structure is known and the objective is optimizing the structure by adjusting sizes of the components. Size of structural elements such as, thickness of structure or cross section area of beams, are design variable in this kind of optimization. In this optimization there is a predefined structure and the size of its member should be optimized [23].

Shape optimization:

In shape optimization, design variables are considered as parameters which control the shape of the structure for instance diameter of holes radius of fillets. No new boundaries and no new holes can be added in this type of optimization.

Topology optimization:

It is a technique that optimizes material of the structure in a specific domain. In topology optimization, the structure is free to have any shape in the given design domain [3]. The shape of the structure is not known. This subject will be discussed with more details in section 3.3.

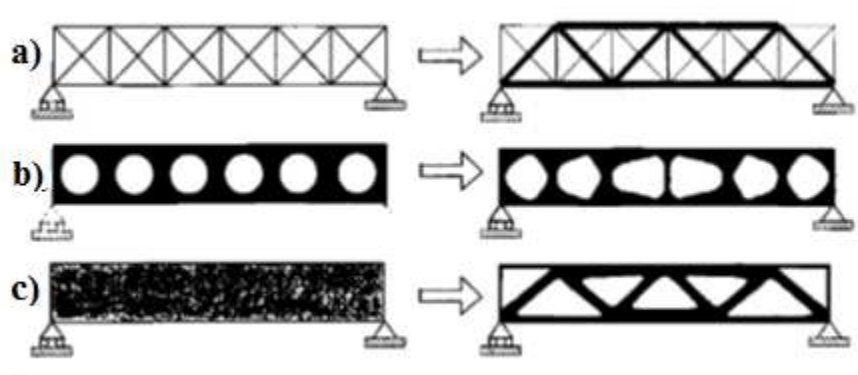


Fig 3.1 Three categories of structural optimization a) Sizing optimization of a truss structure, b) Shape optimization and c) Topology optimization. The initial problems are shown at the left and the optimized solutions are shown at the right [3]

3.3 Topology optimization:

Topology optimization is a mathematical technique that optimizes the material layout in a given design domain. The goal is to find the best layout for the structure that is subjected to the load and defined constraints. Topology optimization carries out the structural optimization by indicating where the material can be removed. The only known values in this kind of problems are the loads and the condition of supports. There are two main approaches for the solving topological optimization problem: the homogenization method and density method. Most of topology optimization software tools use the density method. The density method is also adopted in Optistruct 12 and it is

employed to perform topology optimization in this thesis. Interested readers are referred to references [19]and[24] for more details in regards to other solution approaches for the topological optimization problem.

In the density method a density field of $\rho(x) \in [0,1]$ is defined in the design domain. The topological optimization problem is changed to a problem of an optimal distribution of material density. In spite of the mathematical convenience of the density method it has some weaknesses. Existence of intermediate density values in the structure is one of the most important inconveniences of this technique. For the continuous structure these intermediate density values which result in intermediate stiffness values are meaningless in a design. Element densities should be either zero or one. So to have a manufacturable design it is desired to have only solid (element density equal to one) or avoid (element density equal to zero) in the structure. The majority of density based methods use the SIMP (Solid Isotropic Material with Penalization) method scheme that favors the configuration of zero or one in the structure. This method scales up the design variable (relative density of elements) in regions with high strain energy and scales down the design variable in regions with low strain energy and iteratively creates a new distribution of stiffness in the structure. The SIMP uses the following scheme [25]:

$$\hat{K}(\rho) = \rho^p K \quad (3.1)$$

Here \hat{K} is the penalized stiffness and K is the original stiffness matrix of an element. ρ shows the element density and p the penalization factor (usually $p = 3$) . This method makes material with intermediate stiffness values too expensive, since its volume depends linearly in ρ [26]. The penalization factor is always greater than one and it is usually measured between two and four. This factor is controlled by Optistruct by default. This value is increased iteratively in order to get a more discrete solution. The basic formulation of the topology optimization of minimizing compliance and constrained volume removal is described as follows [27]:

$$C = F^{-1}U \quad (3.2)$$

Here C is the compliance of structure, U is displacement vector and F is the force vector. The strain energy of a structure is defined as

$$S = \frac{1}{2}UF \quad (3.3)$$

Accordingly, under the same loading condition F minimizing S is equivalent to minimizing the formation U or maximizing the stiffness. As a result minimizing compliance means minimizing strain energy in a structure.

$$\begin{aligned} \text{Objective:} \quad \text{Min } C &= (K \cdot U)^{-1}U = \sum_{i=1}^N \frac{u^i}{k^i u^i} \\ &= \sum_{i=1}^N \frac{u^i}{(x^i)^p u^i k_0} \end{aligned} \quad (3.4)$$

$$\text{Subject to:} \quad V = \sum_{i=1}^N x^i v^i \leq V_0 - V_* \quad \text{or}$$

$$VOF = \frac{\sum_{i=1}^N x^i v^i}{V_0} \leq \frac{V_0 - V_*}{V_0}$$

$$KU = F$$

$$k^i = (x^i)^p K_0$$

$$0 < x_{min} \leq x^i \leq x_{max} < 1$$

In above formula K is the stiffness matrix, N is the number of elements in the structure, u^i displacement vector of the node, K_0 is the original stiffness and k^i is the stiffness of optimized element. V is the volume of optimized structure, V_0 is the original volume of the structure, V_* volume of removed material, VOF is the volume fraction (optimized volume divided by the original volume, v^i the element volume after performing optimization, x_{min} and x_{max} are the lower and upper bound of element density respectively. x^i is the design variable of each element between zero and one. p is the penalization factor that decreases the intermediate density elements. p is usually equal to 3 for 3D elements. However, in some more complex structures the penalization scheme is not always evident and there still exist some intermediate density elements. Engineering judgment is required to decide to eliminate or to keep the intermediate

density elements. This interpretation can result in a non-optimal structure. Consequently it is necessary to perform FEA analysis on the interpreted geometry as well to see if the expected result is achieved or not. In this project, the methodology of topology optimization was used to maximize the stiffness of a linear elastic structure guided by a constraint on the volume fraction. That leads to optimizing the material layout and weight reduction of mold.

3.4 Software Selection

An important step to solve the optimization problem is to choose the proper optimization solver. The Hyperworks package contains Hypermesh, a preprocessor that is used for meshing the CAD geometry setting boundary conditions, material properties and generally problem set up for optimization, static analysis and other analysis. It also contains an FEA solver called Optistruct that is used to perform structural optimization. Optistruct is very capable, and different types of FEA analysis can be performed utilizing it, such as static analysis and thermal analysis. Optistruct runs the optimization and modifies the model to achieve the objective given. Optimization with Optistruct can be performed on 2D and 3D models. Hyperview is a post processor in Hyperworks package which is used to evaluate the results. Abaqus is another powerful finite element software which is capable of doing even computationally heavy finite element analysis problems but the standard Abaqus package does not contain a structural optimization solver. There are some packages which can be used along with Abaqus to perform the structural optimization but we didn't have access to them. Therefore, Optistruct was selected for doing the structural optimization.

3.5 SIMP method in Optistruct

In Optistruct usually, the penalization factor P is set to $P = 2$ for shell elements and $P = 3$ for solid elements. When manufacturing constraints are applied the value of P is increased to 3 or 4 [28]. The procedure of topology optimization in Optistruct for minimizing the compliance problem for a specified volume fraction is as follows:

1. At first a homogeneous distribution of density is applied to elements within the design space
2. A volume constraint is applied

- Alternatively the densities are updated based on the previous iteration. Element densities are scaled up for elements with high strain energy and densities are scaled down for elements with low strain energy.
3. For the applied density distribution, FEA analysis is performed and nodal displacements are achieved
 4. The compliance and the corresponding sensitivity of the design variables are calculated and the compliance modification with respect to the objective function is tested.
 5. If the obtained decrease in the compliance is less than the convergence criterion, iteration is stopped. Otherwise the iteration is repeated.

The solution in Optistruct consists of all the elements of design space. However, densities are scaled varying in the range of 0 and 1. The user should determine the threshold density to print out the structure (a random value is assigned to threshold density set by user) [29].

3.6 A trial case for 2D Topology optimization problem

In this example, topology optimization is performed on a model to create new topology for the structure and to remove the unnecessary material from the primary structure. A C-clip is tested in this study. The resulting structure is lighter and satisfies all design constraints. This study is performed theoretically and experimentally and analysis is performed for the original models and optimized ones.

3.6.1 Optimization with Optistruct (software level)

The main parameters are defined as following:

- a. Objective function: Minimizing the volume fraction
- b. Constraints: Displacement at nodes where loads are applied must not exceed 4×10^{-4} (m) in the Z direction
- c. Design variables: Density of each element in design space

The C-clip is demonstrated in figure 3.2. It is a squared shape piece with an opening in the middle of it. This is a 0.1m by 0.1m specimen with 0.018 m thickness. The

Hypermesh software was utilized to set up the optimization problem and the Optistruct solver was used to solve the problem.

The first step was to determine the design domain, optimized domain, and non-design domain, the area that remains unchanged. The design domain and non-design domain are displayed in figure 3.2. The geometry was then meshed. In the next step, a particular type of material should be assigned to the model. Then, loads and constraints were applied on the model. A load equal to 50 N was applied to 60 points that is equal to 3000 N. Constraints were applied on both top part and bottom part of the C-clip. The meshed model loads and constraint are demonstrated in figure 3.2.

Basic FEA was performed and the displacement contour for original model and optimized model is demonstrated figure 3.3 and figure 3.5, respectively. The result of optimization is also shown in figure 3.4.

1. Original C-clip

The following figure shows problem set up for this problem. Non-design spaces are designed to fit the jaws of the tensile test machine.

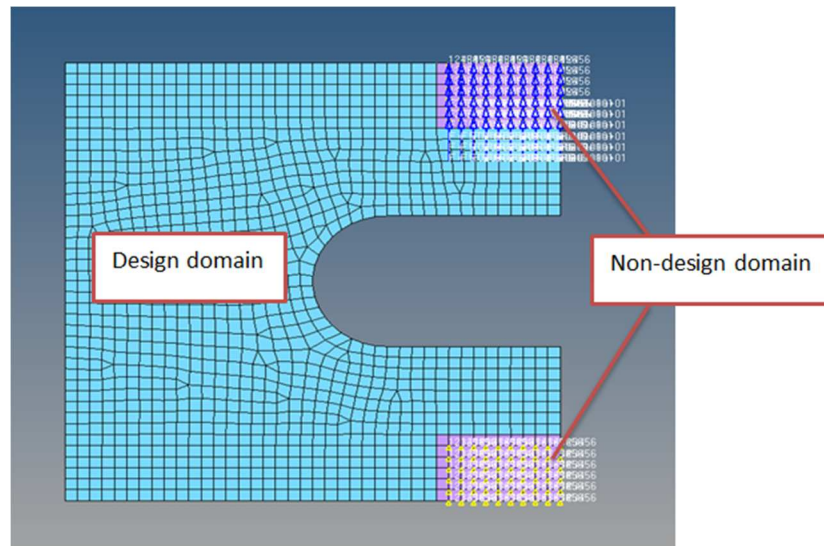


Fig 3.2 Topology optimization problem set up (yellow triangles are constraints and applied loads are demonstrated with blue arrows)

Displacement contour for original C-clip

A basic FEA was performed on the model. For the applied loads and constraints, the resultant displacement contour is demonstrated in figure 3.2.

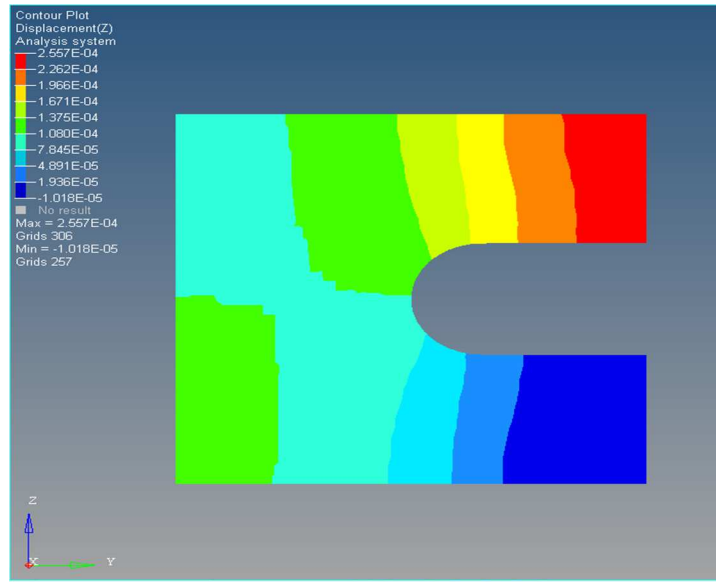


Fig 3.3 Displacement (m) contour for the original c-clip along Z axis each color corresponds to a range of displacement (m), varying between $1.0 \text{ E-}5 \text{ m}$ and $2.6 \text{ E-}4 \text{ m}$

2. Optimized C-clip

The element density contour plot is displayed in figure 3.4. Optimization was carried out and optimized geometry was achieved based on element density contour plot. Blue domains are elements with a density equal to zero and red domains are elements with density equal to one. The remaining elements are intermediate density elements with a density between zero and one. The user have to decide about these elements.

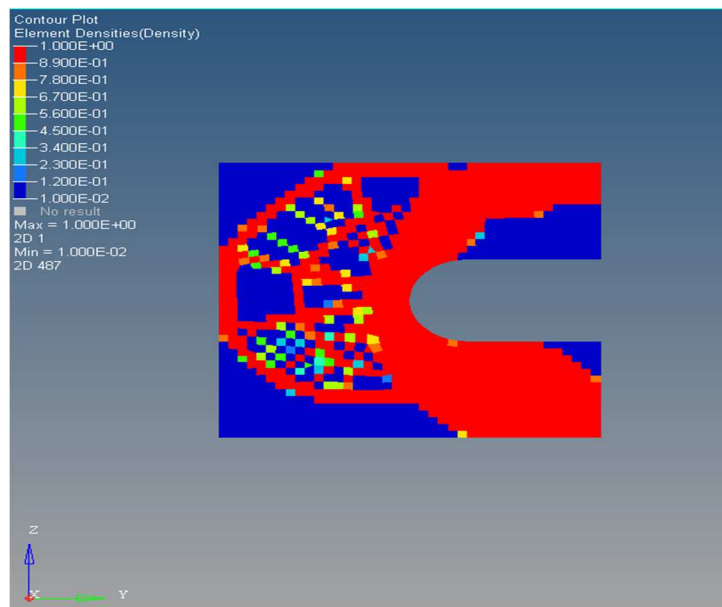


Fig 3.4 Element density contour plot

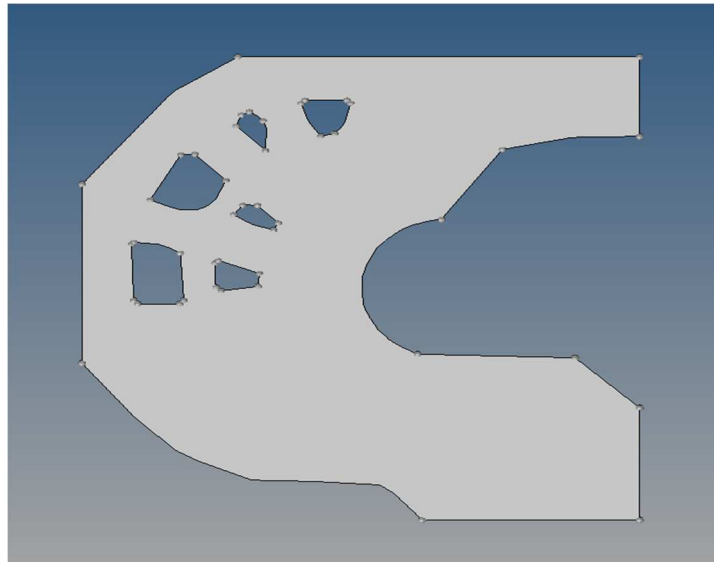


Fig 3.5 Optimized model of c-clip after performing topology optimization

Displacement and Von Mises stresses contour for optimized C-clip

The displacement contour for the optimized geometry in figure 3.6 shows that the optimization has satisfied the constraint and material was removed in a way that the displacement of the optimized model for predetermined load case didn't exceed 4×10^{-4} (m). Von Mises stress contour is displayed in figure 3.7.

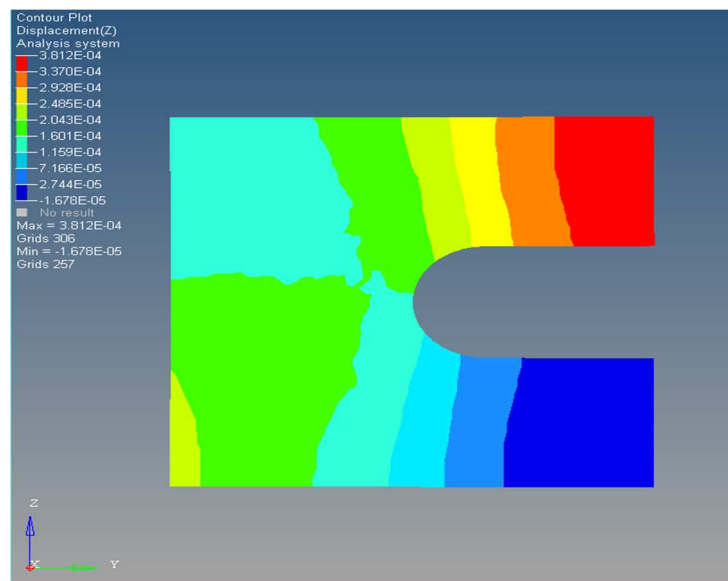


Fig 3.6 Displacement (m) contour for the optimized geometry, each color corresponds to a range of displacement (m) varying between $-1.6 \text{ E-}5 \text{ m}$ and $3.8 \text{ E-}4 \text{ m}$

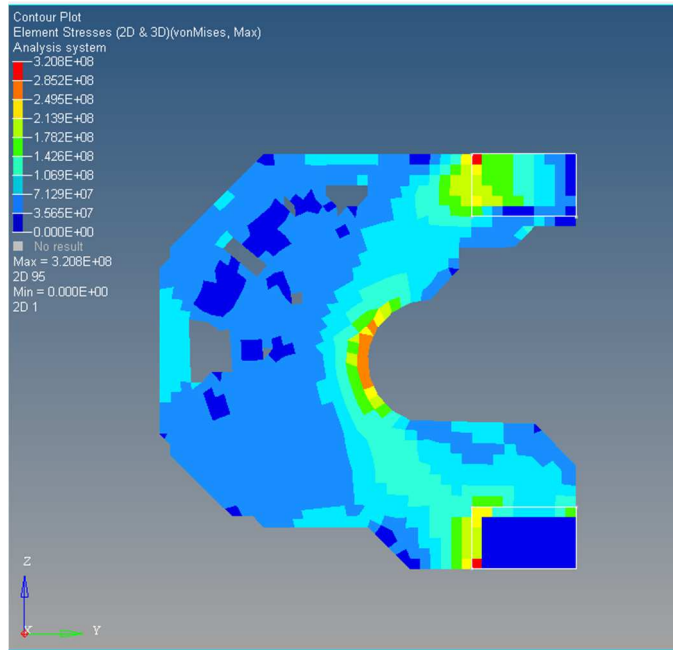


Fig 3.7 Von Mises stresses (Pa) contour for the optimized geometry

Results:

In this example, the load case of 3000 N was applied to the structure and it was predetermined that the displacement of $4 \times 10^{-4}m$ is critical. Hence, this value was defined as a constraint for displacement at points where load was applied. It was desired to analyze reduction in the volume fraction of the structure while the displacement of new structure had constrained to $4E - 4m$. The optimization results showed 28% weight reduction for the optimized structure.

	Original c-clip	Optimized c-clip	weight reduction
Weight	0.125 kg	0.090 kg	28%

Table 3.1 Original and optimized c-clip weight comparison

3.6.2 Experimental tests

In order to validate the results of optimization, physical specimens of primary CAD model and optimized model were built from cold rolled steel sheet with average elastic module of $2 \times 10^{11} \text{ N/m}^2$. Specimens were tested with a tensile test machine. The specimens were cut with EDM machine and were subjected to controlled tension. The Instron tensile test machine was utilized to perform the tensile test.

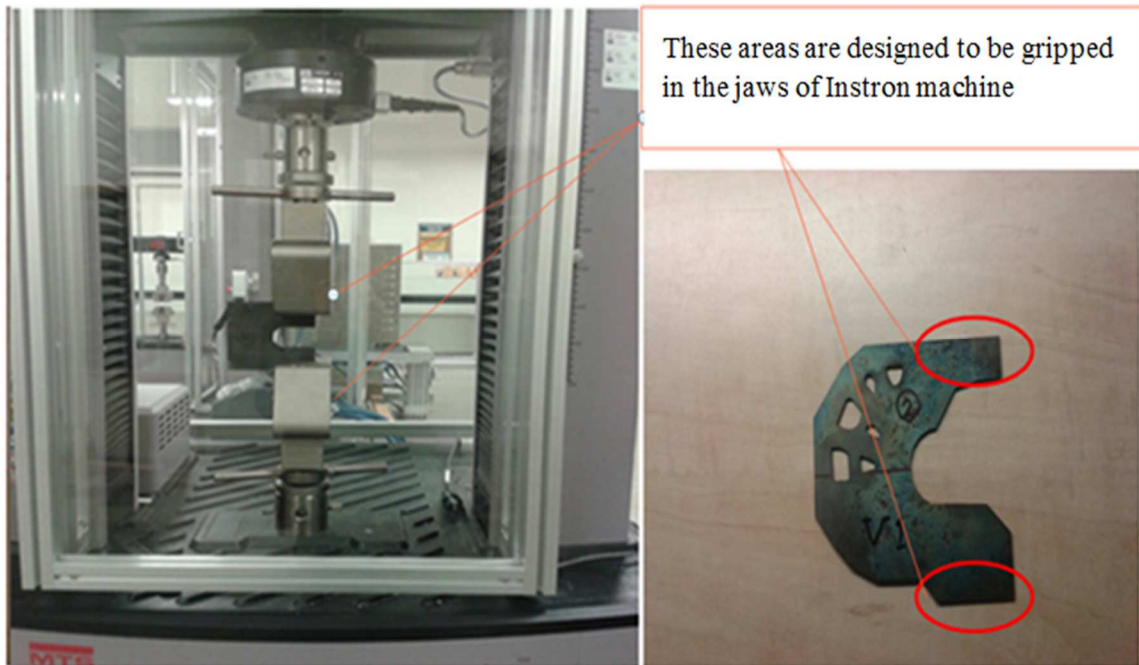


Fig 3.8 C-clip in tensile test machine (Instron)

The test was conducted for the original model and three variation of the optimized model with three different ISO values (normalized element density values between zero and one) of 0.15, 0.3 and 0.6. The manufactured specimen with ISO value of 0.15 shows satisfactory results and less error in comparison with other specimens (The design determined for the iso 0.15 configuration is shown in Figure 3.8). The iso surface presentation is a normalized value between zero and one and it is used to display the concept design of topology optimization results with respect to different element density values. For instance, zero density elements refer to elements without any structural relevance. These elements will be removed from the structure whereas the elements with

density of one refer to elements which bear load in the structure and have to be maintained within the structure. There are also some elements with intermediate density values which the analyst should decide about the existence or removal of them, using an appropriate user-determined iso value. Elements with density above the specified iso value are treated as elements with density of one and would maintain in the structure and elements with density below that iso value are accounted for as elements with a density of zero and are removed from the structure. For instance by specifying the density threshold of 0.3, on the one hand elements with the density of 0.1 or 0.2 or even 0.29 are considered as zero density elements and are removed from the structure however, these elements do have some structural relevance. On the other hand elements with density above the iso value are considered full density elements.

Conventionally, the user specifies the iso values based on engineering judgment. However, there might be a gap between what the theory suggests and what really works in practice. Therefore, in many cases, the iso values picked based on engineering judgment satisfies the constraint in theory, but it might not necessarily lead to a structure that fulfills the predetermined constraint in practice.

Each test was repeated twice; therefore; eight tests were conducted in total. The load was applied with the rate of 0.5 mm per minute to obtain a smooth loading condition. The specimens were fastened into the jaws of Instron machine as demonstrated in figure 3.7. The non-design spaces of specimens (purple areas) were fixed tightly in top and bottom jaws to provide the exact condition of model simulation in Optistruct. The physical test results were analyzed for 3000 *N* load case.



Fig 3.9 Optimized model with iso value of 0.15

Test results for original C-clip and optimized C-clip

1. Original C-clip

The load-displacement table and diagram for original model are given as following:

Cross head (mm)	Load (N)	Time (s)
0.001	17.30	0.23
0.002	24.80	0.34
0.002	32.74	0.44
0.003	41.31	0.54
.	.	.
.	.	.
.	.	.
0.317	2994.76	38.23
0.318	3004.48	38.33
0.319	3009.27	38.43
0.320	3018.95	38.52
.	.	.
.	.	.

3.00	5443.32	360.34
3.00	5442.67	360.44

Table 3.2 Displacement changes based on load and time for original C-clip

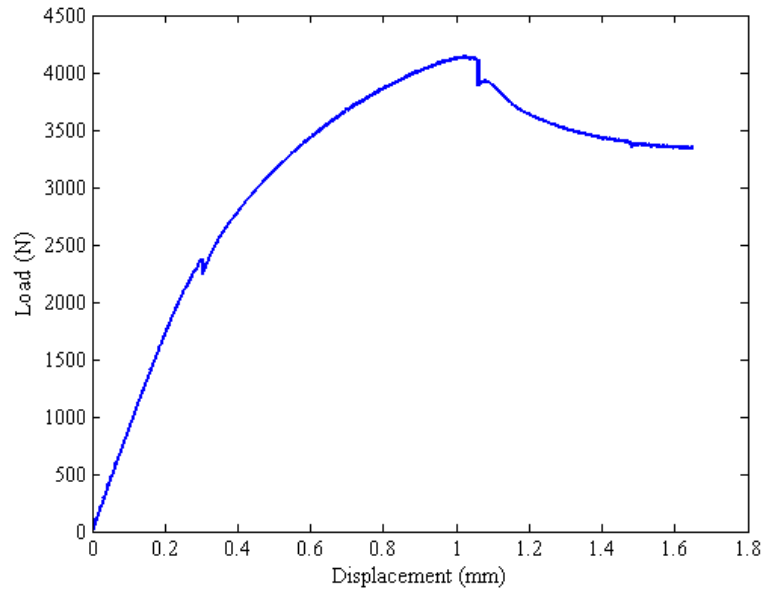


Fig 3.10 Load-displacement diagram, original c-clip

2. Optimized C-clip

The load-displacement table and diagram are as follow

Cross head (mm)	Load (N)	Time (s)
0.00	4.73	0.14
0.001	12.54	0.23
0.002	19.47	0.34
0.003	26.93	0.43
.	.	.
.	.	.
.	.	.
0.45	2995.53	54.84

0.45	2999.17	54.93
0.45	3002.55	55.04
0.45	3007.73	55.13
.	.	.
.	.	.
1.64	3342.58	198.13
1.65	3340.88	198.24

Table 3.3 Displacement changes based on load and time for optimized C-clip

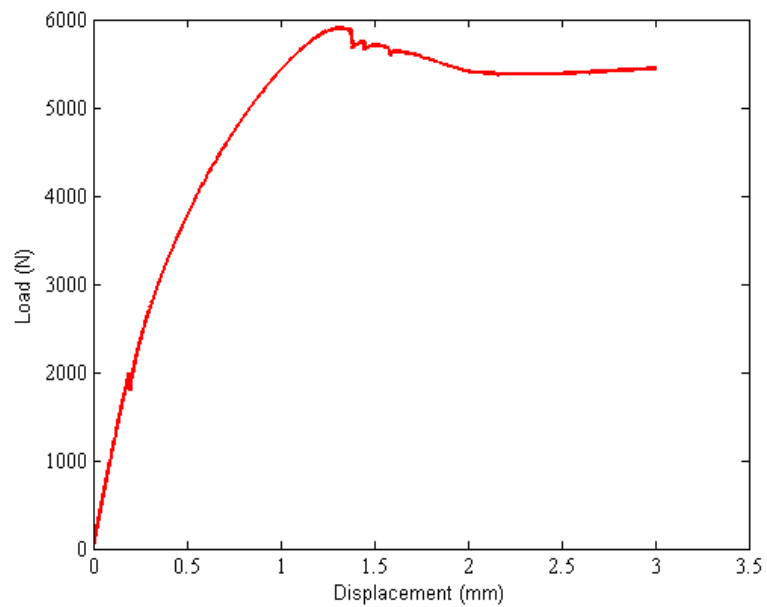


Fig 3.11 Load-displacement diagram, optimized c-clip

Results and discussion:

Table 3.4 compares the theoretical results and experimental results for the load case $F = 3000\text{ N}$.

		Displacement (m)	Error
Original c-clip	Theory	2.5×10^{-4}	24%

	Experiment	3.1×10^{-4}	
Optimized c-clip	Theory	3.8×10^{-4}	18%
	Experiment	4.5×10^{-4}	

Table 3.4 Numerical values of theoretical and experimental displacement for original and optimized c-clip and the calculated error

Discrepancies between theoretical result and experimental result might arise due to different factors such as: difference between mathematical model and physical model (loads are simplified and boundary conditions are idealized), inaccurate material assumption compared to the real material, an inaccurate load application to the specimen which leads to a combined state of tension and bending in the test specimen, error between cross head travel vs extensometer measurement and etc. The key output is that the results are consistent, so a calibrated model can be leveraged.

3.6.3 Geometry extraction for 2D topology optimization problem, based on experiment

It was realized that in experiment test, for the specimen with iso value=0.15, the maximum displacement (4.5×10^{-4}) has exceeded the test limit (displacement at nodes where loads were applied should not exceed 4×10^{-4} m). However, we are looking for a geometry that can satisfy the constraint in physical testing so we have to find a way to extract that reliable geometry.

The theoretical and experimental displacements based on iso values were plotted in a diagram and the appropriate iso value based on experiment was extracted by extrapolating. The geometry based on new iso value is demonstrated in next figure. Based on the following diagram, it can be concluded that for any iso value less than 0.096 we are in the safe zone.

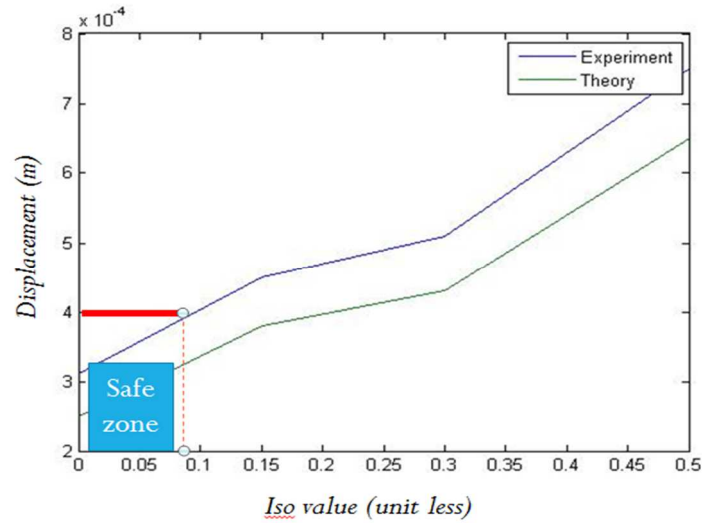


Fig 3.12 Displacement- iso value diagram for theory and experiment tests

3.6.4 Comparison between resultant geometry from theory and experiment

The optimized geometry from result of theory is depicted in figure 3.12 and updated geometry with new iso value is shown in figure 3.13. Weight comparison between original and optimized c-clip for both theory and experiment are presented in tables 3.5 and 3.6 respectively.

Optimization based on theory

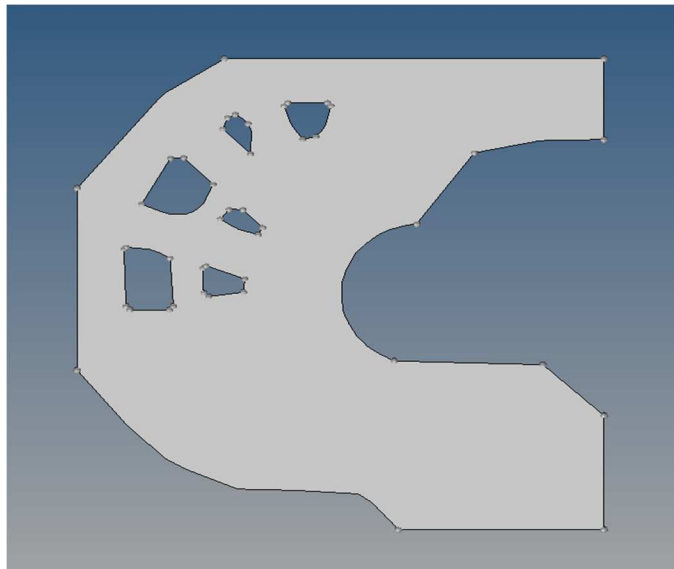


Fig 3.13 Optimized geometry based on theoretical result

	Original c-clip	Optimized c-clip	weight reduction
Weight	0.125 kg	0.090 kg	28%

Table 3.5 Original and optimized c-clip weight comparison based on theory

Optimization based on experiment

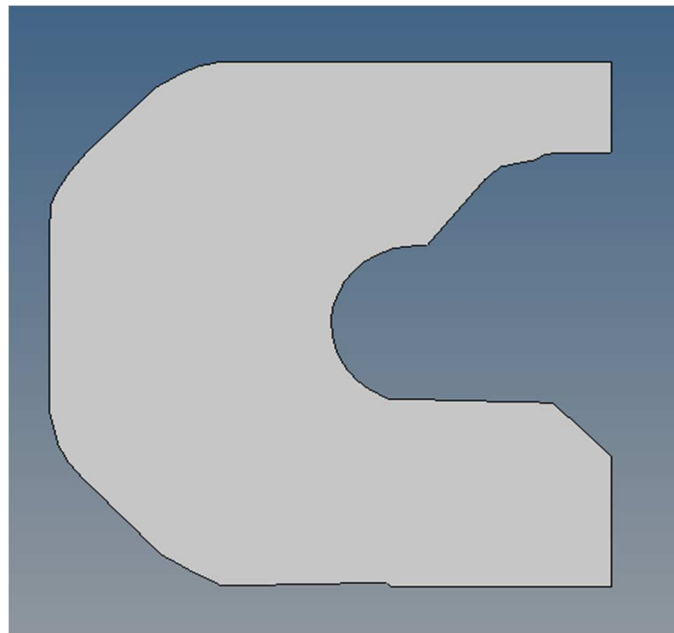


Fig 3.14 Optimized geometry based on experimental result

	Original c-clip	Optimized c-clip	weight reduction
Weight	0.125 kg	0.099 kg	20%

Table 3.6 Original and optimized c-clip weight comparison based on theory

It can be concluded that, the optimized geometry based on experiment (iso value=0.096) is considered as the final optimized design.

CHAPTER 4
MODEL DESCRIPTION, ANALYSIS SETUP, STRUCTURAL OPTIMIZATION AND
VALIDATION

A plastic injection mold consisting of a cavity block and a core block is studied as a 3D topology optimization trial case. The model is described and the steps of problem set up are elaborated, optimization is performed and results are validated.

4.1 Mold geometry

The mold geometry from the industrial partner is shown in figure 4.1. The mold geometry consists of a cavity block (the top part) and the core block (the bottom part). The parting line separates the cavity block from core block. Figures 4.2 show the actual mold mounted on injection molding machine. Figures 4.3, 4.4, 4.5 and 4.6 show front view and side view of cavity block and core block respectively.

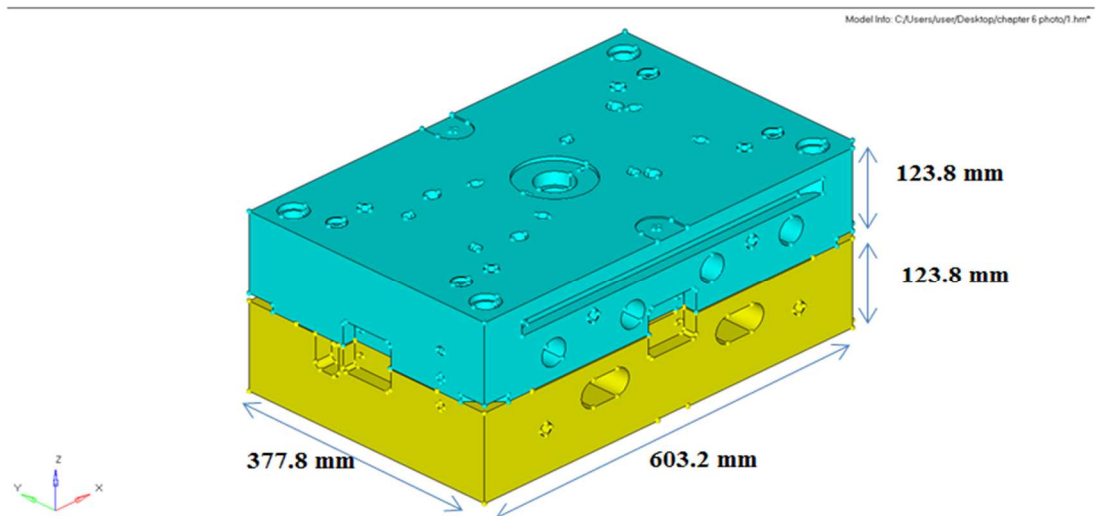


Fig 4.1 Mold block consisting core, yellow part, and cavity, blue part, from industrial partner

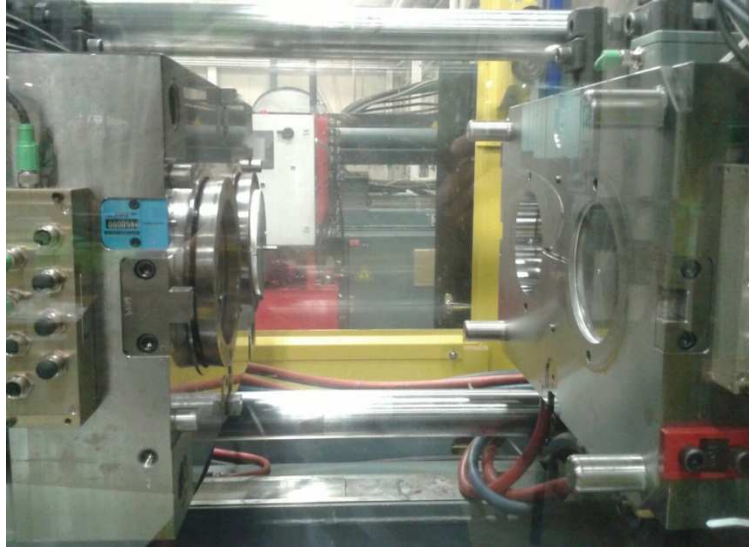


Fig 4.2 Mold block mounted in injection molding machine

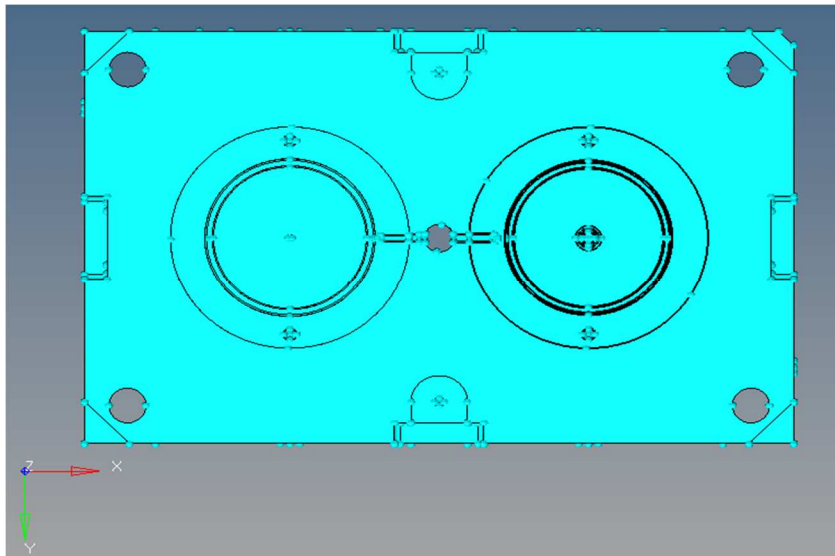


Fig 4.3 Front view of cavity block

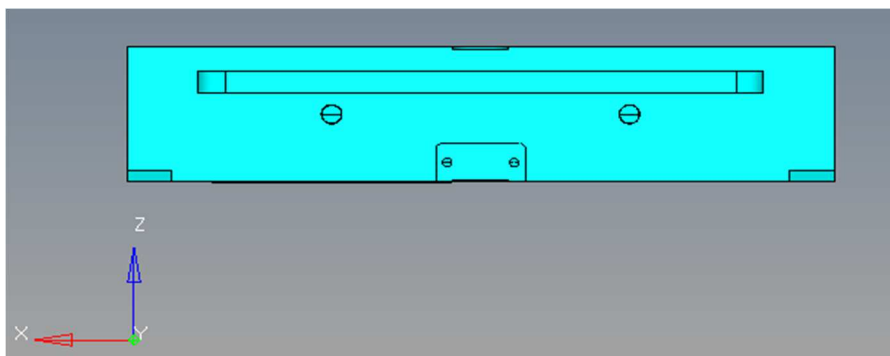


Fig 4.4 Side view of cavity block

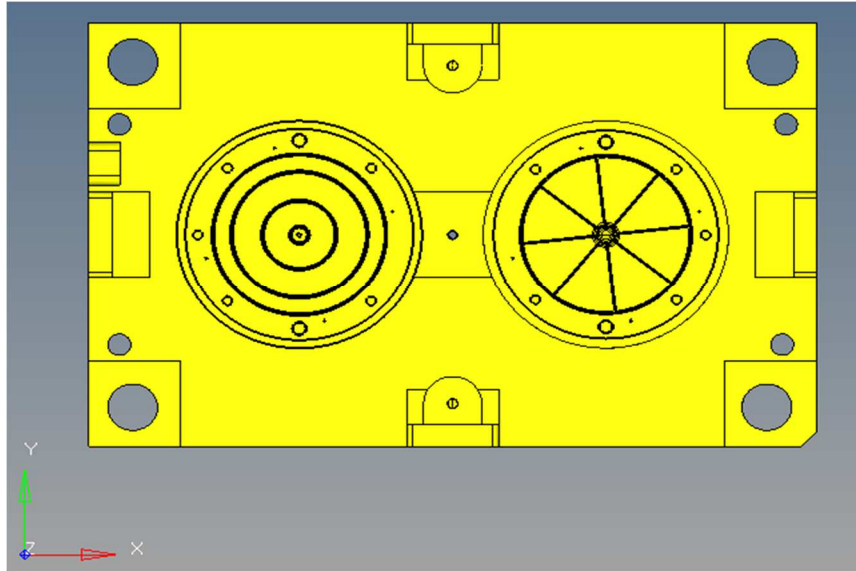


Fig 4.5 Front view of core block

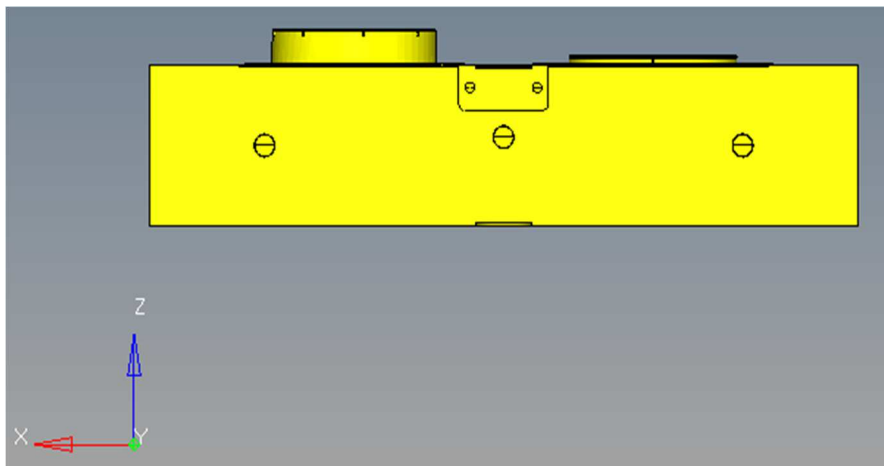


Fig 4.6 side view of core block

The cavity block and core block are made of P20 steel tool. The material properties of P20 steel tool is shown in the table 4.1.

Properties	Values in metric system
Hardness, Brinell	300
Hardness, Rockwell C	30
Tensile strength, ultimate	965-1030 MPa

Tensile strength, yield	827-862 MPa
Compressive strength	862 MPa
Poisson's ratio	0.27-0.3
Elastic modulus	190-210 GPa
Density	7861 Kg/m ³

Table 4.1 Material properties of P20 steel tool

4.2 Geometry cleanup:

Creating a model from designer's point of view is different from an analyst's perspective. Designers consider the structure in very detailed form. However, from an analyst's perspective some details of the structure such as small holes, fillets with small radius, small gaps and groove are not necessary for the analysis [4]. In order to prepare the geometry for meshing and optimization, it is necessary to perform geometry cleanup. Geometry cleanup results in a qualified mesh, created on the entire part with proper connectivity. It also directly influences the quality of the elements. The geometry cleanup is comprised of two stages: removing unnecessary details from geometry and modifying the geometry topology to increase mesh quality. In this thesis, the inner packaging of the mold consisting cooling lines are not considered.

4.2.1 Removing unnecessary details:

This stage of geometry cleanup is related to changing of the shape of the part in order to attain a more simplified geometry. The following pictures demonstrate the geometry before removing details and after performing this step. The four circular holes, where tie bars are located, in the corners will remain constant and will be defined as non-design space.

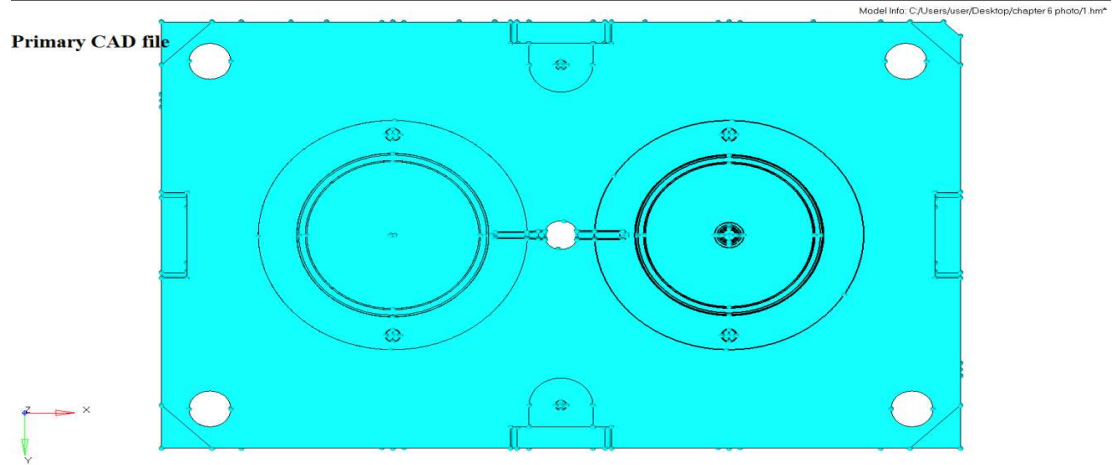


Fig 4.7 Original CAD model

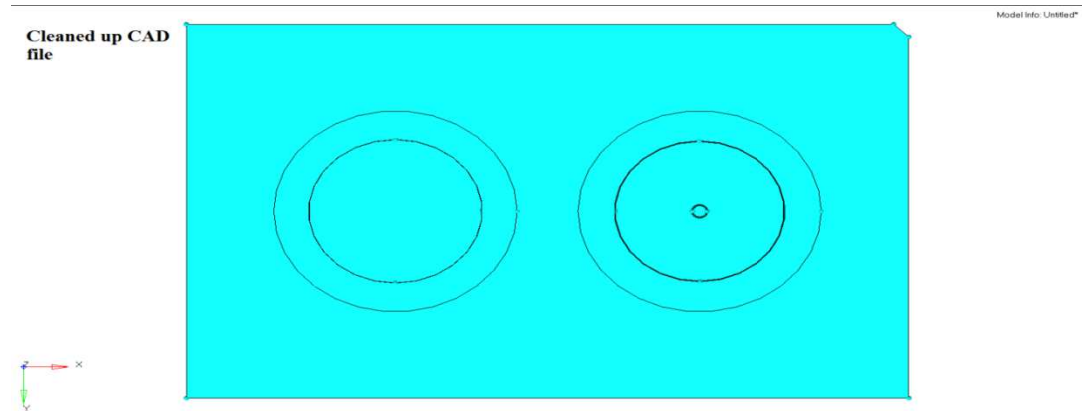


Fig 4.8 Cleaned-up model

4.2.2 Refining topology to achieve a quality mesh

The topological details of the geometry may affect the quality of the mesh. However, these details may not reflect any major feature of the part's shape and can be removed without concern. Adding topological features that do not change the shape of the part, may help to create better mesh. Different aspects of topology refinement are demonstrated in the following examples.

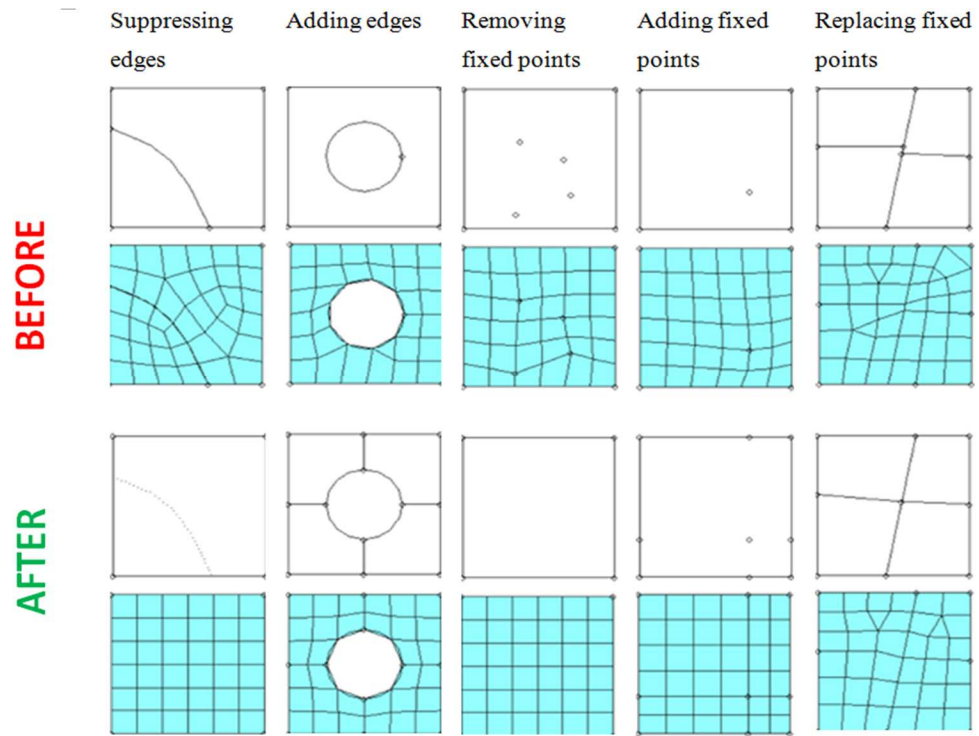


Fig 4.9 Topology refinement examples [4]

4.3 Meshing

Meshing is considered as the process of generating polygonal or polyhedral elements that approximate a geometric domain and split that into subdomains [30]. There are two common types of elements, namely 2D elements and 3D elements.

4.3.1 2D meshing

There are two types of 2D elements triangle elements and quadrilateral elements. Triangle elements are cells with three sides and three nodes and quadrilateral elements are elements with four sides and four nodes.



Fig 4.10 Triangular and quadrilateral elements

4.3.2 3D meshing:

3D elements are used when all dimensions of a structure are comparable. There are three element shapes in 3D meshing consisting tetra, penta, hexa and pyramid elements. HyperMesh can be used to create tetra mesh or hexa mesh. Tetrahedral elements

Tetrahedral elements are elements with four sides and four nodes, penta elements are elements with five sides and six nodes, hexa elements are with eight nodes and six sides

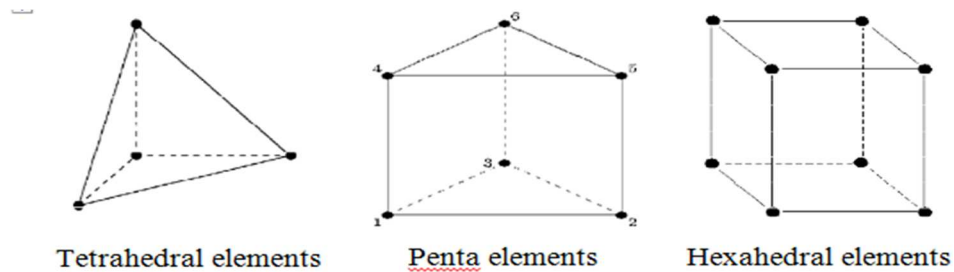


Fig 4.11 3D elements, tetra, penta and hexa

Meshing with hexa elements is usually more time consuming in comparison with tetra elements. Therefore, the model was meshed with tetrahedral elements in our simulations. Meshed model is depicted in figure 4.12

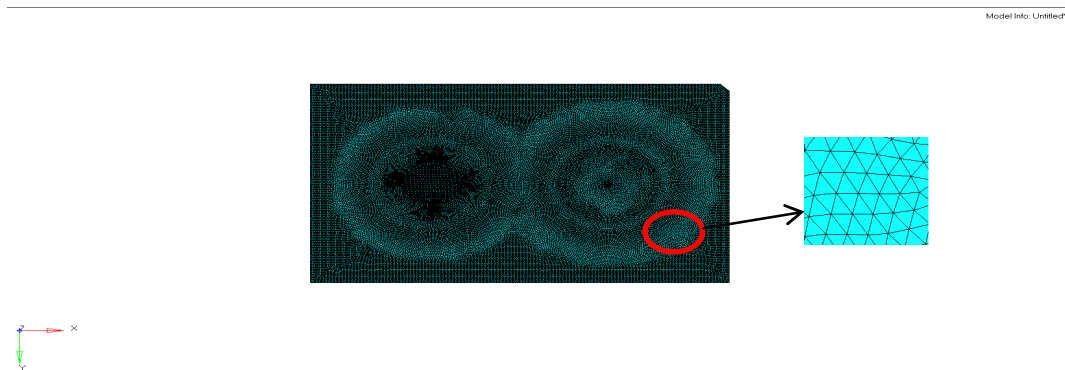


Fig 4.12 Meshed cavity and tetrahedral elements in meshed cavity

4.4 Element quality check

There are not any accurate criteria for element quality. The reason is that the quality is relative and the solution is approximate. The element quality range is represented graphically in the following table.

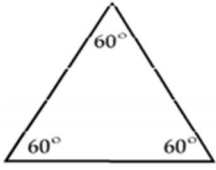
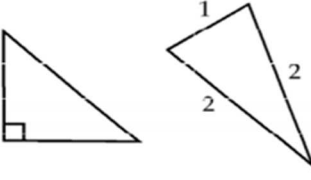
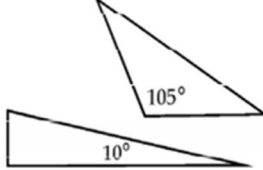
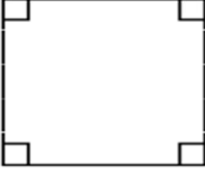
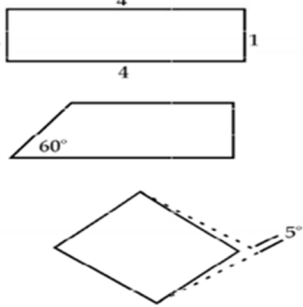
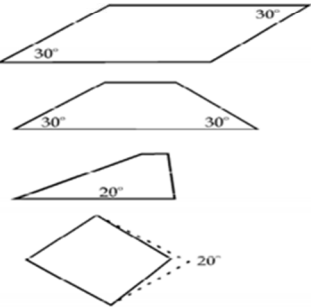
Ideal	OK	Poor quality
		
		

Table 4.2 Demonstration of element quality

To check the quality of 3D tetra mesh, it is necessary to check the quality of each element. The check element panel in Hypermesh was used for this purpose.

While performing the element quality check, the user can save the failed elements and those failed elements plus a layer or two layers of elements in the vicinity of the failed elements would be re meshed later.

4.5 Assigning material and properties

After meshing the model, the material and the properties should be assigned to the elements of the model. The material is P20 steel tool (material data is shown in table 4.1) and it was considered as temperature independent and an isotropic material. The property of PSOLID was assigned to the component since solid elements were used to discretize the model.

4.6 Defining design space and non-design space

In a topology optimization problem, the total volume should be divided into a design space and a non-design space. The design space is the volume from which the material is removed, until the final shape is achieved. The design space is the optimized domain. The non-design space is the volume that stays unchanged during the optimization process. Loads and constraints are applied to the non-design space. The

design space and non-design space of the model are determined. They are shown in figure 4.13. The design space is displayed in purple in the following figure and non-design space is displayed in blue mesh. In this model areas where loads and boundary conditions were applied were considered as the non-design and the rest of geometry was design domain.

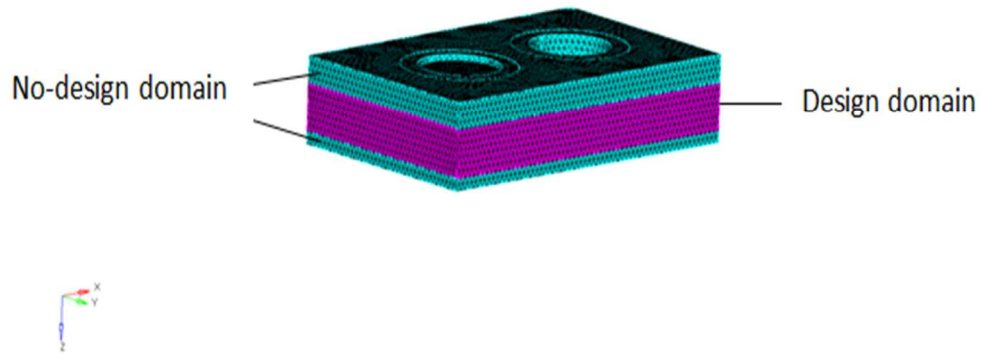


Fig 4.13 Model configuration consisting design space (purple mesh) and non-design space (blue mesh)

4.7 Analysis setup

The last step of problem set up is applying constraints and forces. In the study of this model three different load cases were considered: Weight of the mold, pressure (consisting of the cavity pressure and clamping pressure) and the thermal load. All load cases are considered as linear static loads and dynamic loads such as vibration are not considered in this study. Due to different load cases, structural optimization analysis and thermal analysis were performed. Structural optimization and results validation will be discussed in the rest of this chapter and thermal analysis will be elaborated in chapter 5.

4.7.1 Constraints

The constraints are considered as follows. The back of the cavity block has been fixed. The back plate is constrained in all degrees of freedom. The back of the core block was also constrained in all degrees of freedom except in the z direction. This boundary condition is applied for both static and thermal load cases. Constraints are shown with green triangles.

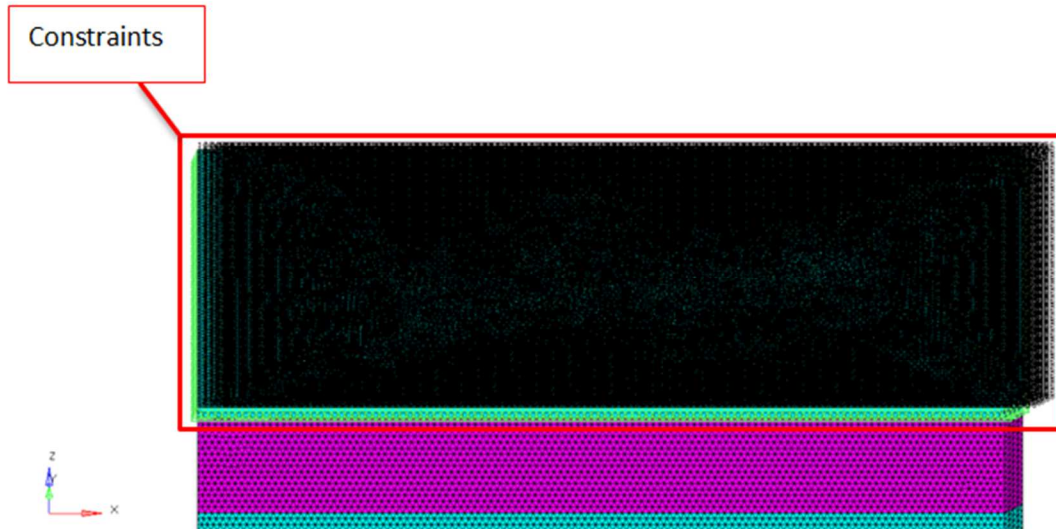


Fig 4.14 Constrained cavity block

4.7.2 Loads

The weight of the die, cavity pressure and clamping pressure, which impacts the back of the core block are the load cases in this optimization. Therefore, the clamping pressure was applied in the back of core block. In this case study the clamping pressure and the weight of the mold were known but the cavity pressure and temperature, both were unknown. However, in order to solve this problem we needed to determine the real load cases applied to the model. Hence, cavity pressure, cavity temperature and mold deflection sensors were installed in the die to measure the unknown values. The eDART system was employed for monitoring of the signals sent from sensors. The eDART system is considered as one of the most comprehensive and powerful process monitoring and control system platforms for plastic injection molding. The location of the sensors needed to be decided about before ordering and installation. Therefore, after consulting with our industrial partner the following decisions were made. Pressure sensors were placed inside the cavity and on the core half. Temperature sensors were placed in the cavity and on the cavity half. Mold deflection sensors were placed on the parting line and on the cavity half. Deciding about sensors placement was based on the application of the sensors and the placing limitation due to existence of cooling lines and plastic injecting lines.

Cavity pressure

The Lynx button style digital pressure sensors were selected as cavity pressure sensor after consulting with RJG corporation consultants.



Fig 4.15 Button style cavity pressure sensor [5]

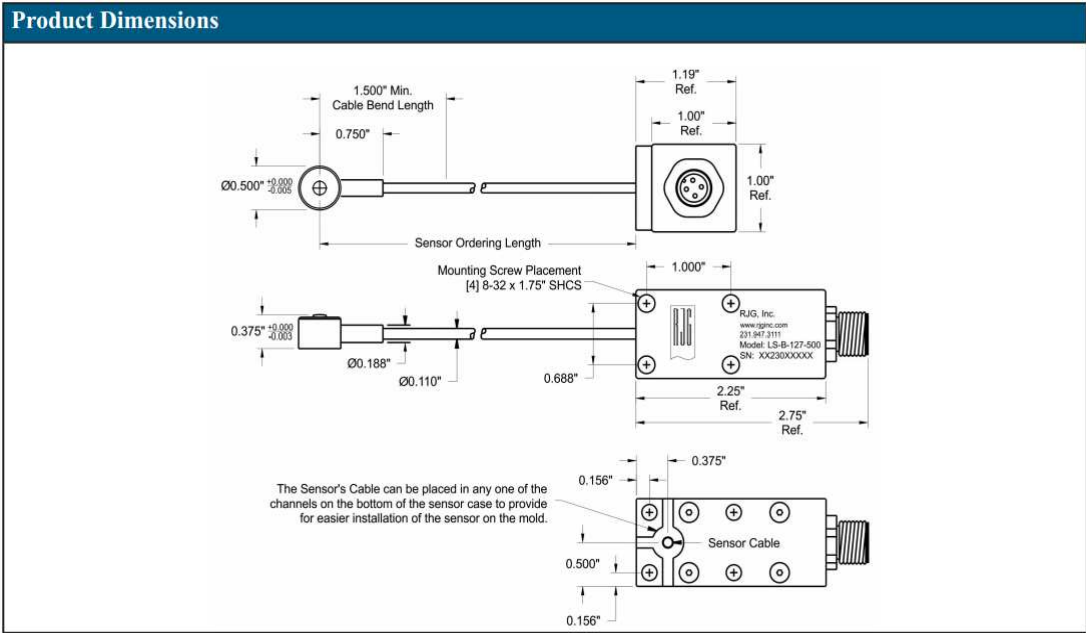


Fig 4.16 Button style cavity pressure sensor dimensions [5]

In the button style sensors (indirect sensors), cavity pressure causes the ejector pin to force itself against the sensor which is located behind the head of the pin. The sensor

creates a voltage that is proportional to the amount of deflection caused by pin being under pressure.

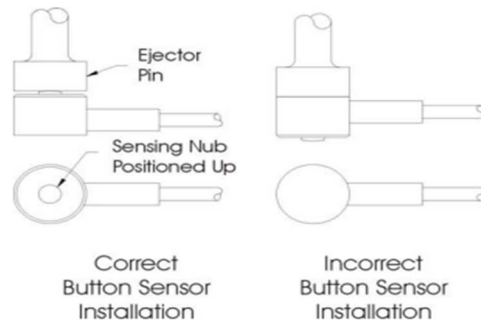


Fig 4.17 Pressure sensors located behind the ejector pin [5]

The mold in our problem had two cavities. As a result, at least two button style pressure sensors were required to be installed in each cavity. One sensor was placed in each cavity. The button style pressure sensors are installed behind the ejector pins in drilled holes. The following picture shows the pressure sensors installed in the mold.

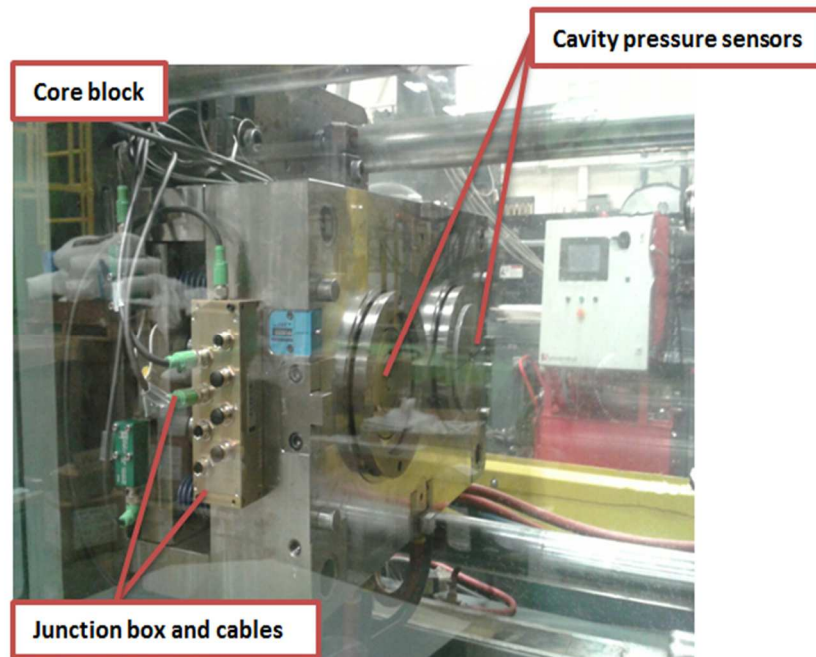


Fig 4.18 Cavity pressure sensors are installed in the core block

The lead wire of the pressure sensor is connected to the junction box. The junction box plays the role of interface between devices and eDART. The cavity pressure data are collected by sensors and transferred to eDART through the cables connected to junction box. This data are displayed on eDART monitor and are also saved. This information extracted from eDART and plotted with Matlab as shown in Figure 4.19.

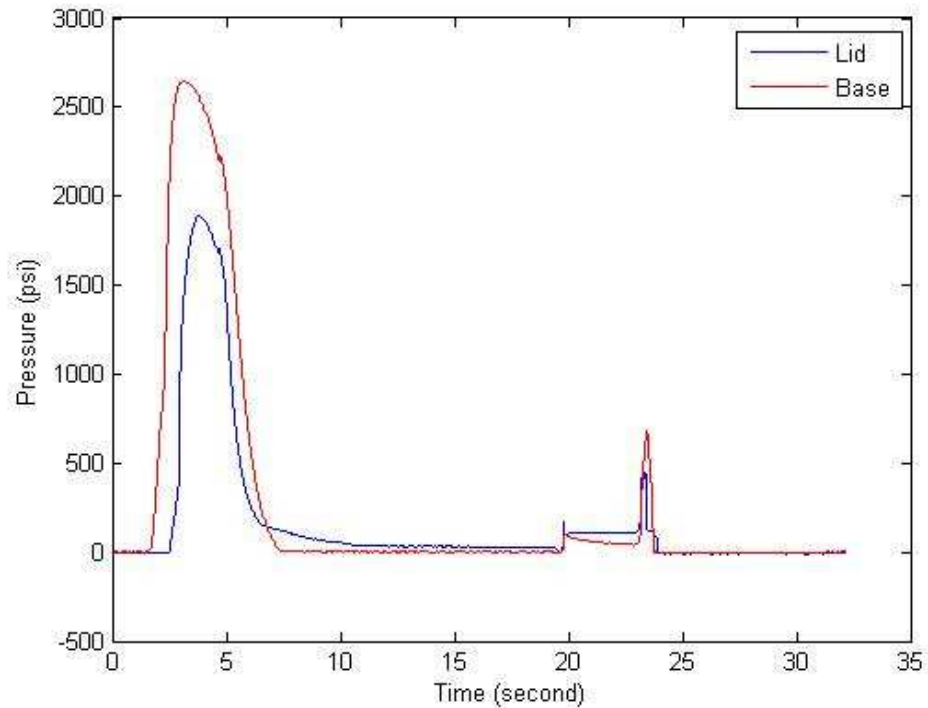


Fig 4.19 Pressure-time diagram, Cavity pressure is plotted for both sensors in each cavity

Clamping pressure

The clamping pressure is the pressure applied to the mold by the clamping unit of the injection machine to keep the mold closed. This pressure opposes the separating force produced due to the injection of plastic into the cavity. The clamping unit of the machine applies the clamping force of 1500 *tonne – force* to the mold which is equal to 6475771 *Pa*.

$$P_{Clamping\ pressure} = \frac{F_{Clamping\ force}}{A_{Effective}}$$

$$F = 1500\ \text{tonne} - \text{force} \quad (4.1)$$

$$\text{one tonne} - \text{force} = 9.80665\ \text{kilonewtons (kN)}$$

$$A_{Effective} = \text{The area of back of core block} = 0.227\ \text{m}^2$$

The following figure 4.20 shows the loaded geometry. In order to make the applied cavity pressure visible the design space has been hidden. Red arrows show the direction of the applied clamping and cavity pressure.

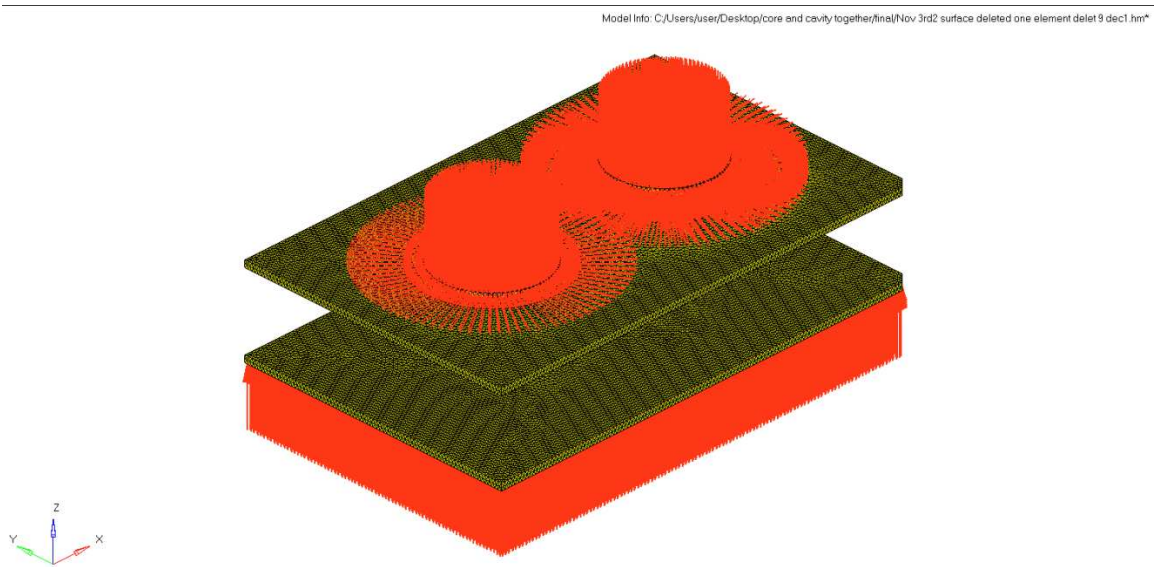


Fig 4.20 Loaded model, red arrows show the applied pressure to the mold

Weight of the mold

The weight of the mold is not applied to the center of gravity, but instead, over the entire volume of the model.

4.7.3 Defining optimization criteria

As mentioned before, the optimum design for the mold geometry is the design in which the mold has an objective function of minimizing the compliance and also has a constraint on volume fraction to make sure that the model does not exceed the volume

fraction limit. The volume fraction is the optimized volume of the design space divided by original volume of the design space in each iteration. The model was developed with different values of volume fraction, but the best result was obtained for the volume fraction of 0.5. So a volume fraction of 0.5 was defined for this problem. The process of defining the optimization criteria is done in several steps in Optistruct. The first step is defining responses to be used as criteria for optimization. The volume fraction and compliance were defined as responses. The next step is assigning objective and constraint to responses. Minimizing the compliance was set to be the objective of optimization and constraint on the volume fraction was set to 0.5 since it gives a clearer distribution of material in the structure. That, means the software takes a minimum 50% of design space for the optimized domain.

Topology optimization results provide a concept design of the structure. The results are sometimes difficult to manufacture due to the limitations of conventional manufacturing methods. The manufacturing constraints option in the Optistruct facilitates producing geometry that can be realistically fabricated. Usually these structures with applied manufacturing constraints need more modifications to become manufacturable. Several constraints to use in Optistruct to control the manufacturability of the design and which was used in this thesis are the symmetry constraint and minimum member size (MMS) control constraint. The MMS is usually decided based on the maximum element size and it is usually three times the maximum element size which is $5E - 3$ m here [28]. The benefit of using a sufficiently large MMS size value is getting clearer picture of the result of the optimization at the end of the analysis. The input values of the model are shown in table 4.3.

Mesh details	
Elements type	CTETRA, four sided and four nodes elements
Element size	$5 \times 10^{-3} m$
Number of elements	1322814
Material properties	

Density	$7861 \text{ Kg}/\text{m}^3$
Elastic module	$E = 210 \text{ GPa}$
Boundary conditions	
Analysis load cases	Pressure, gravity, constraint
Pressure	Clamping pressure= $6.4 \times 10^6 \text{ Pa}$ Cavity pressure $\begin{cases} \text{Lid} = 1.1 \times 10^7 \text{ Pa} \\ \text{Base} = 1.7 \times 10^7 \text{ Pa} \end{cases}$
gravity	$9.8\text{m}/\text{s}^2$
Optimization criteria	
Objective function	Minimizing compliance
Constraint on volume fraction	0.5

Table 4.3 Inputs of FE model in Optistruct

4.8 Results of static analysis of primary model

Before performing optimization, static analysis of the primary model was carried out to have reference values for the displacement and Von Mises stresses (table 4.4 and figure 4.21) since the results of the optimization are compared with the primary model

	Max Displacement (m)	Displacement, Parting line (m)
Original model	1.4×10^{-5}	4.1×10^{-6}

Table 4.4 Results of static analysis of primary model

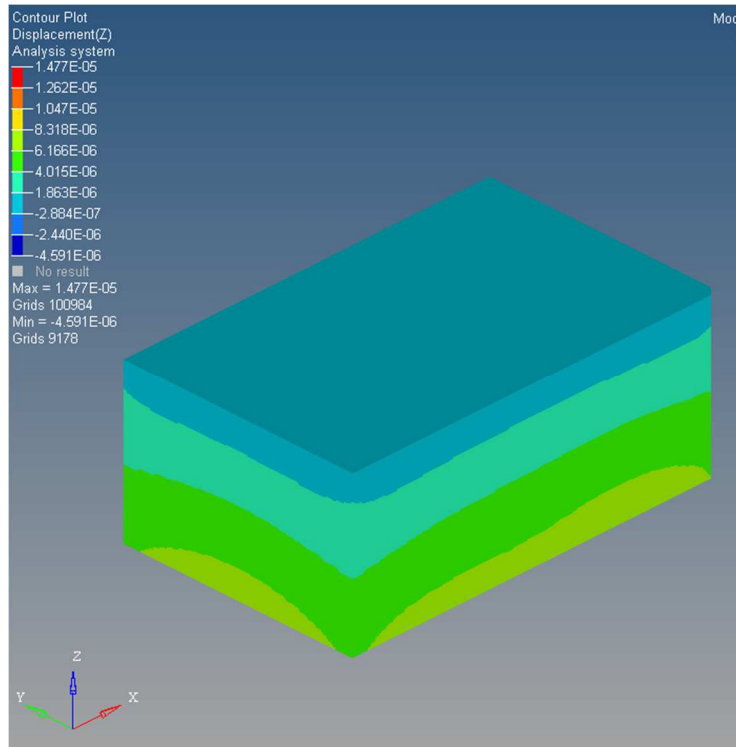


Fig 4.21 Displacement (m) contour plot for primary model

4.9 Results of topology optimization

The results of topology optimization on the mold geometry were later viewed in the Hyperview the post processor that comes with the Hyperworks package. The results satisfied the objective function and constraints. The compliance is minimized for volume fraction of 0.5. The number of iterations to converge to a solution and have a feasible design was 32. The CPU time was 22:13:14 with a 32 GB RAM system.

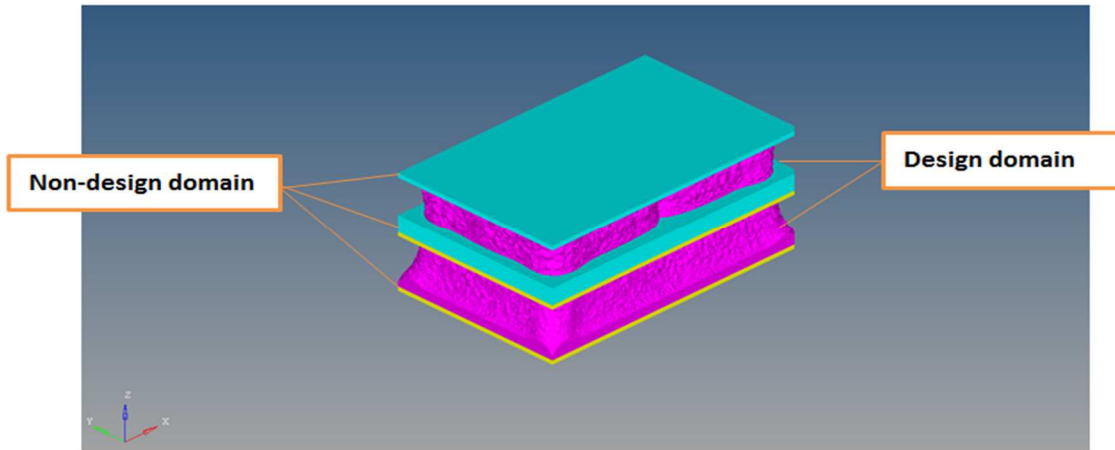


Fig 4.22 Topology optimized mold, top block is the cavity block and bottom block is the core block

The blue and yellow domains show the non-design space of core and cavity. These domains remained unchanged during optimization.

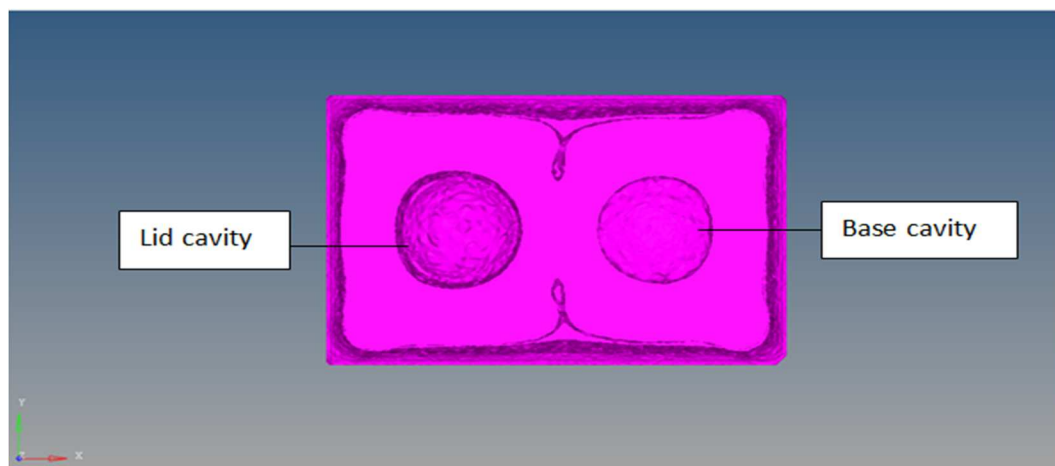


Fig 4.23 Results of topology optimized mold, only the design space has been demonstrated, top view

As it is illustrated in figure 4.23, the material has not been removed evenly from the two cavities. That is due to the difference in cavity pressure of two cavities. The cavity with the higher pressure called the base cavity and the cavity with lower pressure is called the lid. The material removed from the lid was more than the material removed from the base.

The element density plot of the optimization results is shown in figure 4.24. As it can be clearly seen, domains displayed in red show the areas that the material should exist. The element density in these domains is equal to one. The areas depicted in blue are the domains where material can be removed from and the element density is equal to zero. Colors between red and blue show the elements with intermediate density values.

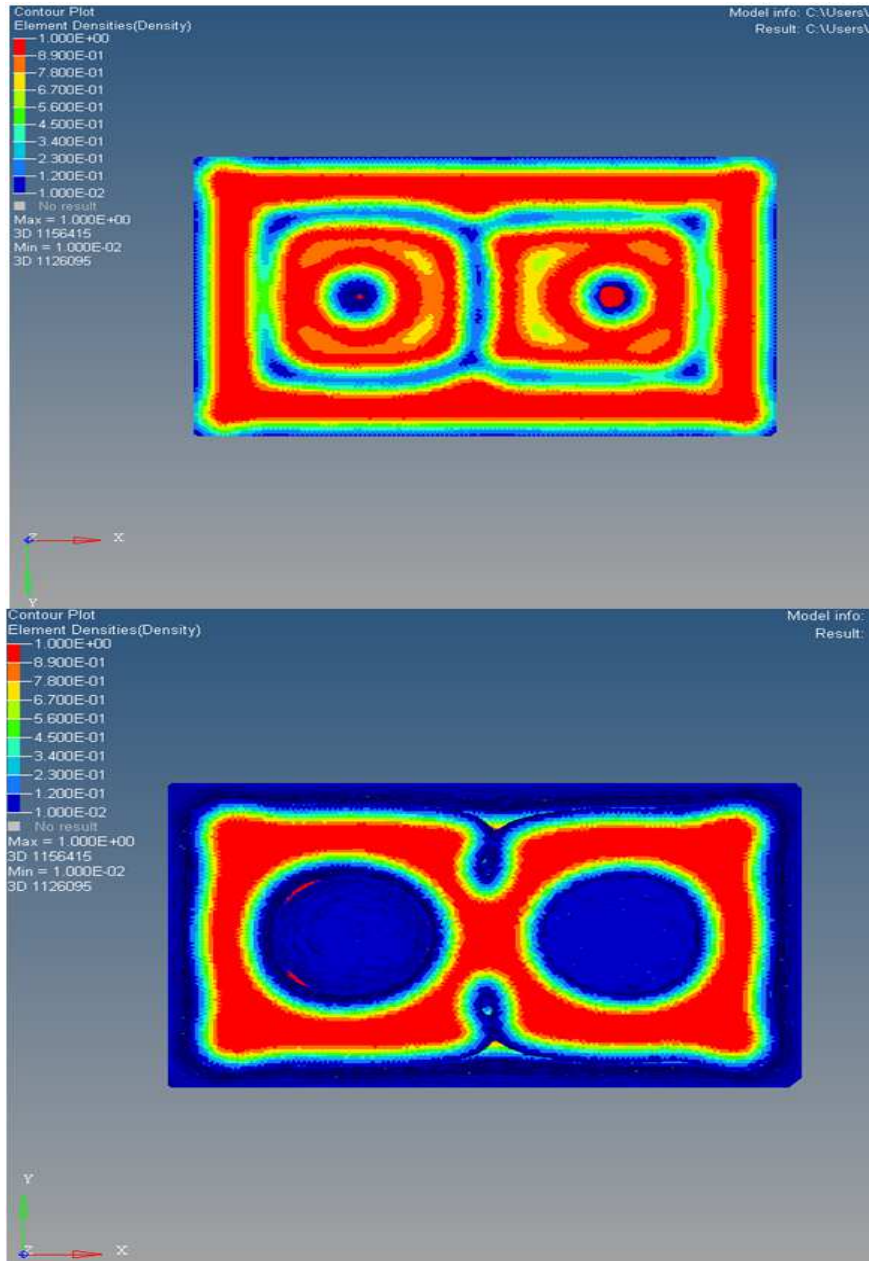


Fig 4.24 Element density plot for topology optimization results, top view and bottom view

The lower the element density in a section is the less material is needed. There is an option in Hyperview that removes the material from some sections of the plot that does not meet the minimum criteria for element density. In the optimized design the material densities are varied between 0 and 1. Zero density elements refer to elements without any structural relevance in contrast elements with density of one refer to elements which bear load in the structure. There are some elements with intermediate

density value, densities between zero and one. The threshold value that mentioned before interpret the importance of these intermediate density elements. There is a slider bar for determining the iso value in Hyperview. By using the slider bar we can view likely design concept with respect to different element density values. By default elements with the density above the user specified value are shown. Frequently this density value is in the range of 0.3 to 0.5 usually. The iso value of 0.3 was selected for this problem since this value was used for most problems of topology optimization problem and also very conservative for this specific problem. It should be emphasized here that topology optimization offers a concept design for structures and it does not provide a detailed size structure.

There is an option in Hypermesh called “Ossmooth”. It is used to create an IGES file format from the result. In order to extract the topology optimization results in iges format “ossmooth” command from Hypermesh was used with “surface reduction” command. The surface reduction option in parameters section is used to reduce the number of surfaces in geometry and make it more smoothed.

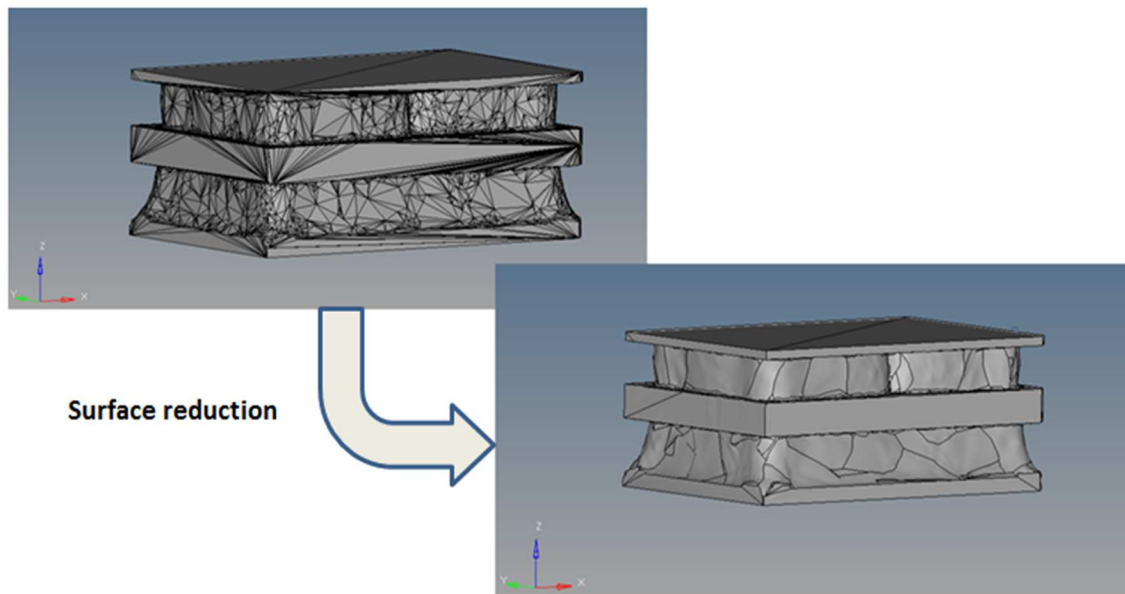


Fig 4.25 IGES file extracted from topology results using Ossmooth

4.10 Results interpretation and redesign of the die

As it was briefly discussed in section 4.7.3, once the optimization is done, we have to interpret the results of optimization. Figure 4.26 shows the interpretation of structure from topology optimization results. Four corners of core and cavity block will remain unchanged since tie bars of injection machine go through them. When interpreting the results, it is important to keep in mind that the extracted geometry is not the exact shape that the software predicted. In this project, it was impossible to machine the inner hollow volumes inside the cavity block and core block with conventional tooling method since they are bounded to non-design spaces. As a result the interpreted geometry does not consist the inner optimized hollow domain due to machining inaccessibility. Solid works software was used to create the CAD model from results interpretation initially but it was slightly modified after consulting with our industrial partner. It should be mentioned that the optimized interpreted geometry is “near optimal”.

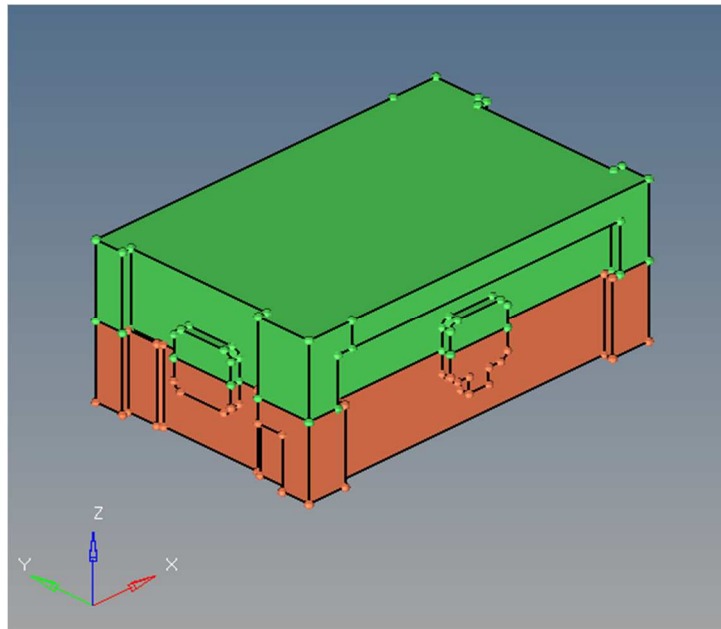


Fig 4.26 Optimized interpreted geometry

Result of analysis for the optimized interpreted model

	Max Displacement (m)	Displacement, Parting line (m)
Optimized interpreted Model	8.3×10^{-6}	3.9×10^{-6}

Table 4.5 Results of static analysis of optimized interpreted model

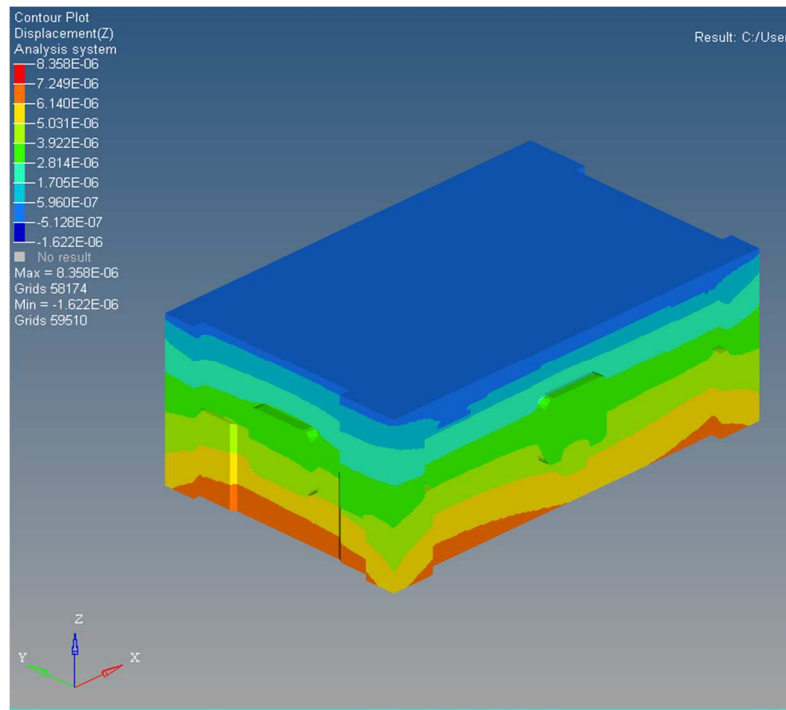


Fig 4.27 Displacement (m) contour plot for optimized interpreted model

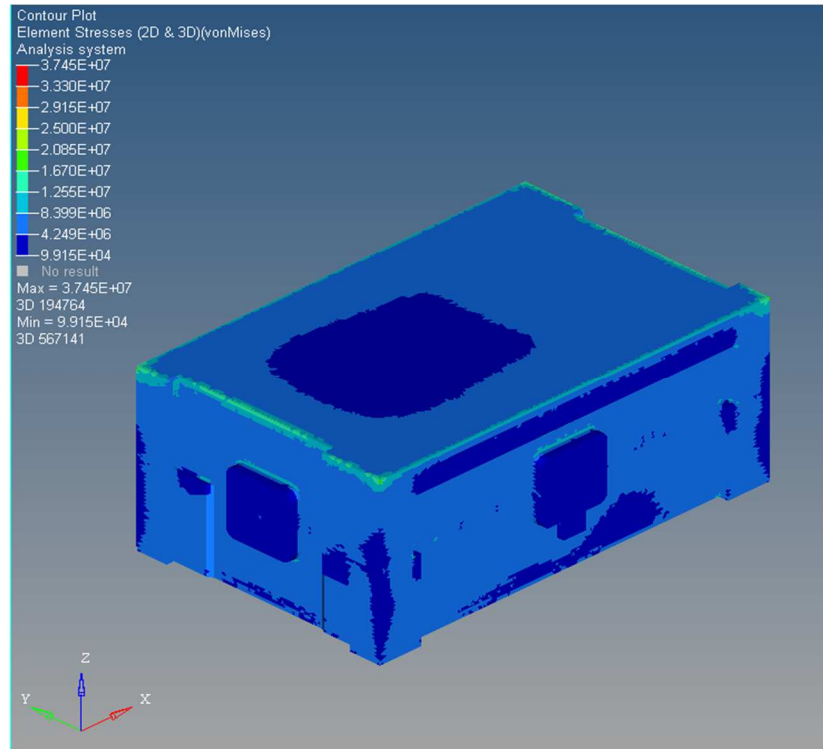


Fig 4.28 Stress (Pa) contour plot for optimized interpreted model

4.11 *Mold with smaller overall size*

Manufacturing the optimized interpreted model that was elaborated in section 4.10 entails spending time and cost for creating pockets which reduce the weight. It was favorable for our industrial partner to choose smaller block size for the mold rather than starting with large block and then machining it according to optimized interpreted model to reduce the weight. In order to save time and cost a new model was proposed that has approximately similar behavior but 12% lighter than the original model. This model does not contain any pockets and is based on selecting smaller block size. The size of the smaller mold is according to minimum width and height of topology optimization output, 5.76×10^{-1} by 3.44×10^{-1} ($\Delta x = 0.273 \times 10^{-1}$, $\Delta y = 0.338 \times 10^{-1}$, $\Delta z = 0$). The proposed model does not need any extra machining operations. Loading conditions for this model varied from previous models and the only different was clamping pressure since the equal force was divided on smaller area and the pressure did increase. The model was meshed and finite element analysis was performed on that. The following table shows the result of static analysis on that.

	Max Displacement (m)	Displacement, Parting line (m)
Proposed model	1.4×10^{-5}	4×10^{-6}

Table 4.6 Results of static analysis of proposed model

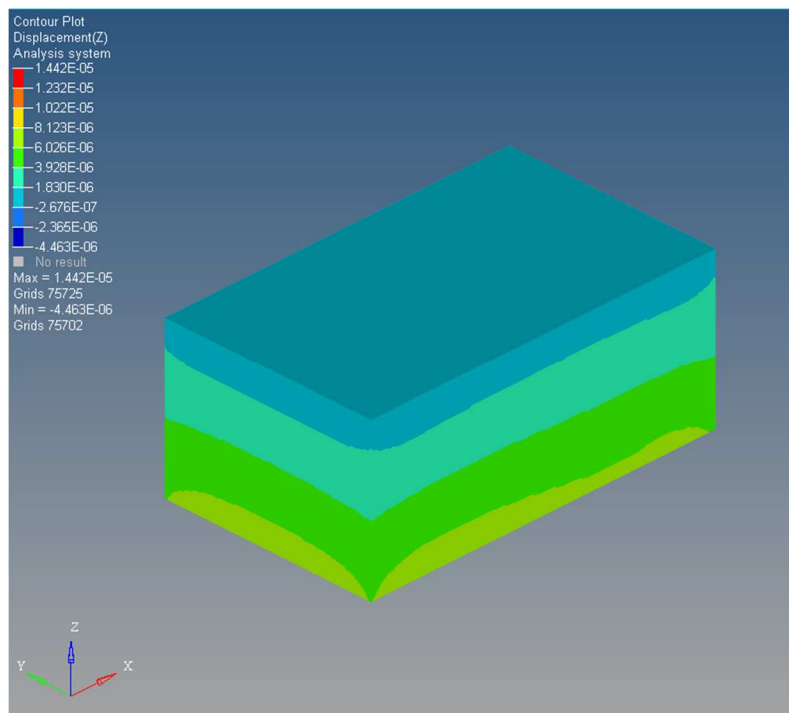


Fig 4.29 Displacement (m) contour plot for smaller model

As it can be seen from results of static analysis of the mold with smaller overall size, the maximum displacement in original model and this model are rather the same.

4.12 Validating results by installing mold deflection sensors

In order to validate the result of the optimization and verify that the optimized structure with less weight has almost similar performance to the original structure and will not fail under applied loading condition and pass the stress limit, deflection sensors were installed in the mold. Sensors were once installed on primary mold (to record the deflection of original model) and then they were uninstalled and again mounted on

optimized model. These sensors were installed in the parting line of the mold on cavity half to measure deflection. The deflection sensors are usually placed in the center of the mold if there is no cavity or runner on the parting line in the center. If there is a cavity in the center then two mold deflection sensors are installed, one on either side of the cavity [6]. In our study, two deflection sensors were installed in the middle on top and bottom of the runner on cavity half. Figure 4.30 shows where deflection sensors are installed and figure 4.31 indicates sensor's configuration in the mold.

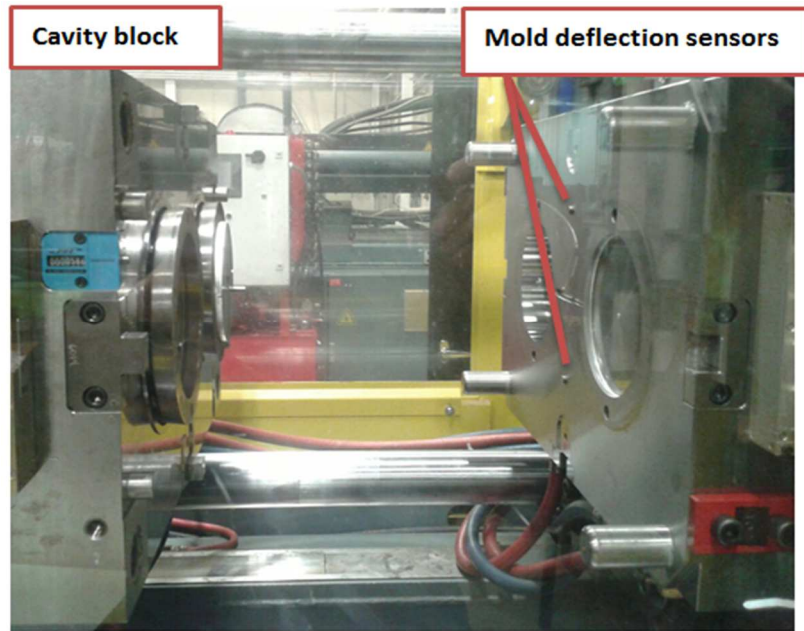


Fig 4.30 Deflection sensors placement on cavity half

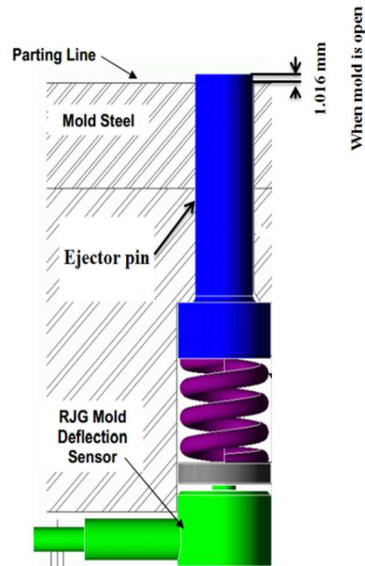


Fig 4.31 Mold deflection sensor installed in cavity block on parting line [6]

Mold deflection sensors were connected to the eDART system to monitor deflection data. Experiments were performed on both original and optimized model and deflections via sensors were recorded. The obtained results are discussed as following. Deflection (mils) - time (s) diagrams are displayed in following figures.

It is worthwhile noting that finite element analysis is an approximate technique and the accuracy of the result might vary with respect to experimental data. The difference of 10% to 15% between theory and experiment is a very good correlation [3].

Original mold

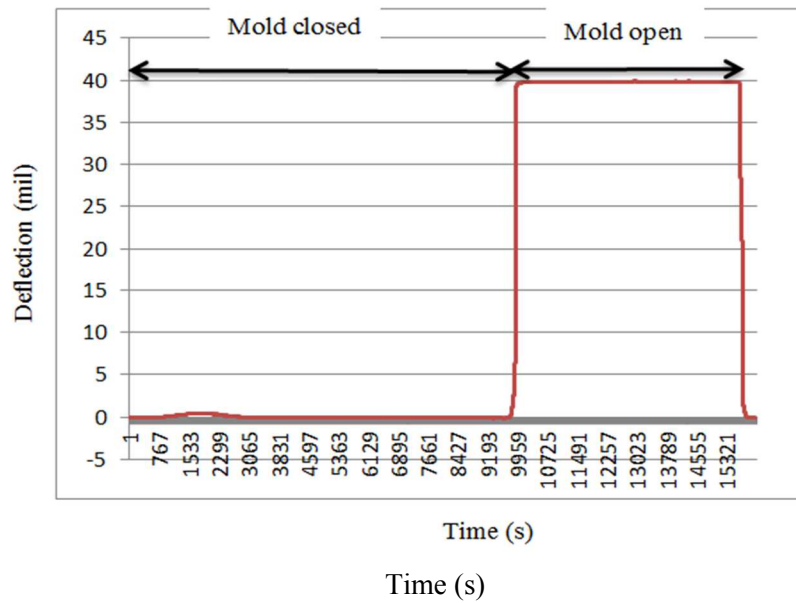


Fig 4.32 Deflection-time diagram, original model

Optimized mold

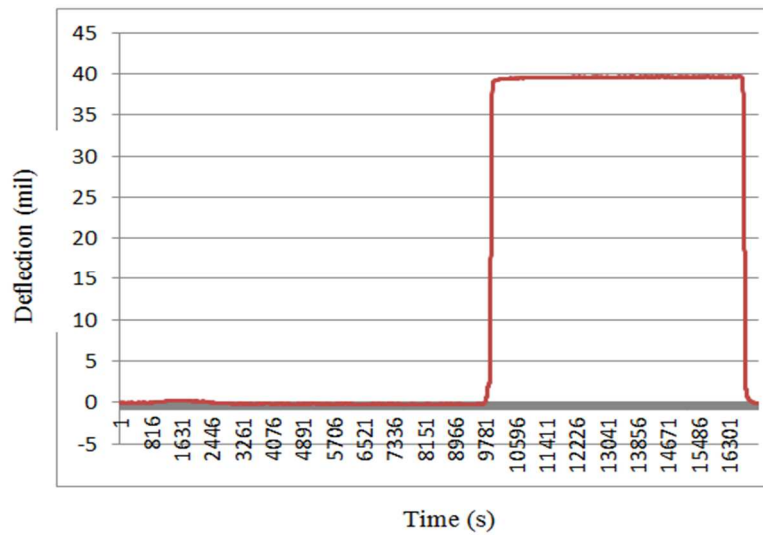


Fig 4.33 Deflection-time diagram, optimized model

Analyzing the mold cycles indicates that, the maximum deflection of mold, where the clamping force is applied to the mold and the injection pressure in cavities are in their peak point, is during the period of $t=2.8$ S to $t=3.2$ S. Two sample cycles are

demonstrated in following figures. The maximum cavity pressure has happened in 3.1 S and 3.3 S respectively.

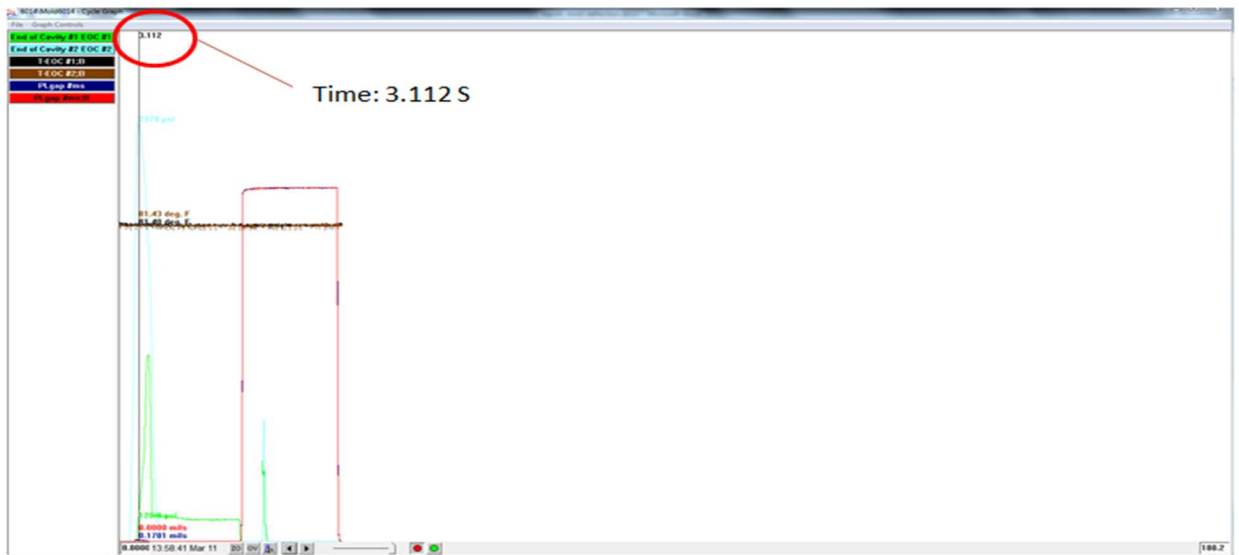


Fig 4.34 The mold is clamped and peak pressure of cavities are demonstrated with green and blue lines) has happened $t=3.112$ S

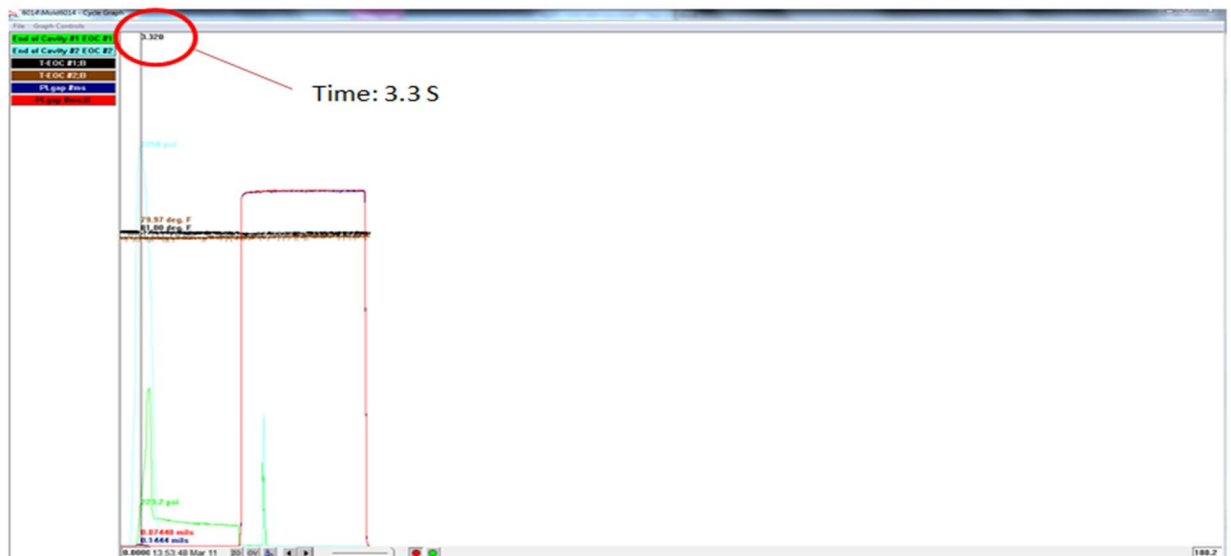


Fig 4.35 The mold is clamped and peak pressure of cavities are demonstrated with green and blue lines) has happened $t=3.3$ S

In order to have better perspective of mold deflection during the period that peak pressures were applied to the mold, the time frame has been narrowed down and period of ($t=2$ S to $t=4$ S) is plotted for both models in figures 4.35 and 4.36.

Original model

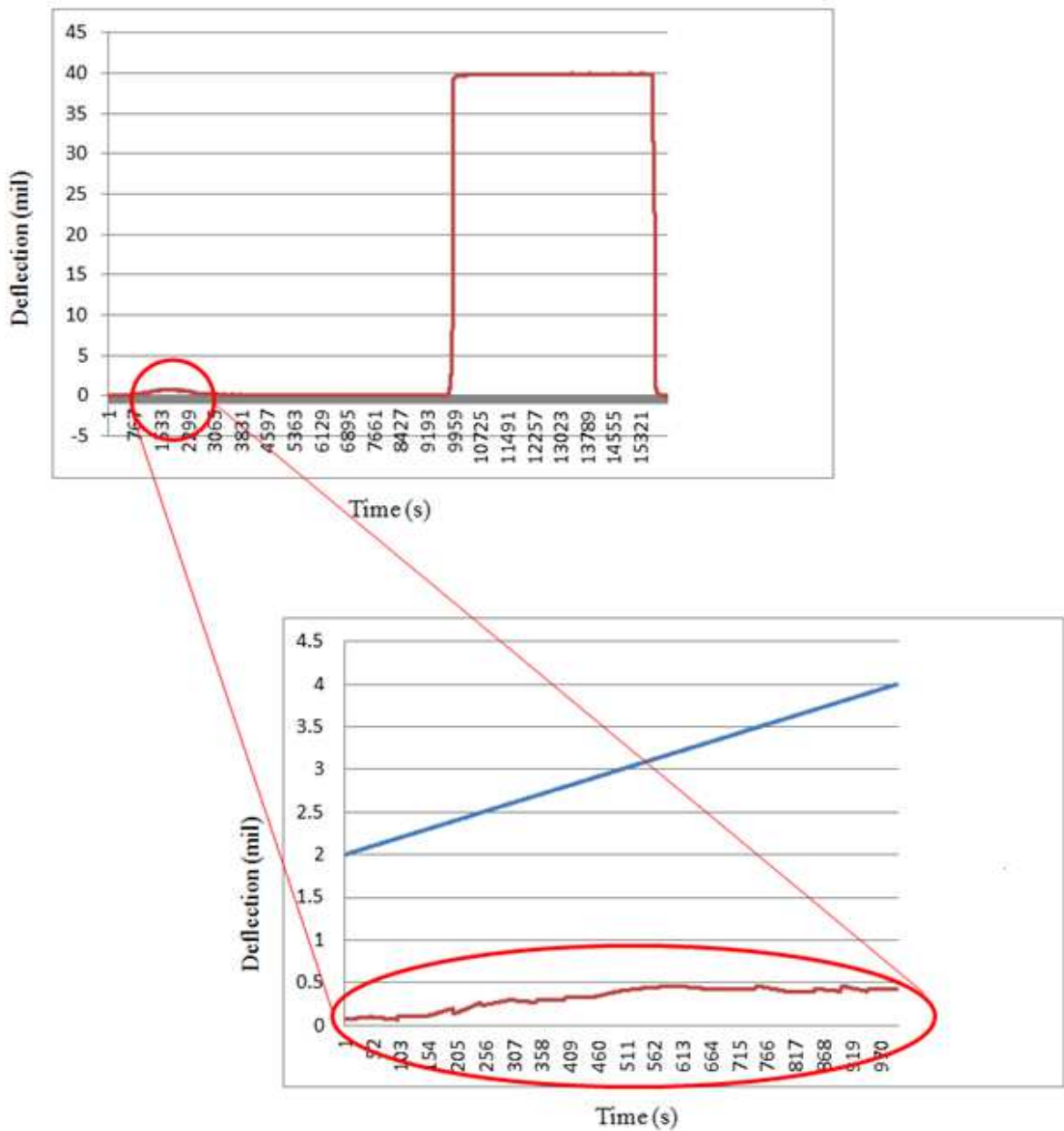


Fig 4.36 Deflection (mils)-time(s) diagram for $t = 2$ S to $t = 4$ S, original structure

Optimized mold

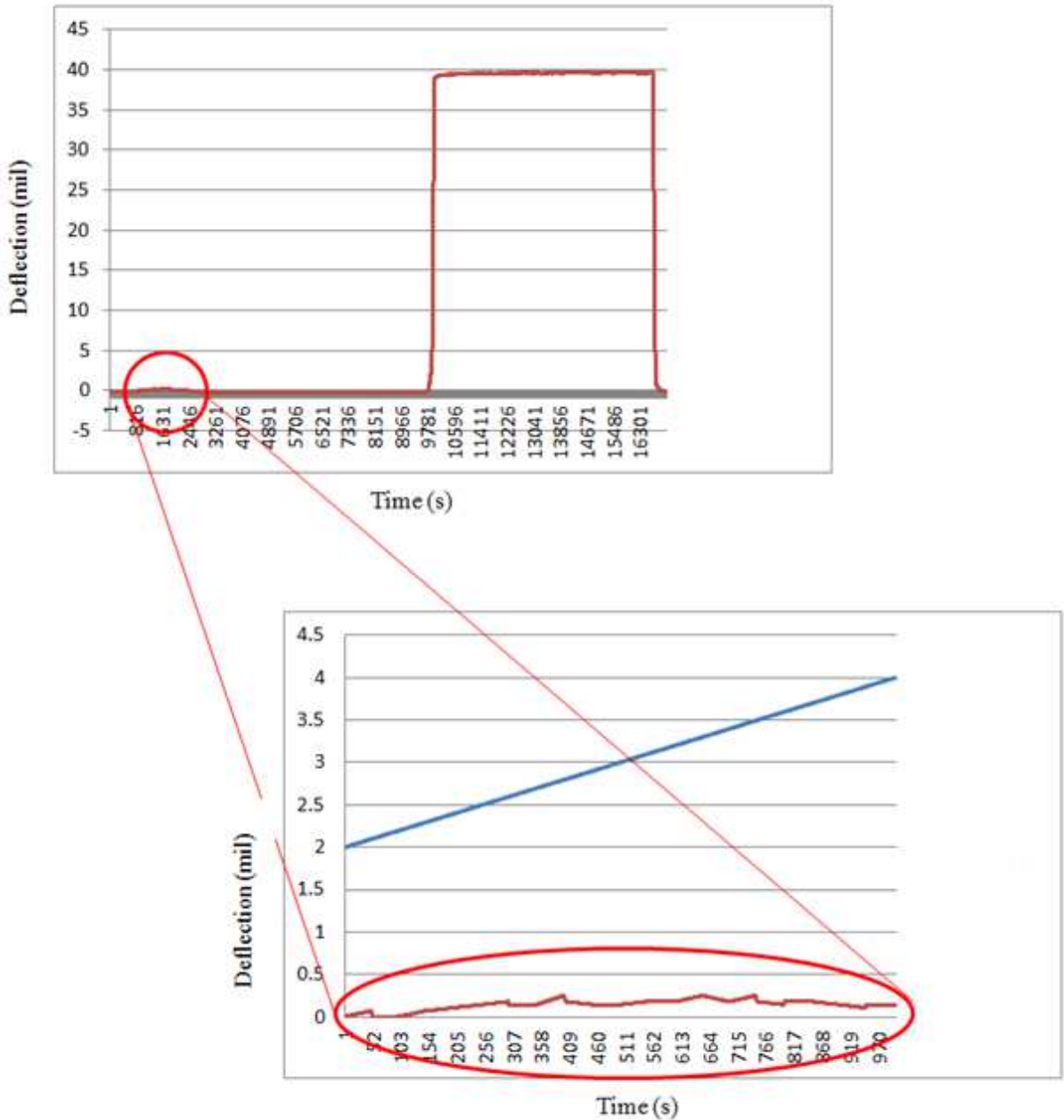


Fig 4.37 Deflection (mils)-time(s) diagram for $t = 2 S$ to $t = 4 S$, Optimized structure

Results of the experiment showed that the optimized structure with less weight has almost similar performance to the original structure and did not fail under applied loading condition. The stress contour plot for the optimized model displayed that, the maximum stress, $37 MPa$, is far from yield stress of steel which is $820 MPa$.

CHAPTER 5

A COUPLED HEAT TRANSFER/STRUCTURAL ANALYSIS OF THE MOLD

The objective in this chapter is to study the thermal effects on mold deflection due to thermal boundary condition of the mold while it is under pressure load case. In other words, a coupled linear heat transfer/structure analysis was performed. However, heat transfer via radiation and convection was not considered and the conduction heat transfer is solely studied. The study was developed on both primary model and the optimized one.

Cavity temperature sensors were needed to be installed in the mold for monitoring temperature and determining the thermal boundary condition. The cavity temperature was considered to be uniform in all surfaces of cavity. Two cavity temperature sensors were needed for two cavities.

5.1 Cavity Temperature

Two 1 mm flush mount temperature sensors were installed in the cavities. Temperature sensors work in conjunction with the eDART process control system. The temperature was monitored through the eDART system. The 1 mm temperature sensor is a miniaturized K type cavity temperature sensor designed for applications where small size is important [7]. Temperature sensors are installed with a distance of less than 1 cm from cavity surface and they do not touch the cavity surface.

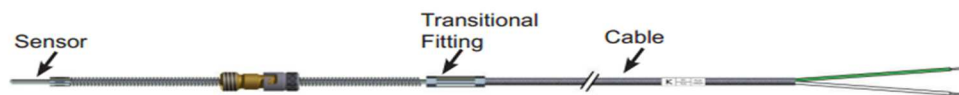


Fig 5.1 Cavity temperature sensors [7]

The sensor tip location and depth (D) are critical if the goal is to monitor plastic flow front arrival timing and/or relative plastic melt temperature (See the table below for applications versus values of D [7]). However, even for detecting mold temperature, it is important to get as close as possible to cavity surface.

Application	Depth to the mold face
-------------	------------------------

Detect melt temperature	D < 0.38 mm
Detect mold temperature	D > 0.38 mm

Table 5.1 Sensor's application and depth of tip to mold surface table

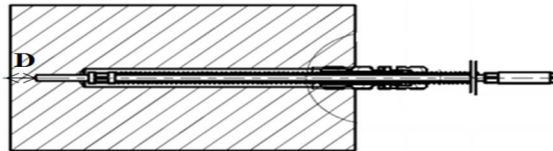


Fig 5.2 Cavity temperature sensor and depth of tip to the cavity surface [7]

The temperature sensors are installed on cavity half. A quad temp module is used to read thermocouple output. Each module is able to monitor four thermocouple outputs.

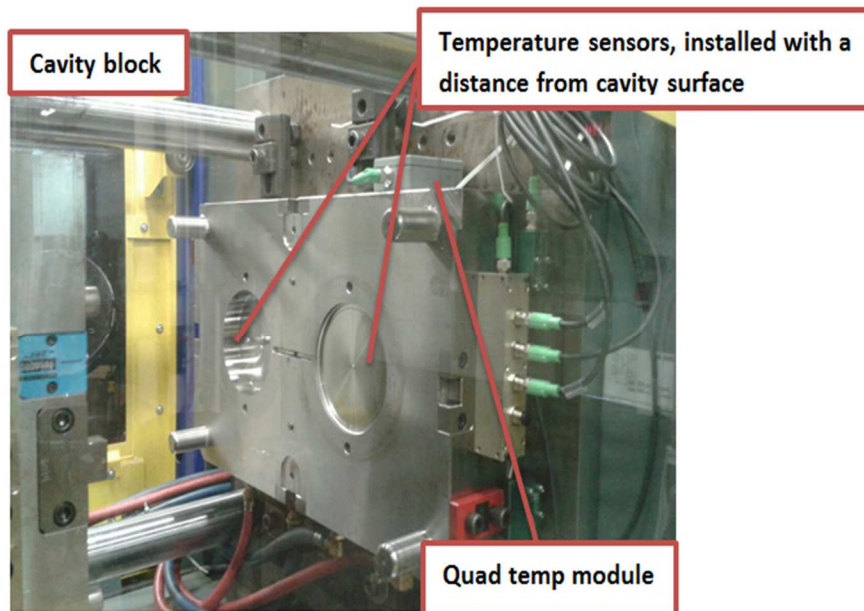


Fig 5.3 Cavity temperature sensors and module, installed in cavity block

The quad temp module is connected to the junction box and the junction box allows the sensor to interface with the eDART. The temperature data is plotted in Matlab and demonstrated in figure 5.4.

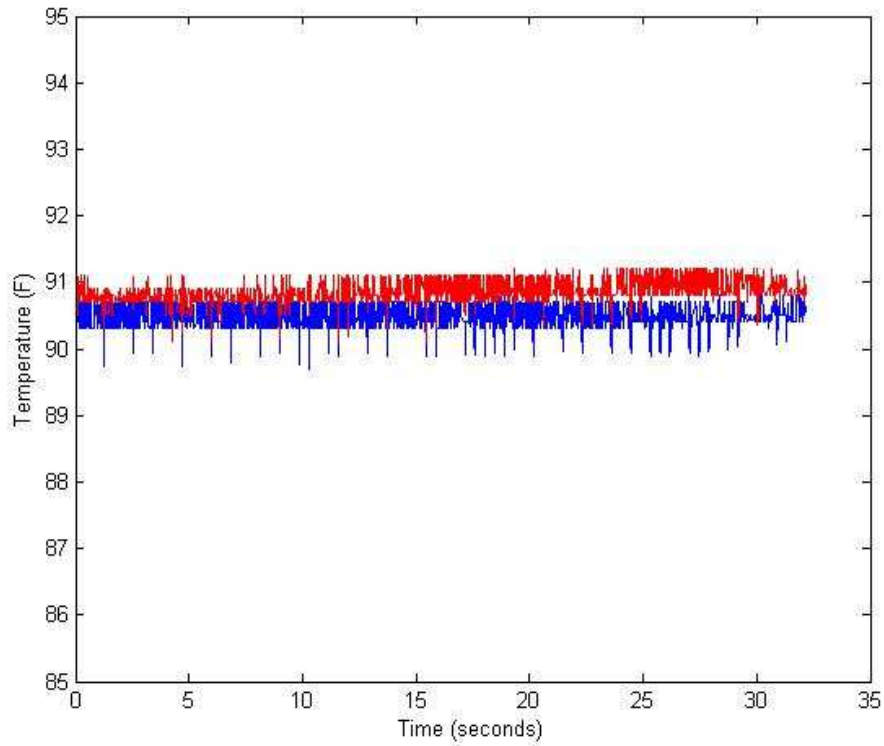


Fig 5.4 Temperature-time diagram, Cavity temperature is plotted for both sensors in each cavity

As it can be seen the temperature sensors monitor the temperature of 90 – 91 °F during one cycle. Since the sensors do not touch the cavity surface, the diagram does not depict a sharp rise and drop in temperature as the melt enter the cavity and it only shows the mold temperature. The following table shows the input data for analyzed models.

Mesh details	
Elements type	CTETRA, four sided and four nodes elements
Element size	$5 \times 10^{-3} m$
Material properties	
Density	$7861 Kg/m^3$
Elastic module	$E = 210 GPa$

Thermal expansion coefficient	$h = 40 \text{ W/m}^2\text{K}$
Thermal conductivity	$K = 73 \text{ W/mK}$
Boundary conditions	
Analysis load cases	Pressure, gravity, constraint, surface temperature
Pressure	Clamping pressure = $6.4 \times 10^6 \text{ Pa}$ Cavity pressure $\begin{cases} \text{Lid} = 1.1 \times 10^7 \text{ Pa} \\ \text{Base} = 1.7 \times 10^7 \text{ Pa} \end{cases}$
Temperature	$T_{\text{ambient}} = 20^\circ\text{C}$ and $T_{\text{cavity}} = 32^\circ\text{C}$
gravity	9.8m/s^2

Table 5.2 Inputs of FE model in Optistruct

5.2 Coupled thermal/ structure analysis result

Figures 5.5, 5.6 and 5.7 show the result of coupled structure/thermal analysis for original model, optimized model and model with smaller overall size.

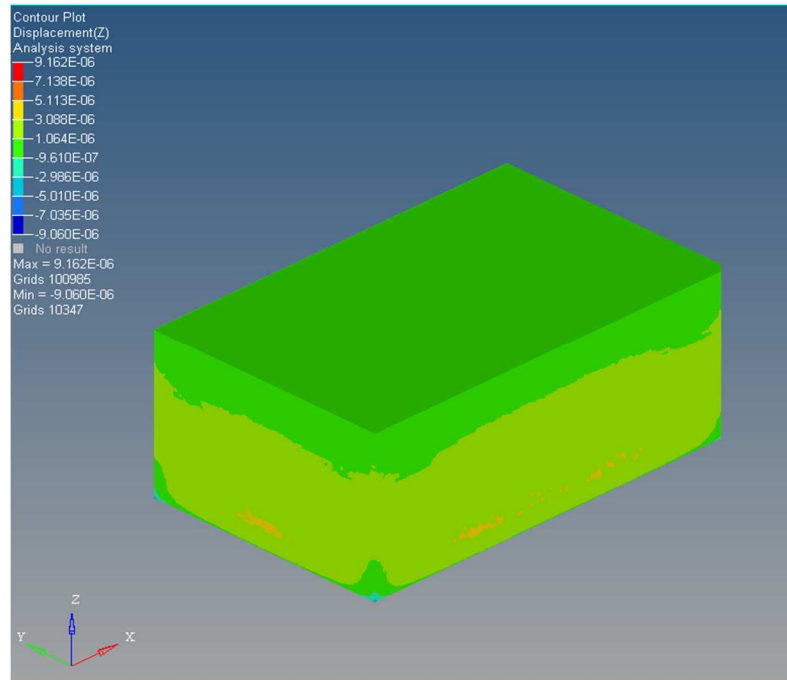


Fig 5.5 deflection (m) contour due to coupled thermal structure analysis of original model

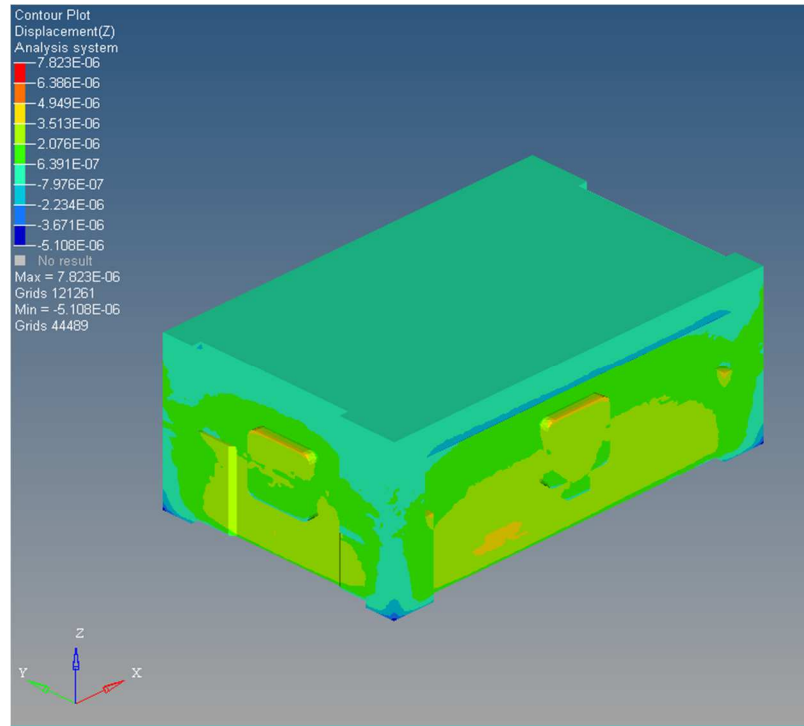


Fig 5.6 deflection (m) contour due to coupled thermal structure analysis of optimized interpreted model

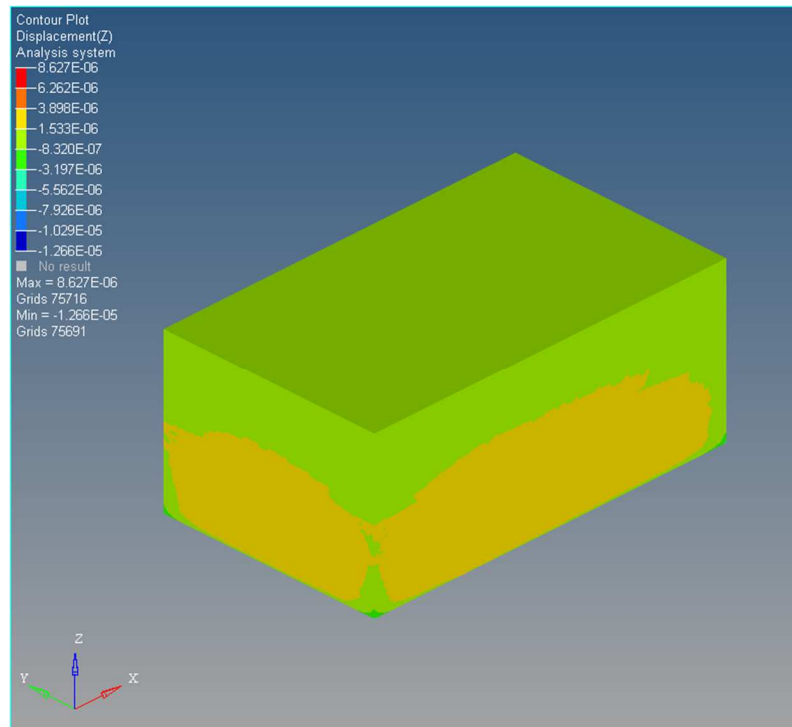


Fig 5.7 deflection (m) contour due to coupled thermal structure analysis of smaller model

As it can be observed from the coupled structure/thermal analysis of primary model, the optimized model and smaller model, thermal expansion in all models has worked in reverse of displacement due to pressure. In another words thermal expansion has decreased the maximum displacement due to pressure and in general it has decreased the pressure effects. However as it can be clearly seen thermal expansion does not have a significant effect since temperature difference between mold and ambient temperature is not considerable.

CHAPTER 6
SUMMARY, CONCLUSION AND FUTURE WORKS

6.1 Summary and conclusion

In this study, it is shown both virtually and experimentally that, a mold with less weight can be achieved from the results of topology optimization. Effort was made to achieve a satisfactory design of the mold from topology optimization results. The model was elaborated for different values of a volume fraction and the best result was achieved when volume fraction of 0.5 was used (volume fraction less than this amount resulted in a discrete structure). From the primary results of the optimization, it could be concluded which areas are loaded more and from which areas the material can be removed more. The optimized interpreted model is 8% lighter than the original model. The key point was that the theoretical results were validated and it was verified that optimized structure has very similar performance to the original structure. Figure 5.1 shows compliance curve vs iteration for volume fraction of 0.5 (compliance is minimized for volume fraction of 0.5)

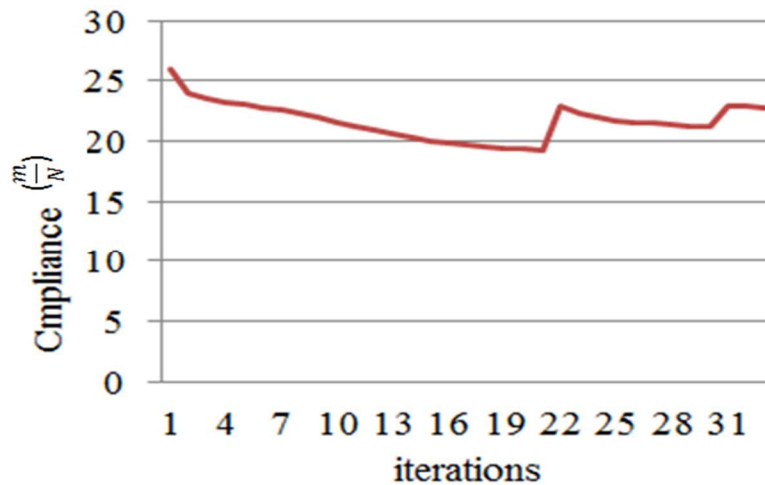


Fig 6.1 Compliance curve vs iteration numbers for optimization with VOF of 0.5

Topology optimization results are not usually feasible to be manufactured. This is due to limitation of conventional manufacturing methods. Additive manufacturing is an alternative technique for manufacturing topology optimization results without the

necessity of post-processing the model. Optistruct does not have proper tool for creating geometry directly from topology optimization results. The problem is the geometry directly exported from results of Optistruct has thousands of faces and creating a manufacturable geometry from that is somehow impossible. Utilizing the Ossmooth command in Optistruct might help to reduce the number of faces but it still doesn't offer a satisfactory result. Therefore a CAD software is needed to be utilized to extract the key surfaces of structure as reference from the results. These surfaces are used to form the actual final CAD geometry. It should be noted that that the final geometry is near optimal in real world.

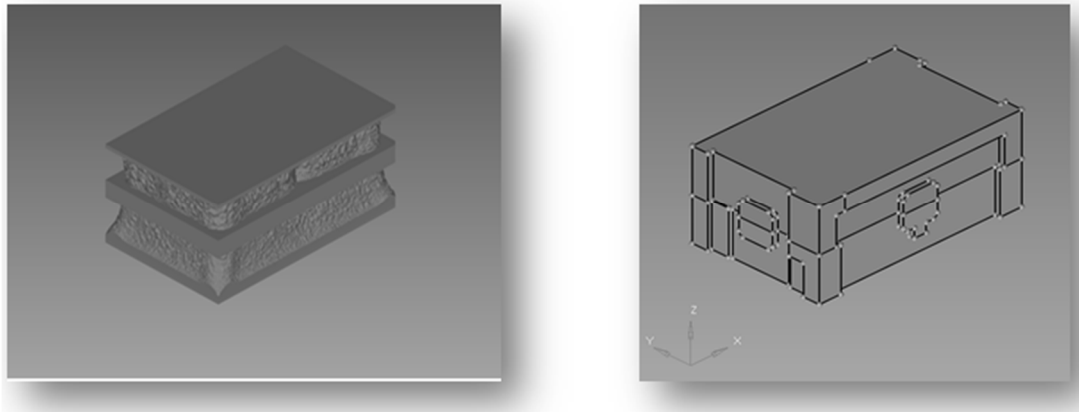


Fig 6.2 Demonstration of real optimal and optimized interpreted model

Thermal expansion in both the original and optimized models has worked in reverse of displacement due to pressure and thermal effect decreased the maximum displacement.

In this thesis a multi load cases optimization with respect to minimizing compliance was performed instead of considering each load case in single optimization and performing several optimization. Therefore the obtained result was due to multi load case optimization.

6.2 Future works

Conventional manufacturing methods have disabled users to manufacture the exact optimal structure and the optimized interpreted model is near optimal. Additive

manufacturing techniques can be proposed as an alternative solution in many cases. This technique omits the post processing step from the process.

Considering convection and radiation in thermal analysis of the mold would be a subject for future works.

There are many parameters in Optistruct which affect the final result in optimization such as volume fraction, threshold value and MMS. It is valuable to conduct a parameter study for each optimization and write a program that checks all combination of parameters to find the best combination of aforementioned parameters will increase the accuracy of optimum result. This work can improve the final result, if optimal solutions are evaluated with respect to optimality and assuring that the global optimum structure is achieved.

In this study length and width of the mold were subjected to optimization and height of the mold was bounded to non-design spaces. Hence, the height stays unaffected from the optimization. Incorporating the mold height could be a subject for future studies.

REFERENCES

- [1] "What is plastic injection molding?" [Online]. Available: <http://www.vulcanmold.com/article/Plastic-Injection-molding-process.html>.
- [2] G. Menges, W. Michaeli, and P. Mohren, *How to make injection molds*. Carl Hanser Verlag GmbH & Co. KG, 2001.
- [3] M. P. Bendsoe and O. Sigmund, *Topology optimization: theory, methods and applications*. Springer, 2003.
- [4] "HyperMesh QuickStart - Refining Geometry." [Online]. Available: http://www.altairhyperworks.com/training/self_paced/hm_quickstart_preview/content/refine_geom.htm. [Accessed: 04-Dec-2014].
- [5] "LS-B-127-500 - Products - Injection Molding | Injection Molding Training, eDART System, RJG Inc. Traverse City, Michigan, MI - RJG Inc." [Online]. Available: <https://www.rjginc.com/products/92-ls-b-127-500>. [Accessed: 12-Dec-2014].
- [6] "LS-MD-040 - Products - Injection Molding | Injection Molding Training, eDART System, RJG Inc. Traverse City, Michigan, MI - RJG Inc." [Online]. Available: <http://www.rjginc.com/products/495-ls-md-040>. [Accessed: 03-Jan-2015].
- [7] "TS-FM01-K-1 - Products - Injection Molding | Injection Molding Training, eDART System, RJG Inc. Traverse City, Michigan, MI - RJG Inc." [Online]. Available: <https://www.rjginc.com/products/423-ts-fm01-k-1>. [Accessed: 17-Dec-2014].
- [8] "Tutorial: Injection molded parts." [Online]. Available: <http://www.sinotech.com/injectionMolded.html>. [Accessed: 05-Jan-2015].
- [9] P. E. Allen, "Injection-mold venting: the hidden processing parameter," *Plast. Eng.*, vol. 35, no. 1, pp. 43–50, 1979.
- [10] L. M. Pintelon and L. F. Gelders, "Maintenance management decision making," *Eur. J. Oper. Res.*, vol. 58, no. 3, pp. 301–317, 1992.
- [11] W. Michaeli and M. Thornagel, "Mechanical design of plastics injection moulds by means of FEA," *J. Polym. Eng.*, vol. 24, no. 1–3, pp. 1–14, 2004.
- [12] K. K. Alaneme, B. O. Adewuyi, and F. A. Ofoegbu, "Failure analysis of mould dies of an industrial punching machine," *Eng. Fail. Anal.*, vol. 16, no. 7, pp. 2043–2046, 2009.
- [13] D.-G. Ahn, H.-W. Kim, S.-H. Park, and H.-S. Kim, "Manufacture of Mould with a High Energy Efficiency Using Rapid Manufacturing Process," in *NUMIFORM 2010: Proceedings of the 10th International Conference on Numerical Methods in Industrial Forming*

Processes Dedicated to Professor OC Zienkiewicz (1921--2009), 2010, vol. 1252, no. 1, pp. 185–191.

- [14] F. Shi, Z. L. Lou, Y. Q. Zhang, and J. G. Lu, "Optimisation of plastic injection moulding process with soft computing," *Int. J. Adv. Manuf. Technol.*, vol. 21, no. 9, pp. 656–661, 2003.
- [15] Z. Chen and L.-S. Turng, "A review of current developments in process and quality control for injection molding," *Adv. Polym. Technol.*, vol. 24, no. 3, pp. 165–182, 2005.
- [16] A. G. M. Michell, "LVIII. The limits of economy of material in frame-structures," *London, Edinburgh, Dublin Philos. Mag. J. Sci.*, vol. 8, no. 47, pp. 589–597, 1904.
- [17] U. L. F. T. RINGERTZ, "On topology optimization of trusses," *Eng. Optim.*, vol. 9, no. 3, pp. 209–218, 1985.
- [18] W. Achtziger and M. Stolpe, "Global optimization of truss topology with discrete bar areas—Part II: Implementation and numerical results," *Comput. Optim. Appl.*, vol. 44, no. 2, pp. 315–341, 2009.
- [19] Sükrü Karakaya and Ö. Soykasap, "Natural frequency and buckling optimization of laminated hybrid composite plates using genetic algorithm and simulated annealing," *Struct. Multidiscip. Optim.*, vol. 43, no. 1, pp. 61–72, 2011.
- [20] G. I. N. Rozvany, "A critical review of established methods of structural topology optimization," *Struct. Multidiscip. Optim.*, vol. 37, pp. 217–237, 2009.
- [21] S. H. Tang, Y. M. Kong, S. M. Sapuan, R. Samin, and S. Sulaiman, "Design and thermal analysis of plastic injection mould," *J. Mater. Process. Technol.*, vol. 171, no. 2, pp. 259–267, Jan. 2006.
- [22] J. C. Youngs, "Structural Optimization of a Thermally Loaded Functionally Graded Pressure Vessel," Rensselaer Polytechnic Institute, 2009.
- [23] P. W. Christensen and A. Klarbring, *An introduction to structural optimization*, vol. 153. Springer Science & Business Media, 2008.
- [24] M. P. Bendsøe and O. Sigmund, "Material interpolation schemes in topology optimization," *Arch. Appl. Mech.*, vol. 69, no. 9–10, pp. 635–654, 1999.
- [25] J. C. Youngs, "Structural Optimization of a Thermally Loaded Functionally Graded Pressure Vessel by," no. August, 2009.
- [26] T. Renault, "Doctor of Ecole Polytechnique Manufacturing Constraints and Multi-Phase Shape and Topology Optimization via a Level-Set Method Georgios MICHALIDIS Grégoire ALLAIRE," 2014.

- [27] D. Xiao, X. Liu, W. Du, J. Wang, and T. He, "Application of topology optimization to design an electric bicycle main frame," *Struct. Multidiscip. Optim.*, vol. 46, no. 6, pp. 913–929, 2012.
- [28] O. Help, "HyperWorks 13.0_Optistruct help."
- [29] A. Mechanics, "Substructure Topology Optimization of an electric machine," 2013.
- [30] P. J. Frey and P.-L. George, *Mesh Generation: Application to Finite Elements*. Hermes Science, 2000.

APPENDICES

Appendix A: Deflection contour for original model, optimized interpreted model and smaller model

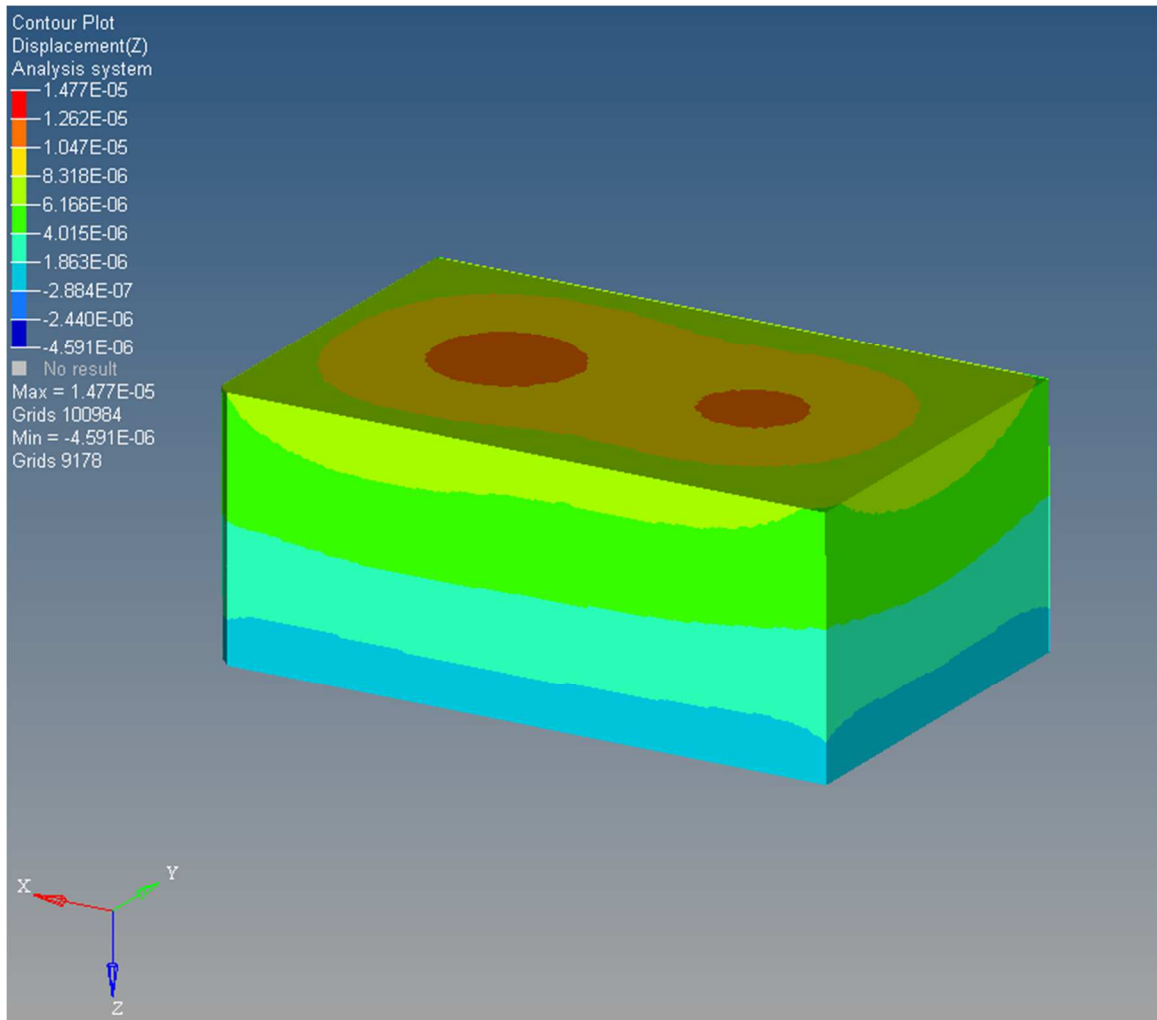


Fig A.1 Displacement (m) contour plot for primary model

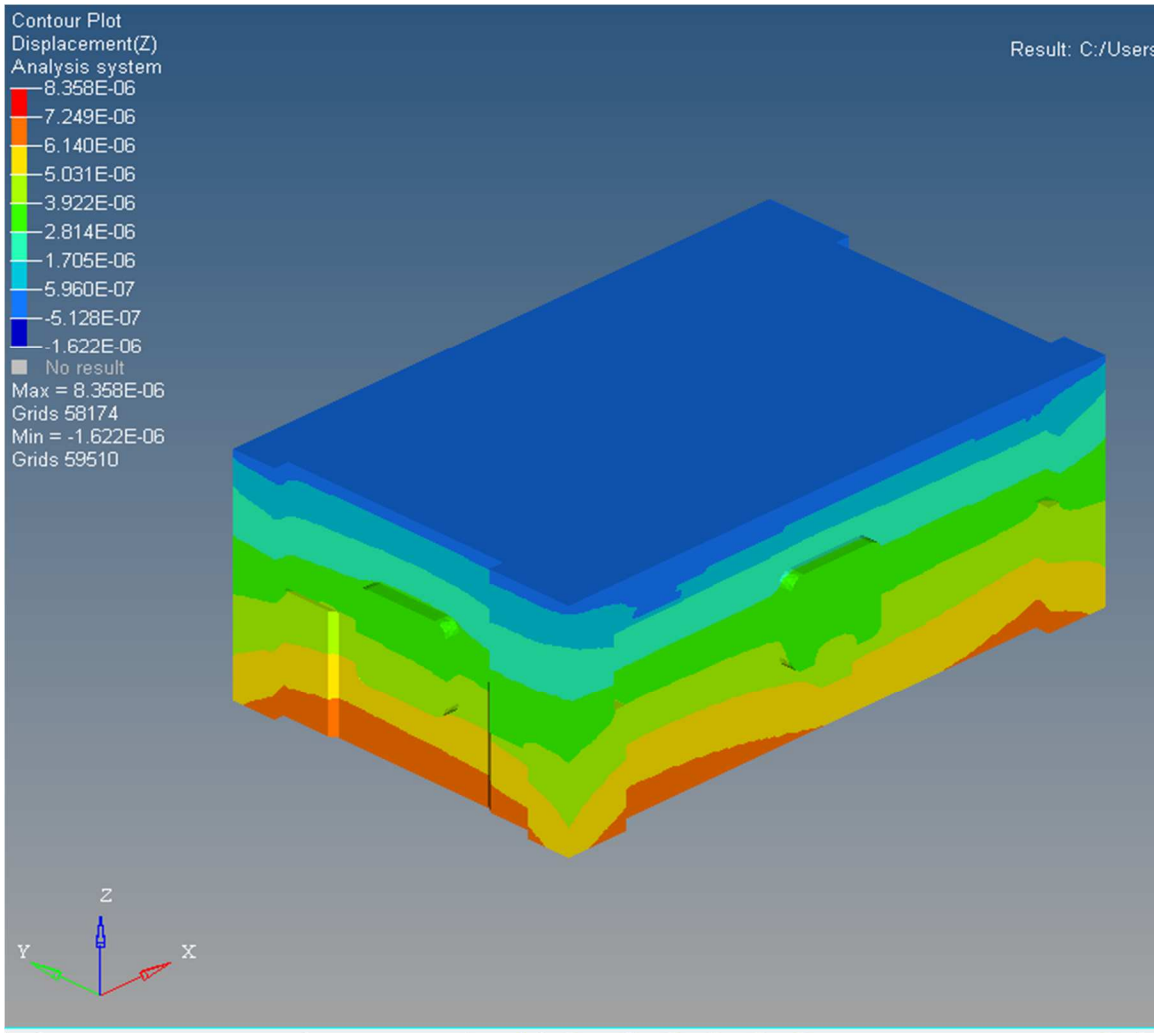


Fig A.2 Displacement (m) contour plot for optimized interpreted model

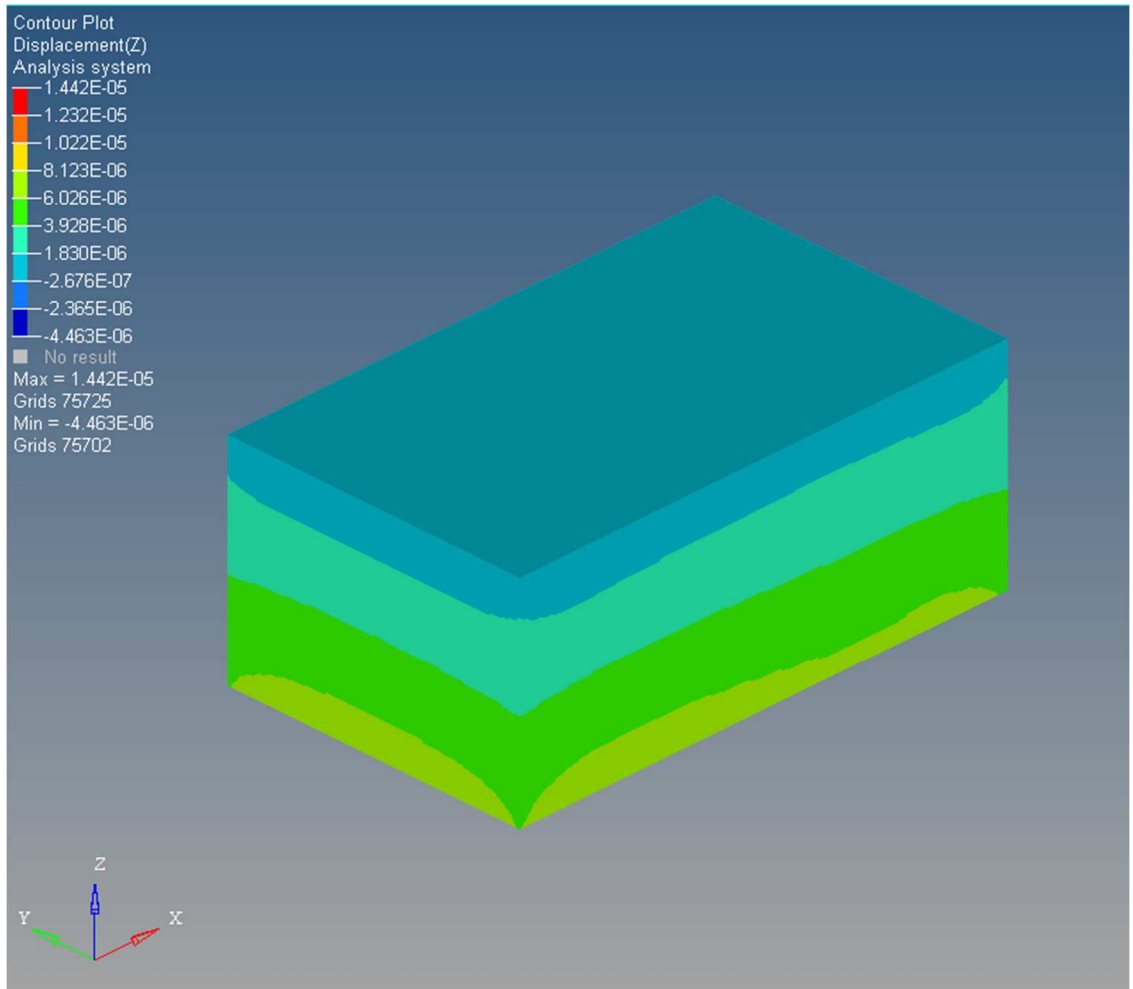


Fig A.3 Displacement (m) contour plot for proposed model

Appendix B: Deflection contour for coupled structure/thermal analysis results

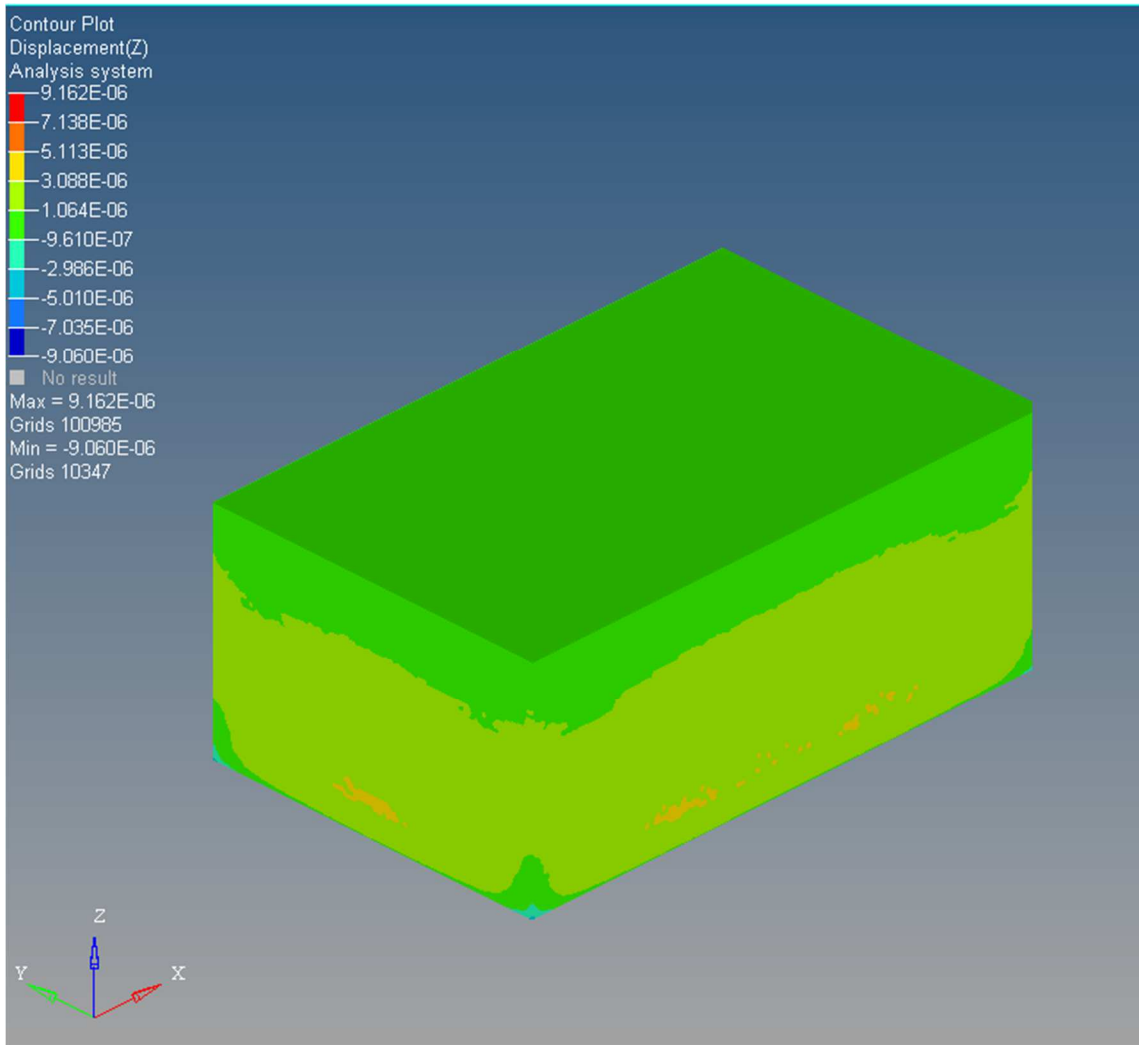


Fig B.1 Deflection (m) of original model under coupled heat/structure analysis

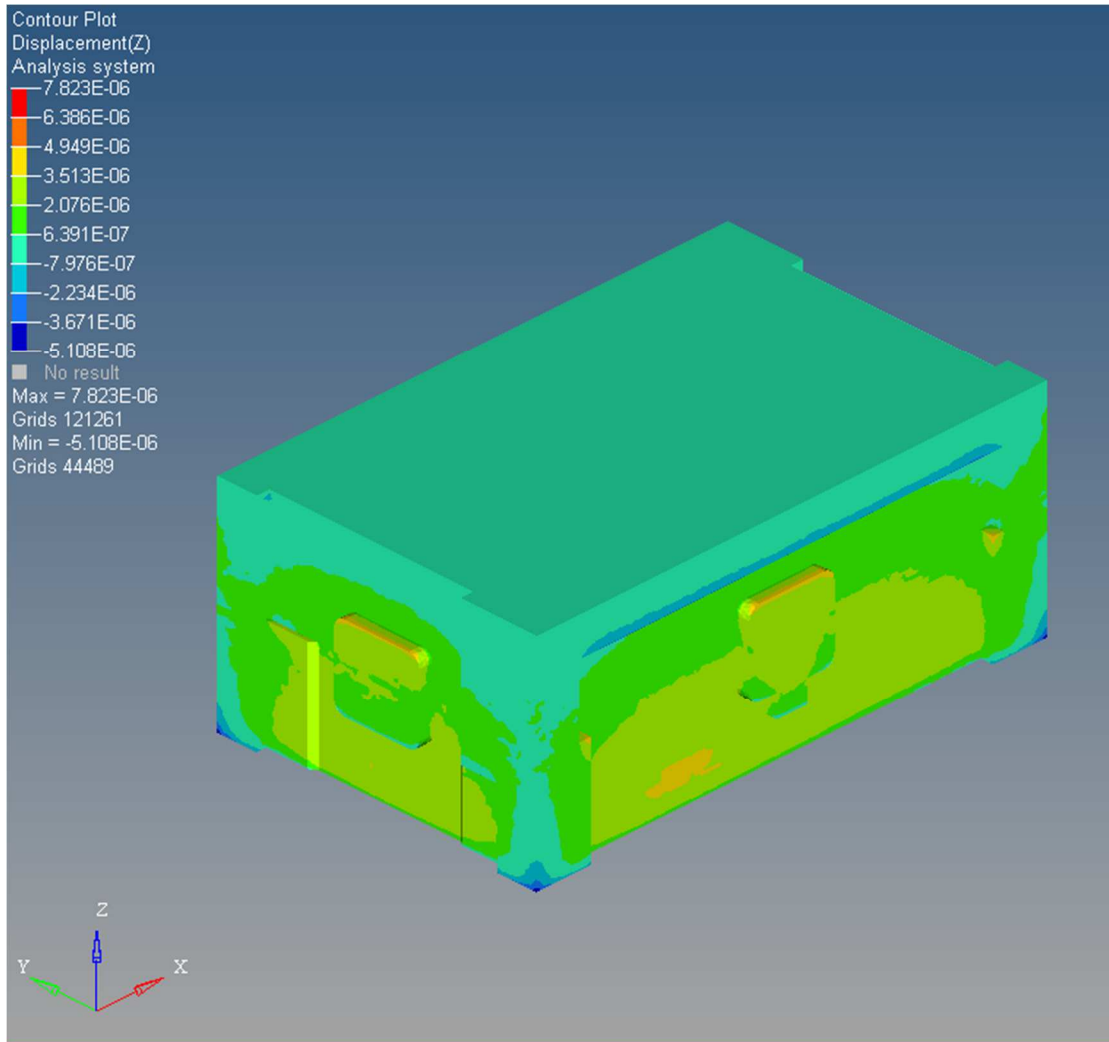


Fig B.2 Deflection (m) of optimized interpreted model under coupled heat/structure analysis

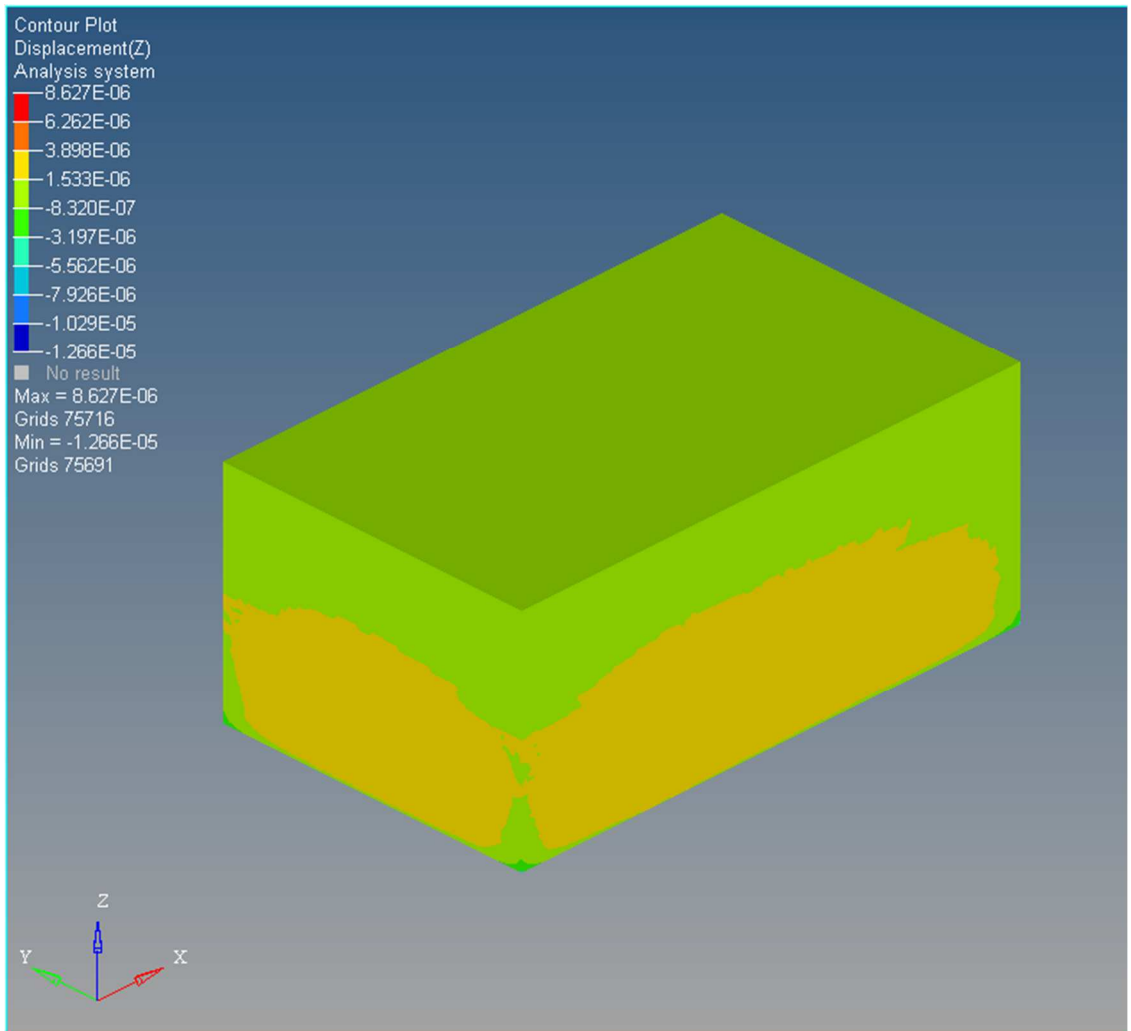


Fig B.3 Deflection (m) contour due to coupled thermal structure analysis of smaller model

Appendix C: Mesh quality check

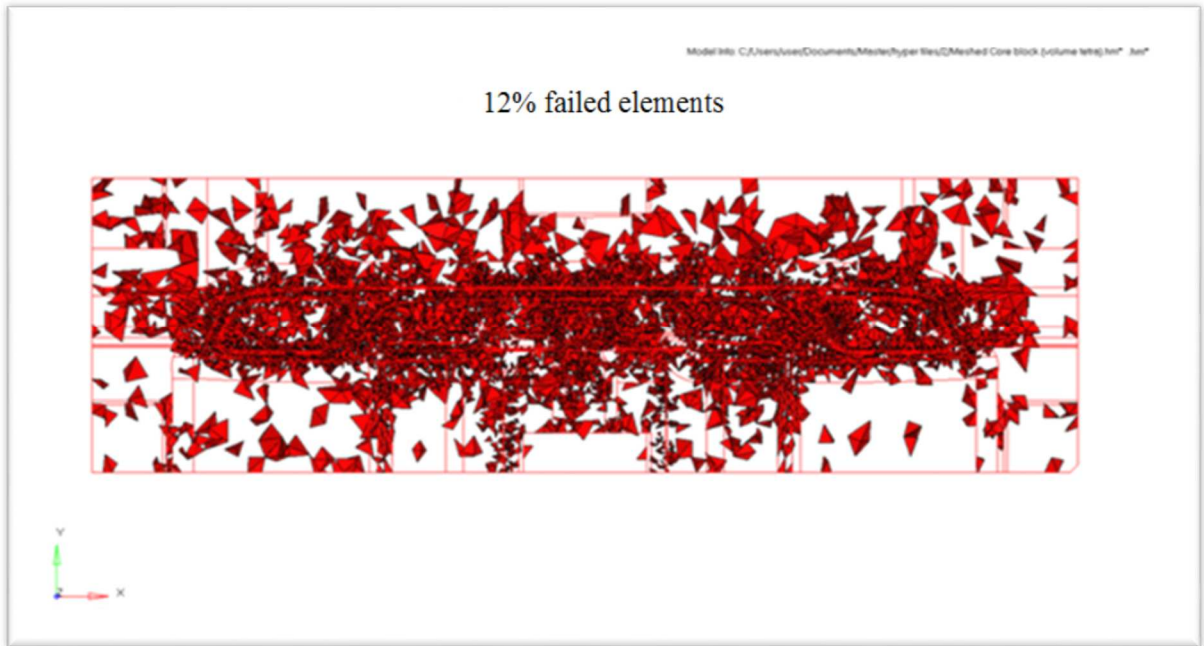


Fig C.1 Element quality check and determining failed elements

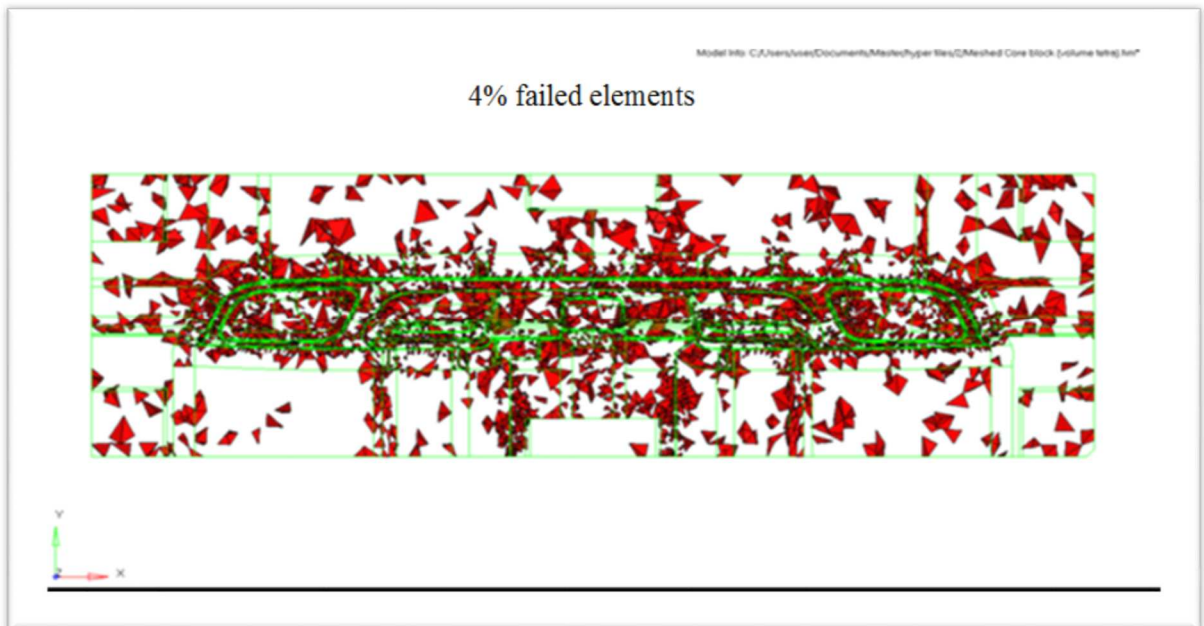


Fig C.2 Re meshing failed elements to increase the quality of the mesh

Appendix D: Workflow of structural optimization

1) **Problem set up**

- i. Determining design space and non-design space using any kind of CAD software or finite element analysis software
- ii. Specifying loading condition and boundary condition applied to the model
- iii. Meshing the model based on needs of topology optimization
- iv. Defining contact surfaces where necessary

2) **Topology Optimization**

- i. Defining objective function, constraints and design variables
- ii. Determining topology optimization criteria such as minimum member size and symmetry constraint
- iii. Running several optimizations to check the predetermined parameters
- iv. Using Hyperview, post processing software, and deciding on a feasible structure
- v. Checking results of FEA analysis on structure with defined parameters

3) **Result interpretation**

- i. Using Osmooth command in Hypermesh to reduce the number of structure's faces to make it more appropriate and saving it into IGES format Exporting topology optimization result
- ii. Using any kind of CAD software to extract the key surfaces of structure as reference from the results. These surfaces are used to form the actual final CAD geometry.

4) **Finite element analysis on optimized interpreted model**

- i. Importing optimized interpreted geometry to the FEA analysis software
- ii. Meshing, applying loads and boundary conditions on optimized interpreted geometry and running the FEA analysis
- iii. Checking the Von Mises stresses and displacement for optimized interpreted geometry

iv. Performing design modifications and adjustments if necessary for stress concentration spots

5) **Fine tuning the final CAD geometry**

VITA AUCTORIS

NAME: Bita Mohajernia
PLACE OF BIRTH: Mashhad, Iran
YEAR OF BIRTH: 1987
EDUCATION: Ferdowsi University of Mashhad, B.Sc., Iran, 2011
University of Windsor, M.Sc., Windsor, ON, 2015